TECHNICAL REPORT STANDARD TITLE PAGE

1. Report No.	2. Government Accession No.	3. Recipient's Catalog No.
FHWA/TX-87/43+415-1		

4. Title and Subtitle	5. Report Date
EVALUATION AND DEVELOPMENT OF P-Y BASED PROCEDURES FOR ANALYSIS OF "SHORT" DRILLED SHAFTS SUBJECTED TO LATERAL LOADS	November 1986
	6. Performing Organization Code
7. Author(s)	8. Performing Organization Report No.
Christopher W. Swan and Stephen G. Wright	Research Report 415-1
9. Performing Organization Name and Address	10. Work Unit No.
Center for Transportation Research The University of Texas at Austin Austin, Texas 78712-1075	11. Contract or Grant No. Research Study 3-5-85-415
	13. Type of Report and Period Covered
12. Sponsoring Agency Name and Address Texas State Department of Highways and Public Transportation; Transportation Planning Division P. O. Box 5051 Austin, Texas 78763-5051	Interim
	14. Sponsoring Agency Code

15. Supplementary Notes

Study conducted in cooperation with the U. S. Department of Transportation, Federal Highway Administration

Research Study Title: "Design Method for Vertical Drilled Shafts"

16. Abstract

This report presents the results of theoretical studies performed to understand and be able to predict better the response of "short" drilled shafts. A "short" drilled shaft has been defined as a shaft which undergoes less than two points of zero deflection when subjected to lateral loads. The first portion of this study was directed towards developing simplified procedures for estimating when a drilled shaft would respond as a "short" shaft, taking into account at least approximately the nonlinear response of the soil. The second portion of this study was directed toward improving the present procedure for predicting the response of "short" drilled shafts. Several modifications were made to existing procedures based on "p-y" curves to improve their ability to predict the response of short drilled shafts. These modifications were incorporated into a computer program with other modifications, which are presented in a companion project report.

17. Key Words	18. Distribution Statement
drilled shafts, "short," response, prediction, procedures, modifications, p-y curves, computer program	No restrictions. This document is available to the public through the National Technical Information Service, Springfield, Virginia 22161.

19. Security Classif. (of this report)	20. Security Classif. (of this page)	21. No. of Pages	22. Price
Unclassified	Unclassified	202	

Form DOT F 1700.7 (8-69)

EVALUATION AND DEVELOPMENT OF P-Y BASED PROCEDURES FOR ANALYSIS OF "SHORT" DRILLED SHAFTS SUBJECTED TO LATERAL LOADS

by

Christopher W. Swan
Stephen G. Wright

Research Report Number 415-1

Design Method for Vertical Drilled Shafts
Research Project 3-5-85-415

conducted for

Texas State Department of Highways
and Public Transportation

in cooperation with the
U.S. Department of Transportation
Federal Highway Administration

by the

CENTER FOR TRANSPORTATION RESEARCH
BUREAU OF ENGINEERING RESEARCH
THE UNIVERSITY OF TEXAS AT AUSTIN

November 1986

The contents of this report reflect the views of the authors, who are responsible for the facts and the acuracy of the data presented herein. The contents do not necessarily reflect the official views or policies of the Federal Highway Administration. This report does not constitute a standard, specification, or regulation.

PREFACE

The response of drilled shafts and pile foundations to lateral loads is routinely computed using computer programs and procedures developed during the past 30 years at the University of Texas. The procedures are based on a numerical solution of the differential equation for a beam on an elastic foundation and employ nonlinear p-y curves to describe the soil response. The procedures are based to a large extent on the results of full-scale load tests on piles and drilled shafts. However, experience with these procedures has shown that they produce relatively poor agreement between predicted and measured response for relatively short drilled shafts. In order to understand better the reasons for the discrepancies between predicted and measured response for such short piles and drilled shafts the studies presented in this report were undertaken.

ABSTRACT

This report presents the results of theoretical studies performed to understand and be able to predict better the response of "short" drilled shafts. A "short" drilled shaft has been defined as a shaft which undergoes less than two points of zero deflection when subjected to lateral loads. The first portion of this study was directed towards developing simplified procedures for estimating when a drilled shaft would respond as a "short" shaft, taking into account at least approximately the nonlinear response of the soil. The second portion of this study was directed toward improving the present procedure for predicting the response of "short" drilled shafts. Several modifications were made to existing procedures based on "p-y" curves to improve their ability to predict the response of short drilled shafts. These modifications were incorporated into a computer program with other modifications, which are presented in a companion Project report.

SUMMARY

Simplified procedures were examined for use in determining whether a laterally loaded drilled shaft or pile would respond such that there were at least two points of zero deflection along its length. Shafts in which there are not at least two points of zero deflection are considered "short" drilled shafts and the simplified procedures presented in this report enable an estimate to be made of whether a shaft or pile should be treated as "short" or "long."

Previous experience had revealed that existing procedures for calculating the response of laterally loaded piles and piers produced relatively poor agreement between measured and predicted response for "short" lengths. Existing procedures were examined and modified to model more properly the behavior of "short" drilled shafts and piles. Results from a series of load tests on a variety of drilled shafts were compared to predicted response based on previous procedures and those developed as part of the current study. The modified procedures were found to produce much better agreement with the measured response and, accordingly, are recommended for use in computations for "short" drilled shafts and piles.

IMPLEMENTATION STATEMENT

The simplified procedure presented for estimating the minimum length of drilled shaft or pile required to produce at least two points of zero deflection is recommended for at least preliminary estimates of shaft length. In general, use of drilled shaft and pile lengths producing at least two points of zero deflection under lateral loading is recommended because of greater overall shaft stability.

In cases where "short" drilled shaft and piles, having less than two points or zero deflection, are employed, the modifications developed in this study to existing procedures, based on use of "p-y" curves, are believed to produce more reliable predictions and are recommended for use in place of previously existing procedures. A computer program and procedures implementing these recommendations is presented in a companion Project report.

TABLE OF CONTENTS

LIST OF TABLES

Table | Page

LIST OF FIGURES

Figure Page

Figure Page

Figure Page

CHAPTER 1. INTRODUCTION

The Texas State Department of Highways and Public Transportation has used cast-in-place concrete drilled shafts as retaining walls with the drilled shafts placed in a single line. Drilled shafts used as retaining structures may differ significantly from those used for conventional foundations, especially with regard to the length of the shafts. The length of drilled shafts used as conventional foundations is governed primarily by the axial loads, rather than the lateral loads. Consequently, the length which is required for design of conventional foundations is often relatively large compared to what would be required to support lateral loads. In contrast, the design of drilled shafts which are used as retaining structures may be governed primarily by lateral loads.

The current procedures for analysis of laterally loaded piles and drilled shafts are largely empirical and are based heavily on the results of actual load tests, most of which have been performed on relatively "long" members. A substantial amount of experience with these procedures has shown that they produce reasonably reliable results for relatively long piles and drilled shafts for which they were developed. A much smaller amount of experience with the application of such procedures to shorter piles and drilled shafts has indicated that the procedures do not work as favorably for such "short" members (Reese, 1986; Leicht, 1986). Although no precise definition exists to distinguish "short" from "long", it is generally accepted that a "long" shaft is one that has two or more points of zero deflection (Fig. 1.1a). For shorter lengths of shaft, the shaft deflects more rigidly with the deflected shape of the shaft having only a single point of zero deflection (Fig. 1.1b).

The study, reported herein, was undertaken to investigate the validity of current procedures for analyses of laterally loaded piles and drilled shafts for cases where the shaft is relatively short. In Chapter 2, current analytical procedures for the analyses of laterally loaded piles and drilled shafts are briefly discussed. In Chapter 3, present procedures for determining the minimum length of shaft required to achieve two points of zero deflection are examined, and a simplified procedure for estimating this

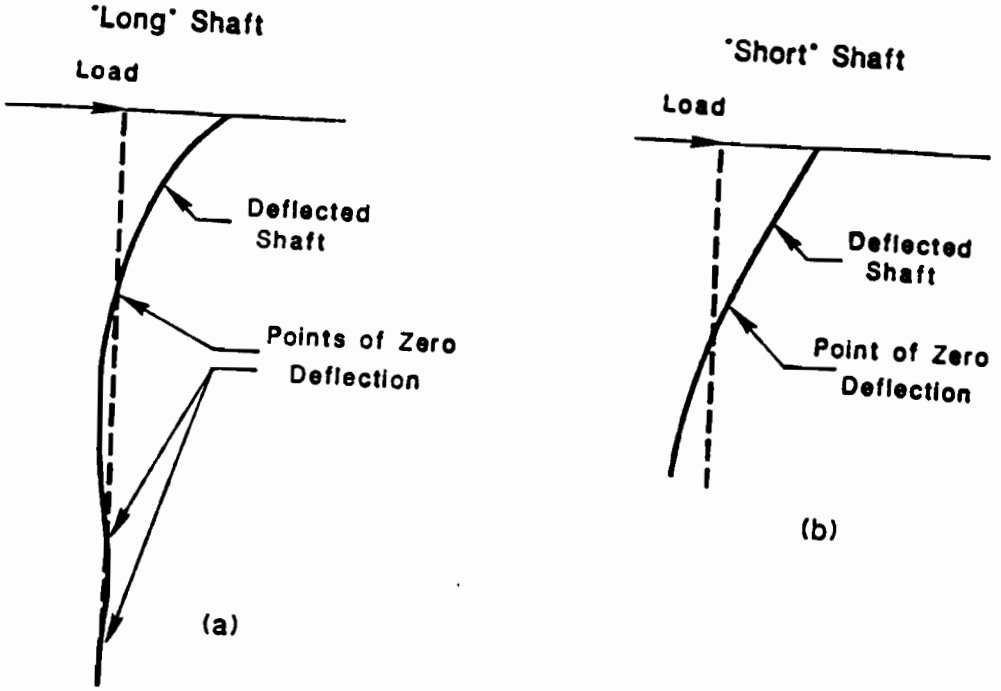

Figure 1.1: Deflected Shape of (a) "Long" Shaft and (b) "Short" Shaft

minimum length is developed. Data from a series of load tests on "short" drilled shafts, sponsored by the Electric Power Research Institute, EPRI, are presented in Chapter 4. In Chapter 5, results from analyses of the drilled shafts, employing current analytical procedures, are presented and compared to the measured results from the load tests. Proposed modifications to the current procedures are presented in Chapter 6, and the results from analyses of the EPRI drilled shafts, using the modifications, are presented in Chapter 7. Analyses were performed on additional "short" drilled shafts with data from the actual load tests and the results of analyses presented and compared to the measured results in Chapter 8. Chapter 9 contains a summary, conclusion, and recommendations.

CHAPTER 2. PROCEDURES FOR ANALYZING LATERALLY LOADED DRILLED SHAFTS

The analysis of a laterally loaded drilled shaft involves a complex interaction between the drilled shaft and soil. Both simple and complex methods of analysis have been developed and are available to the practicing engineer. One of the more widely accepted methods of analysis is that developed by researchers at the University of Texas at Austin. The method utilizes a finite difference solution along with nonlinear "p-y curves" to describe the interaction between the drilled shaft and soil. An overview of this method is presented in this chapter with emphasis on the development of the finite difference solution and p-y curves and a description of the computer program used for analysis, COM624.

2.1 DEVELOPMENT OF FINITE DIFFERENCE SOLUTION

The finite difference solution, used to describe the interaction between the soil and shaft, was derived from Hetenyi's (1946) differential equation which relates the lateral deflection of the drilled shaft to the resistance of the soil:

$$E_p I_p \frac{d^4y}{dx^4} + P_x \frac{d^2y}{dx^2} - p = 0 \qquad (2.1)$$

where y is the lateral deflection at a point x along the drilled shaft, $E_p I_p$ is the structural stiffness of the drilled shaft which is the product of the shaft's elastic modulus (E_p) and moment of inertia (I_p), P_x is the axial force applied to the drilled shaft and p is the soil resistance.

The soil resistance can be related to the lateral deflection of the drilled shaft by the soil modulus, K_s, as

$$p = -K_s y \qquad (2.2)$$

Substituting this expression for the soil resistance into Eq. 2.1 yields

$$E_p I_p \frac{d^4y}{dx^4} + P_x \frac{d^2y}{dx^2} + K_s y = 0 \qquad (2.3)$$

For most soils, the relationship between the soil resistance, p, and lateral deflection, y, is nonlinear and can be represented by nonlinear p-y curves (Fig. 2.1). The secant slope of the nonlinear p-y curve represents the soil modulus where

$$K_s = -p/y \qquad (2.4)$$

In the analysis of a laterally loaded drilled shaft, the deflections are not the same at every point along the length of the shaft; therefore, soil moduli vary nonlinearly with the deflection of the shaft and, therefore, nonlinearly with depth. For such a nonlinear variation in soil modulus, Eq. 2.3 can be solved for the deflections, y, along the drilled shaft using finite differences.

Finite difference solutions have been developed by Gleser (1953), Focht and McClelland (1955), Howe (1955) and others. Briefly stated, in a finite difference solution, the shaft is represented by a series of nodal points, and algebraic expressions, called difference equations, are formed to de scribe the deflection, slope, moment and shear at each nodal point along the entire shaft. The finite difference solution allows a different soil modulus (p-y curve) to be used at each nodal point. With this ability, an arbitrary set of p-y curves can be used to define the soil resistance deflection (p-y) relationship along the entire length of the drilled shaft.

2.2 CRITERIA FOR p-y CURVES

Several criteria for p-y curves have been developed to model the various types and classes of soil. Currently, there are four established p-y curve criteria which are widely used in the analysis of piles and drilled shafts under lateral loads. These criteria were developed from load tests on instrumented piles in sand and clay soils. The four criteria are Matlock's

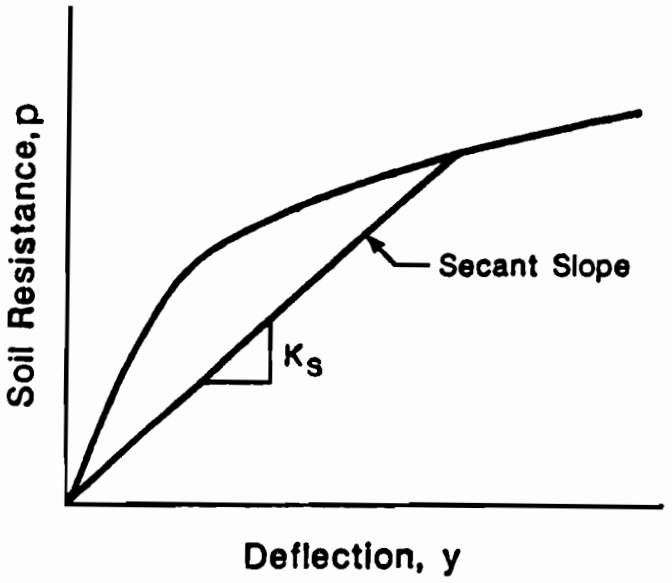

Figure 2.1: Form of Nonlinear p-y Curve

(1970) for soft-clay; Reese, Cox and Koop's (1975) for stiff-clay-below-the-water-table; Reese and Welch's (1975) for stiff-clay-above-the-water-table and Reese, Cox and Koop's (1974) for sands.

There are certain elements that are common to all of the above p-y curve criteria. The p-y curves are limited to an ultimate soil resistance, p_{ult}, based on equations developed from two assumed modes of failure; wedge-type failure and flow-around failure. The p-y curves are also influenced by the unit weight and shear strength of the soil, the diameter of the drilled shaft and the type of loading; static or cyclic. In the present study, only static loading is considered. Construction of the four p-y curves is briefly discussed in the following section.

A p-y curve represents how the soil resistance varies with the deflection of a drilled shaft at a particular depth below the ground surface. In constructing the p-y curve, the appropriate depth is chosen, then, at this depth, the value of the ultimate soil resistance is calculated for both modes of failure; wedge-type failure and flow-around failure. The lowest value of the two resistances is then used to construct the p-y curve. The shape of the actual curve is defined by equations to relate the soil resistance to lateral deflection. Often, more than one equation is used to describe the complete p-y curve. For p-y curves in clay, the curves and the point(s) where one equation ends and another equation begins are governed by a characteristic deflection, y_{50}, which is a function of the diameter of the drilled shaft, b, and a strain, ε_{50}. The strain, ε_{50}, is the axial strain in a triaxial compression test at 50 percent of the axial load at failure.

The three p-y curve criteria for clays produce curves which differ in their shapes. The p-y curves, for static loading, for the soft-clay criteria and stiff-clay-above-the-water table criteria (Figs. 2.2 and 2.3, respectively) have an increasing soil resistance with increasing deflection up to a point, beyond which the p-y curve is assumed to be horizontal. For the criteria for stiff-clay-below-the-water-table, a peak soil resistance is reached, after which the soil resistance decreases with continued deflection until a residual value is reached (Fig. 2.4). The criteria for soft-clay and stiff-clay-above-the-water-table produce curves which are nonlinear throughout

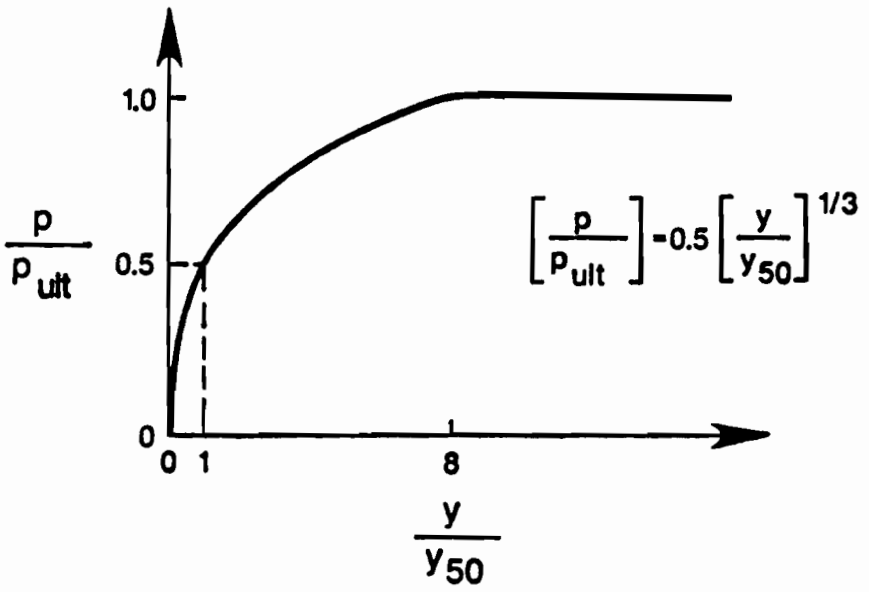

Figure 2.2: Typical p-y Curve for Soft Clay (after Reese, 1983)

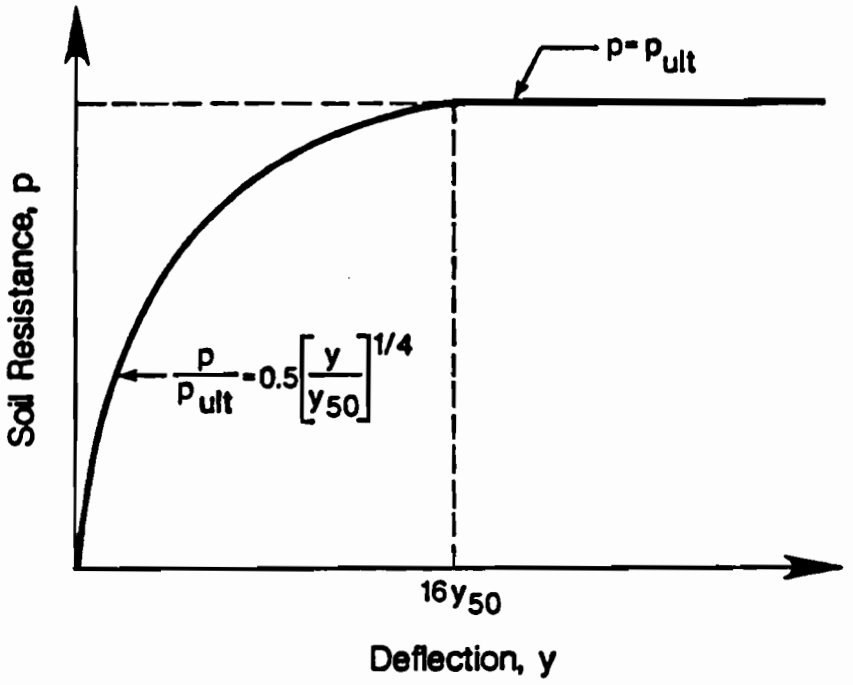

Figure 2.3: Typical p-y Curve for Stiff Clay Above the Water Table (after Reese, 1983)

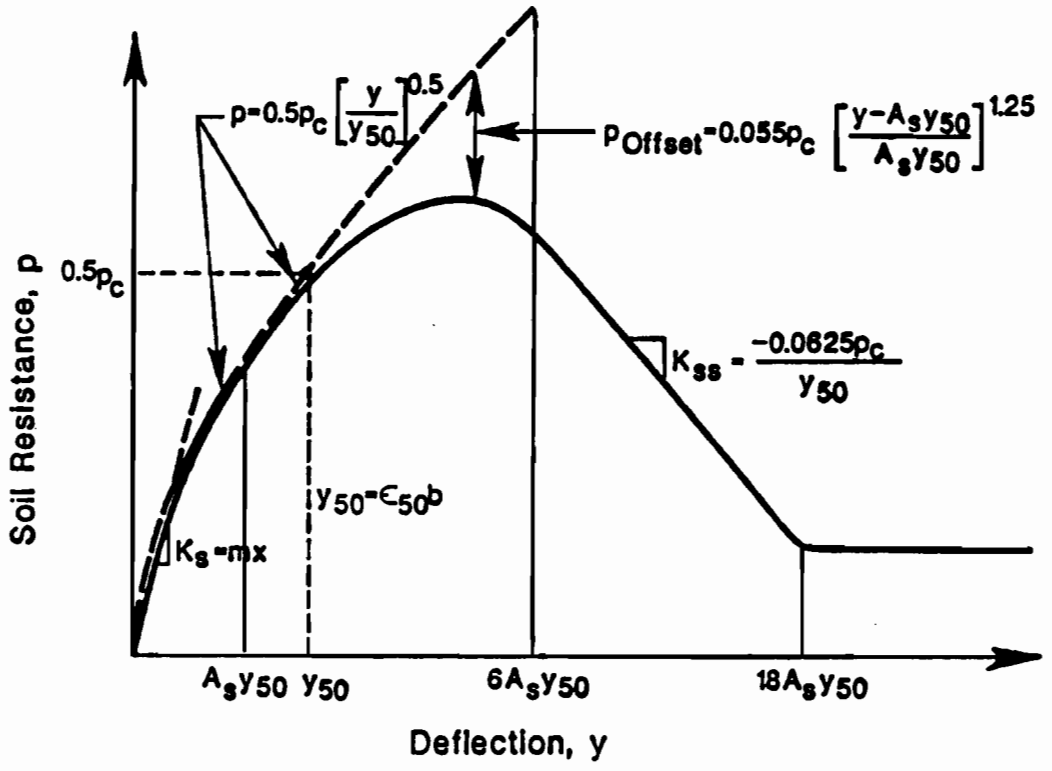

Figure 2.4: Typical p-y Curve for Stiff Clay Below the Water Table (after Reese, 1983)

the range of deflections. The criteria for stiff-clay-below-the-water table produces a p-y curve with an initial, linear portion whose slope (soil modulus) is the product of the depth and a parameter, m, which is a function of the clay's shear strength. The parameter, m, represents the variation of the soil modulus with depth.

The p-y curve criterion for sands is similar to those for clays; however, there is no characteristic deflection, y_{50}. Points which define the various portions of the curve and the transformations from one portion (equation) to another are based solely on the diameter of the drilled shaft. The p-y curves also have an initially linear portion described by the product of the depth and the soil modulus variation with depth, m. The shape of a typical p-y curve for sands is shown in Fig. 2.5.

2.3 COMPUTER PROGRAM COM624

COM624 is a computer program developed for the analysis of laterally loaded piles and drilled shafts (Reese and Sullivan, 1980). The program is used to compute the response of a laterally-loaded member using variable soil and structural properties with depth and nonlinear p-y curves. The program also has the capability either to generate p-y curves according to the four p-y curve criteria described above, or to use p-y curves supplied as input data by the user.

The number of nodal points used to describe the drilled shaft must be input by the user. The number of points should be enough to aptly describe the soil conditions along the drilled shaft and the drilled shaft's structural behavior. Pertinent input variables of the properties for the drilled shaft include the elastic modulus, moment of inertia, diameter and area. The distribution of the soil's unit weight, shear strength parameters, values of the strain, ε_{50}, and the soil modulus variation with depth, m, are also supplied by the user.

Output results include the deflection, slope, shear and moment at every nodal point used to describe the drilled shaft. The program will display error messages if data are input incorrectly or if an applied loading can not be analyzed. COM624 was used to perform the computations de scribed in the following chapters.

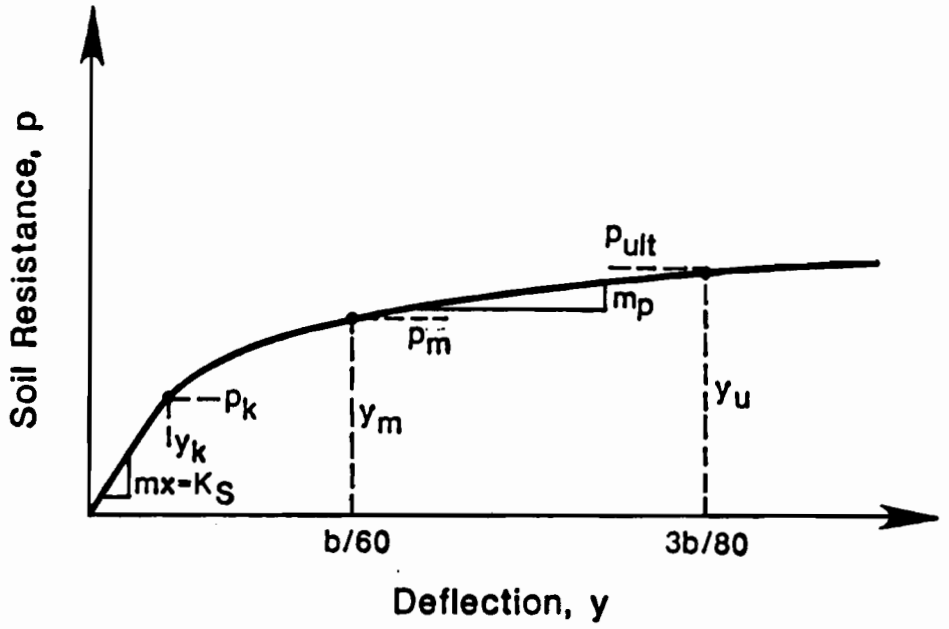

Figure 2.5: Typical p-y Curve for Sands (after Reese, 1983)

CHAPTER 3. PROCEDURES TO DETERMINE TWO POINTS OF ZERO DEFLECTION

For "long" laterally loaded drilled shafts, with two points of zero deflection, the larger, most significant deflections along the drilled shaft occur between the groundline and the first point of zero deflection as shown by curve (a) in Fig. 3.1. Although deflections occur further down the drilled shaft, they are small compared to those above the first point of zero deflection. Thus, it appears that the length of drilled shaft below the first point of zero deflection is largely ineffective in carrying the applied lateral load. However, for shorter shafts, with only a single point of zero deflection, significant deflections occur above and below the point of zero deflection as indicted by curve (b) in Fig. 3.1. In some cases, the deflections of a "short" drilled shaft become excessive and the shaft becomes unstable. Accordingly, the length of a drilled shaft should be one where at least two points of zero deflection will develop, but any additional length can be considered unnecessary. In addition, a reduction of both time and cost in the design and construction of laterally loaded drilled shafts would be possible if the length of a drilled shaft required to achieve two points of zero deflection could be calculated quickly and easily. In this chapter, various procedures for determining the length of shaft required to achieve two points of zero deflection are examined. In addition, a simplied procedure for estimating the minimum length of drilled shaft required to achieve two points of zero deflection is presented for the case where the soil modulus varies nonlinearly with depth and deflection.

3.1 PREDICTING TWO POINTS OF ZERO DEFLECTION

Three different cases are examined for determining the length of shaft required to achieve two points of zero deflection. These cases are distinguished by the characterization of the soil modulus: constant modulus, linear variation in modulus with depth and arbitrary variation in modulus with depth (Fig. 3.2). For all cases, a lateral force was assumed to be applied to the top of the shaft and the top was assumed to be free to rotate. In the

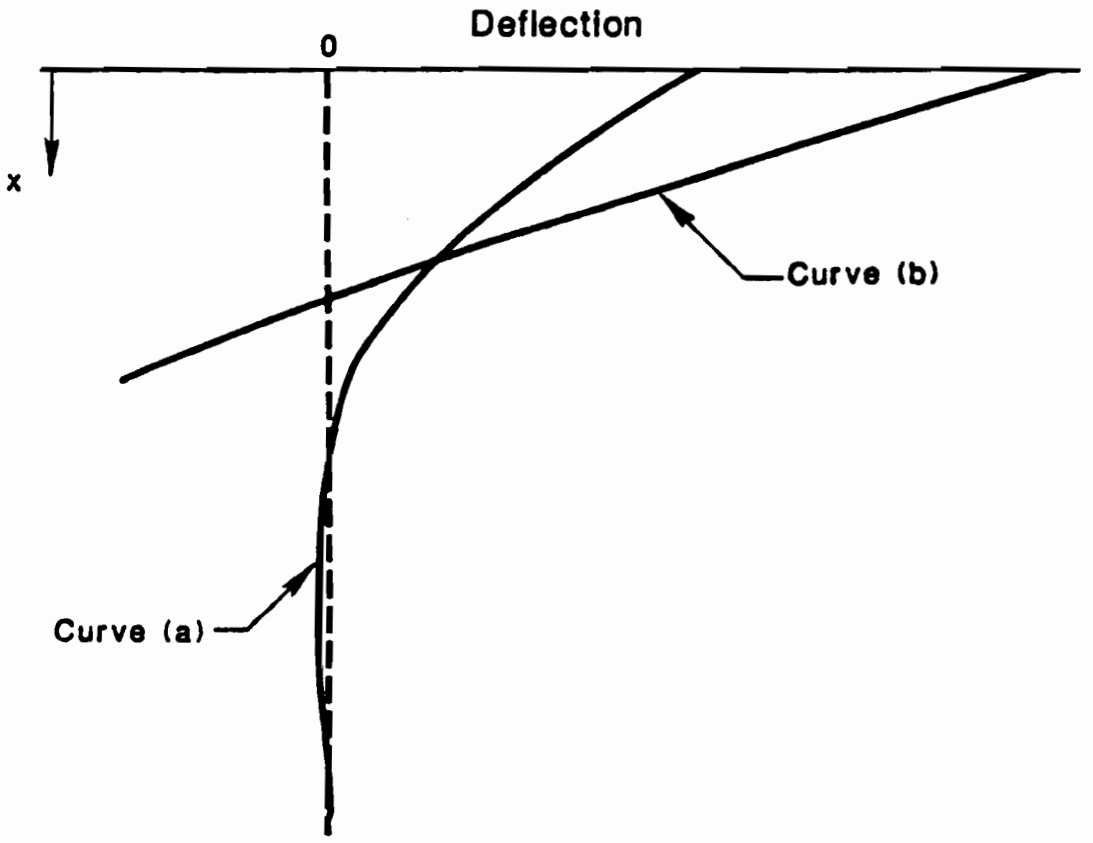

Figure 3.1: Deflected Shapes of Drilled Shafts and Piles

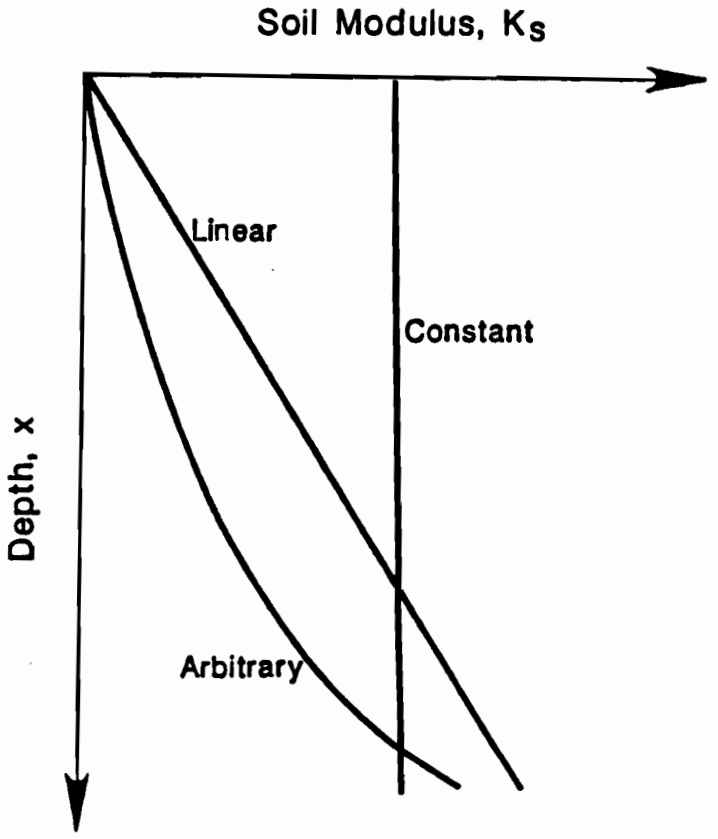

Figure 3.2: Forms of Soil Moduli with Depth

following sections, the minimum length of drilled shaft required to achieve two points of zero deflection is designated L_e.

The length, L_e, is determined based on the assumption that the base of the shaft will experience no shear or moment. This assumption is still valid for a shaft with length, L_e because movements of the shaft at or be low the second point of zero deflection are small; thus, only negligible amounts of shear and moment are developed at the second point of zero deflection (the base of a shaft with length L_e).

The simplest case, that of a constant soil modulus, has been studied by Timoshenko (1941) and Hetenyi (1946). It has been found that the minimum length of drilled shaft required to achieve two points of zero deflection, L_e, can be expressed as

$$L_e = 4.8/\beta \tag{3.1}$$

where β is termed the "relative stiffness factor", with the units of the inverse of length. The relative stiffness factor is defined by

$$\beta = [K_s/4E_pI_p]^{0.25} \tag{3.2}$$

where K_s is the soil modulus and E_pI_p is the structural stiffness of the shaft. The "relative stiffness factor" relates the stiffness of the soil (soil modulus) to the stiffness of the drilled shaft (structural stiffness).

3.2 LINEAR SOIL MODULUS WITH DEPTH

For many soils, the soil modulus can be considered to vary linearly with depth (Fig. 3.3). The rate of increase in the soil modulus with depth is designated by the parameter, m, and the soil modulus at any depth can be expressed as

$$K_s = mx \tag{3.3}$$

Matlock and Reese (1962) performed non-dimensional analyses, in conjunction with a finite difference solution, to develop a solution for the

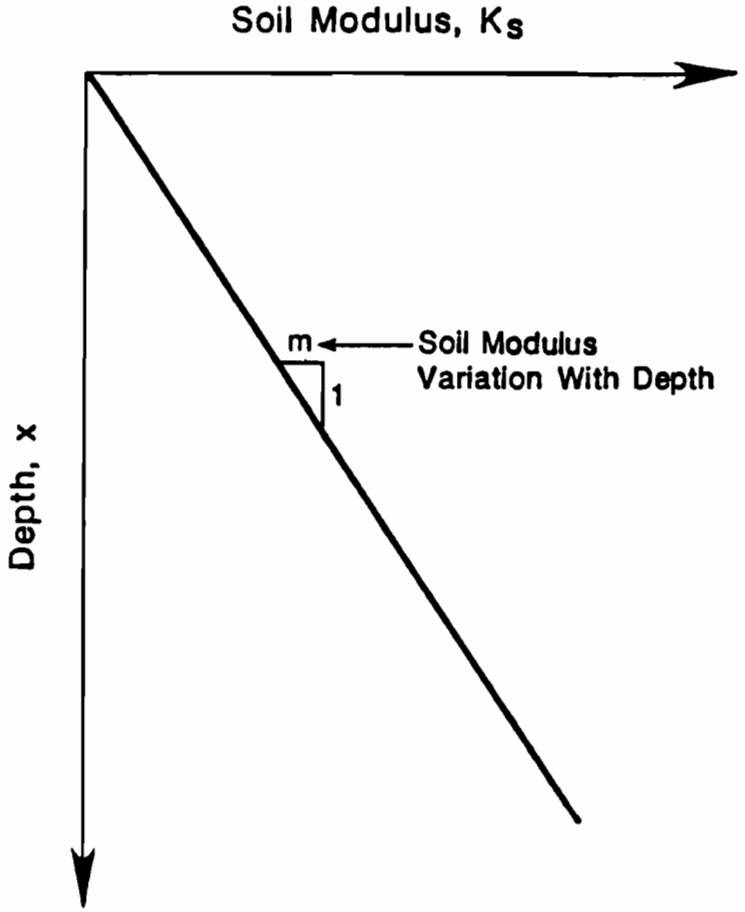

Figure 3.3: Linear Soil Modulus with Depth

response of a drilled shaft where the soil modulus varies linearly with depth. They considered the deflections, y, along the shaft to be a function of the following variables:

- x - depth
- L - length of shaft
- K_s - soil modulus
- E_pI_p - structural stiffness of shaft
- P_t - lateral load
- T - a dimensional quantity which can also be termed a "relative stiffness factor", having units of length and calculated, for a linear soil modulus, as

$$T = [E_pI_p/m]^{0.2} \tag{3.4}$$

For a drilled shaft which is free to rotate and loaded by a lateral force applied at the groundline, the deflection at any point along the embedded length of the shaft can be expressed as

$$y = A_y \frac{P_t T^3}{E_pI_p} \tag{3.5}$$

where P_t is the applied lateral force, E_pI_p is the structural stiffness of the shaft, T is the aforementioned dimensional quantity and A_y is a dimensionless coefficient. The value of A_y is a function of the non-dimensional depth coefficient, Z, expressed as

$$Z = x/T \tag{3.6}$$

The maximum depth coefficient, Z_{max}, corresponds to the total length of the shaft such that

$$Z_{max} = L/T \tag{3.7}$$

Values of A_y versus the depth coefficient are plotted in Fig. 3.4. The smallest depth coefficient where two points of zero deflection occurs is 4.8.

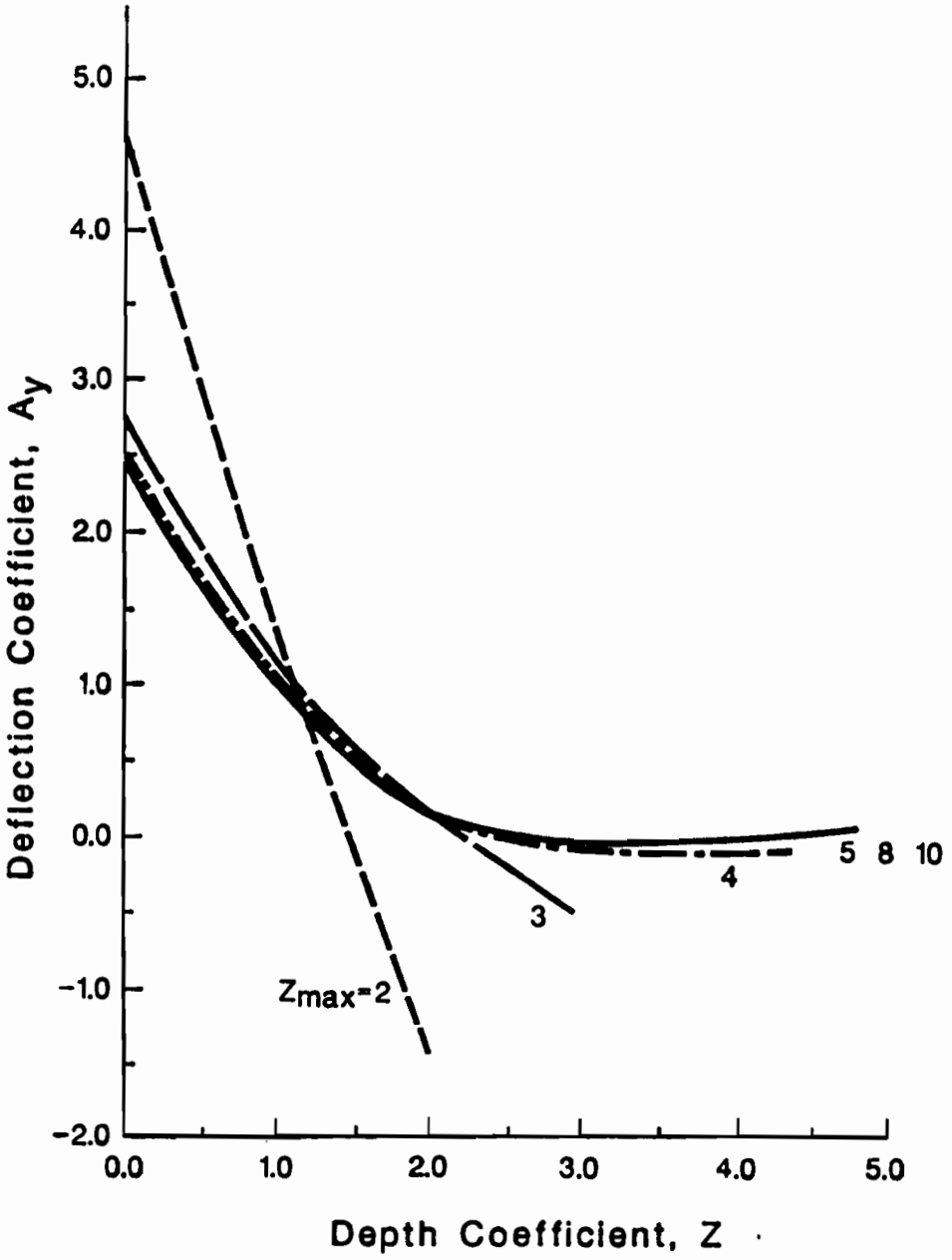

Figure 3.4: Values of A_y for Shafts of Various Maximum Depth Coefficients (after Reese, 1983)

Thus, the minimum length of shaft required to achieve two points of zero deflection (L_e) can be expressed as

$$L_e = 4.8\ T \tag{3.8}$$

3.3 NON-LINEAR SOIL MODULUS WITH DEPTH

The third case to be considered examines a soil modulus which varies nonlinearly with the deflection of the shaft and, consequently, varies nonlinearly (arbitrarily) with depth. The minimum length of shaft required to achieve two points of zero deflection can be obtained by trial-and-error using nonlinear p-y curves and the existing procedures of analysis. However, this process can become tedious; thus, creating the need for a simpler procedure which will estimate the length, L_e. Parametric studies were performed in order to establish such a simplified procedure for estimating the minimum length of shaft required to achieve two points of zero deflection. Computations with a variety of soil and drilled shaft properties were performed, using the nonlinear p-y criteria employed by COM624. The results of these computations were then examined to determine if simple relationships could be established between soil and shaft properties and the length, L_e.

3.3.1 Development of Simplified Procedure

In the past, favorable results have been obtained for drilled shafts which were analyzed using solutions developed for a linear soil modulus (Reese and Matlock, 1956 and McClelland and Focht, 1958). Therefore, it may be possible to develop the simplified procedure for the case of a non linear soil modulus by adapting the form of the procedure for the linear soil modulus (Section 3.2). For the parametric studies, two p-y curve criteria were used: the criterion for stiff-clay-below-the-water-table and the criterion for sands. These two criteria were selected because their p-y curves produce soil moduli which, with small deflections, vary linearly with depth; then, as deflection increases, vary nonlinearly with depth. A basis is now provided for correlating analyses with nonlinear soil moduli to analyses with linear soil moduli.

The soil and drilled shaft parameters used in the parametric studies are presented in Tables 3.1 and 3.2, respectively. Sets of all possible combinations of the various soil and shaft parameters were formed, and, for each set of parameters, computations were performed for a wide range in lateral forces, P_t. The length of the shaft was varied, under each lateral load, until the minimum length required to achieve two points of zero deflection was found.

3.3.2 Computation of "Equivalent" Factors

Once the minimum length of shaft required to achieve two points of zero deflection was determined, a set of "equivalent" quantities were calculated so that the length determined in nonlinear, p-y curve analyses would be the same as the length calculated using a linear soil modulus (Section 3.2). This was accomplished by determining equivalent soil moduli which translated the soil moduli developed in nonlinear p-y curve analyses into ones which varied linearly with depth (Fig. 3.5). Accordingly, the equivalent linear moduli can be expressed in terms of the parameter, m, discussed earlier, which represents the rate of increase in moduli with depth. In the case of equivalent moduli, the parameter, m, has been designated m'. The equivalent variation of the moduli with depth, m', were calculated by first calculating an equivalent value of the dimensional quantity, T, which was also discussed earlier. The equivalent value for T was termed T'. By rearranging Eq. 3.8, the following expression can be written for T':

$$T' = L_e/4.8 \tag{3.9}$$

where L_e is the length determined from the nonlinear p-y curve analyses. Once the equivalent quantity T' was calculated, a corresponding value for m' was calculated by rearranging Eq. 3.4 to give,

$$m' = E_p I_p / T'^5 \tag{3.10}$$

The values of the m' and T' for the lengths, L_e, found in the nonlinear p-y curve analyses are presented in Appendix A.

Table 3.1

Soil Parameters For Stiff Clay

Below the Water Table

Medium Stiff Clay	Very Stiff Clay
$\gamma = 110$ lb/ft^3	$\gamma = 110$ lb/ft^3
$\gamma_w = 62.4$ lb/ft^3	$\gamma_w = 62.4$ lb/ft^3
$s_u = 1500$ lb/ft^2	$s_u = 6000$ lb/ft^2
$\phi = 0$	$\phi = 0$
$\varepsilon_{50} = 0.007$	$\varepsilon_{50} = 0.004$
$m = 500$ lb/in^3	$m = 2000$ lb/in^3

Soil Parameters For Sand

Loose Sand	Medium Dense Sand
$\gamma = 120$ lb/ft^3	$\gamma = 120$ lb/ft^3
$\gamma_w = 62.4$ lb/ft^3	$\gamma_w = 62.4$ lb/ft^3
$c = 0$	$c = 0$
$\phi = 30$ deg.	$\phi = 38$ deg.
$m = 20$ lb/in^3	$m = 60$ lb/in^3

Very Dense Sand

$\gamma = 120$ lb/ft^3

$\gamma_w = 62.4$ lb/ft^3

$c = 0$

$\phi = 45$ deg.

$m = 125$ lb/in^3

Table 3.2
Drilled Shaft Dimensions and Properties

Shaft Diameter (in)	Structural Stiffness $E_p I_p$ ($lb\text{-}in^2$)
12	3.67×10^9
30	1.43×10^{11}
48	9.40×10^{11}
60	2.29×10^{12}

Table 3.3
Results for Analyses in Stiff Clay

Medium Stiff Clay m = 500 lb/in^3

Diameter (in)	Length (in)	Deflection y_t (in)	Lateral Force ($\times 10^3$ lb)
12	114	0.0730	7.5
12	117	0.116	10
12	143	0.575	20
30	236	0.028	13.5
30	242	0.0486	20
30	250	0.0867	30
30	270	0.193	50
30	300	0.401	75
30	322	0.738	100
48	344	0.00952	10
48	345	0.0202	20
48	353	0.0348	30
48	373	0.0721	50
48	393	0.131	75
48	413	0.205	100
48	449	0.401	150

Table 3.3 (cont.)

Medium Stiff Clay m = 500 lb/in^3

Diameter (in)	Length (in)	Deflection y_t (in)	Lateral Force ($\times 10^3$ lb)
60	410	0.0152	22
60	415	0.0228	30
60	430	0.0465	50
60	455	0.0837	75
60	475	0.128	100
60	515	0.239	150

Very Stiff Clay m = 2000 lb/in^3

12	86	0.0987	23
12	89	0.168	30
12	91	0.248	35
12	95	0.375	40
30	179	0.0602	65
30	185	0.113	100
30	195	0.241	150
30	209	0.462	200
30	231	0.919	250
48	260	0.0382	89
48	263	0.0443	100
48	275	0.117	200
48	290	0.233	300
48	308	0.416	400

Table 3.3 (cont.)

Very Stiff Clay $m = 2000$ lb/in^3

Diameter (in)	Length (in)	Deflection y_t (in)	Lateral Force ($\times 10^3$ lb)
60	312	0.0353	115
60	325	0.0746	200
60	335	0.136	300
60	350	0.218	400
60	367	0.329	500
60	383	0.477	600

Table 3.4
Results for Analyses in Sand

Loose Sand m = 20 lb/in^3

Diameter (in)	Length (in)	Deflection y_t (in)	Lateral Force ($\times 10^3$ lb)
12	216	0.191	3
12	228	1.06	10
12	250	5.31	25
12	285	20.9	50
30	449	0.576	38
30	460	0.873	50
30	480	1.58	75
30	480	2.44	100
48	654	1.02	140
48	660	1.13	150
48	680	1.76	200
48	680	2.45	250
60	782	1.35	262
60	790	1.67	300
60	800	2.12	350
60	810	2.59	400

Table 3.4 cont.

Medium Dense Sand m = 60 lb/in^3

Diameter (in)	Length (in)	Deflection y_t (in)	Lateral Force ($\times 10^3$ lb)
12	173	0.0798	2.5
12	190	0.616	10
12	205	2.73	25
12	229	10.4	50
30	360	0.304	38
30	373	0.472	50
30	385	0.904	75
30	400	1.39	100
30	412	2.63	150
30	425	4.29	200
30	450	9.11	300
48	525	0.541	140
48	530	0.600	150
48	545	0.924	200
48	570	1.84	300
48	585	2.86	400
60	627	0.676	250
60	638	0.890	300
60	665	1.74	450
60	690	2.72	600

Table 3.4 cont.

Very Dense Sand m = 125 lb/in^3

Diameter (in)	Length (in)	Deflection y_t (in)	Lateral Force ($\times 10^3$ lb)
12	150	0.0625	3
12	163	0.381	10
12	175	1.56	25
12	191	5.59	50
12	214	18.2	100
30	311	0.189	38
30	314	0.271	50
30	340	0.833	100
30	359	2.47	200
30	375	5.01	300
48	453	0.336	140
48	460	0.550	200
48	489	1.38	350
48	505	2.42	500
48	525	3.70	650
60	550	0.536	300
60	560	0.990	450
60	580	1.60	600
60	600	2.29	750
60	605	3.05	900

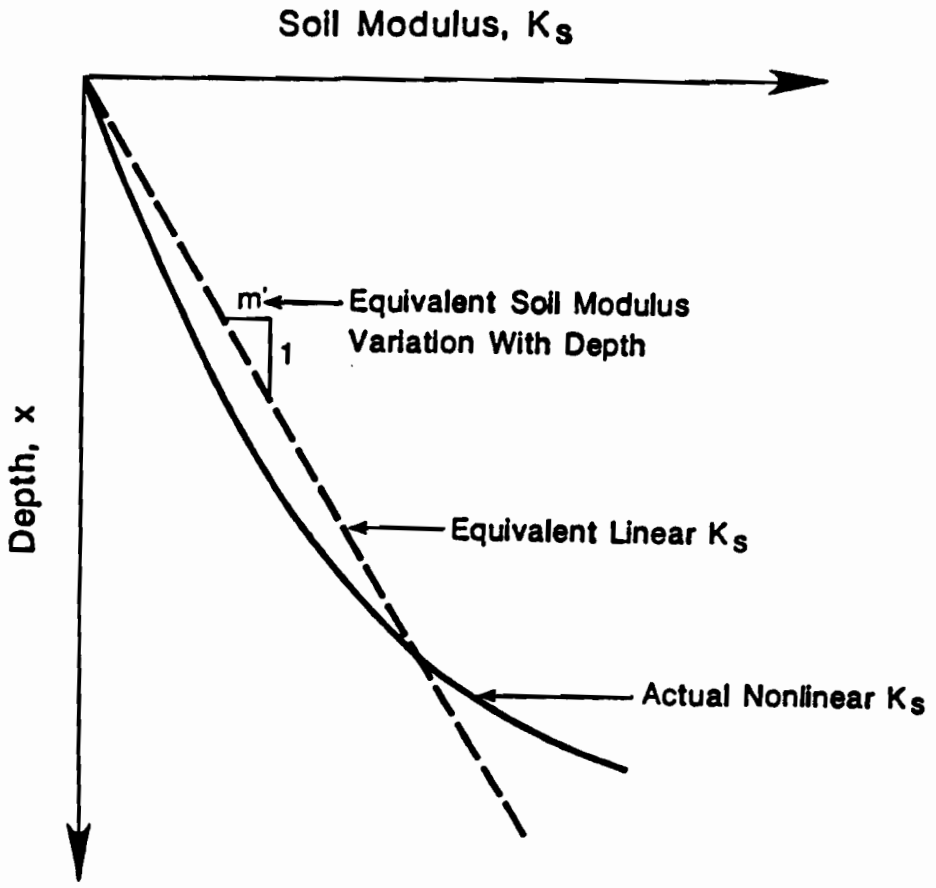

Figure 3.5: Formation of Equivalent Soil Modulus from Nonlinear Soil Modulus

The final step in relating the results of analyses using nonlinear p-y curves to analyses using the procedure for linear moduli involved comparing equivalent variations in the modulus with depth, m', to variations in moduli with depth, m, used to describe the initial, linear portion of the p-y curves. As noted earlier, the p-y curve criteria selected for these studies produced p-y curves with initial, linear portions. For these curves, when the loads are very small, the soil modulus is linear, and there is no difference between the equivalent variation in modulus with depth (m') and the variation in the initial modulus with depth (m). However, as the loads increase, the equivalent variation in modulus with depth becomes smaller than the variation in the initial modulus with depth. That is, the soil modulus is no longer linear but can be represented by an equivalent modulus. The degree of nonlinearity between the initial and equivalent moduli can be expressed as a non dimensional ratio, m'/m_i, where m_i represents the variation in initial modulus with depth. As deflection of the shaft increases and the soil modulus becomes more nonlinear, the ratio, m'/m_i, becomes smaller (lesser than unity). The degree of nonlinearity can also be approximately expressed by the non-dimensional ratio of the deflection of the top of the shaft to the diameter of the shaft, y_t/D. This ratio (y_t/D) was chosen for correlation with the ratio, m'/m_i. Values of the these two ratios for the analyses are presented in Appendix A.

3.3.3 Statistical Analysis on Non-Dimensional Ratios

Linear regression analyses were performed to define a relationship between m'/m_i and y_t/D ratios from the results of the analyses for each of the two p-y curve criteria. For the regression analyses, deflections (y_t) in excess of 10 percent of the shaft diameter ($y_t/D > 0.1$) were considered excessive; thus, these data were excluded from the regression analyses. Data where the ratio m'/m_i was unity corresponded to linear conditions where the procedure for the linear soil modulus (Section 3.2) could be used directly; therefore, these data were also excluded.

For the acceptable data from the analyses in stiff clay, shown in Fig. 3.6, the regression line can be represented by the expression

$$m'/m_i = 0.692\ [9.946\ (y_t/D)] \qquad (3.11)$$

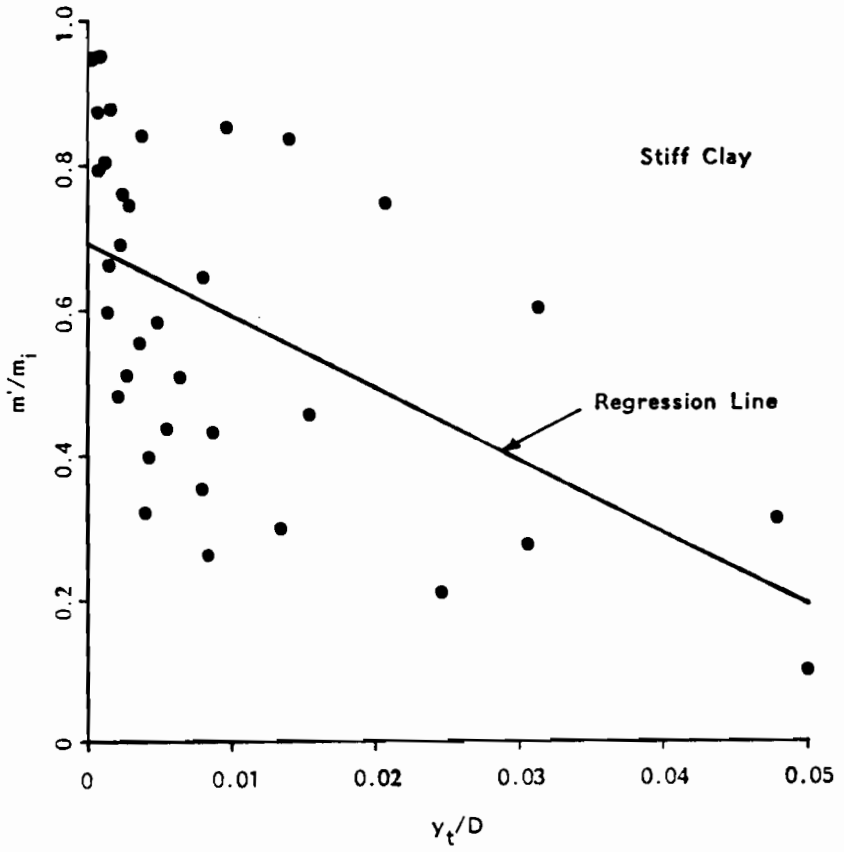

Figure 3.6: Plot of y_t/D versus m/m_i for Stiff Clay with Regression Line

This expression is limited to y_t/D values less than 0.073. Values of y_t/D greater than 0.073 produce negative and, thus, useless values of m'/m_i. The regression line for the acceptable data from the analyses in sands (Fig. 3.7), can be expressed as

$$m'/m_i = 0.932\ [4.708\ (y_t/D)] \tag{3.12}$$

Equation 3.12 is valid for values of y_t/D less than 0.10; the limiting value used to exclude excessive deflections from the regression analyses.

3.3.4 Application of Simplified Procedure

Based on the parametric studies and the correlations described above, the following procedure can now be stated for determining the minimum length of shaft required to achieve two points of zero deflection. First, a diameter of drilled shaft, D, and value of initial soil modulus variation with depth, m_i, must be chosen. A value of the deflection at the top of the shaft, y_t, that is acceptable for design, also must be estimated. This top of shaft deflection is then divided by the diameter of the drilled shaft to compute a value of y_t/D. The deflection chosen for design must be less than 7.3 percent of the shaft's diameter ($y_t/D < 0.073$) for a stiff clay of less than 10 percent of the shaft's diameter ($y_t/D < 0.1$) for a sand to use the suggested procedure. A value of the ratio, m'/m_i, now can be determined using the appropriate regression equation. From this value, an equivalent soil modulus variation with depth, m', can be calculated. The drilled shaft's structural stiffness, E_pI_p, is calculated, and, along with the value of the equivalent soil modulus variation with depth, a value of the dimensional quantity, T', can be calculated base on Eq. 3.4 written in the form,

$$T' = [E_pI_p/m']^{0.2} \tag{3.13}$$

Finally, the value of the dimensional quantity can be used in Eq. 3.8 to calculate the length of drilled shaft required to achieve two points of zero deflection:

$$L_e = 4.8\ T' \tag{3.14}$$

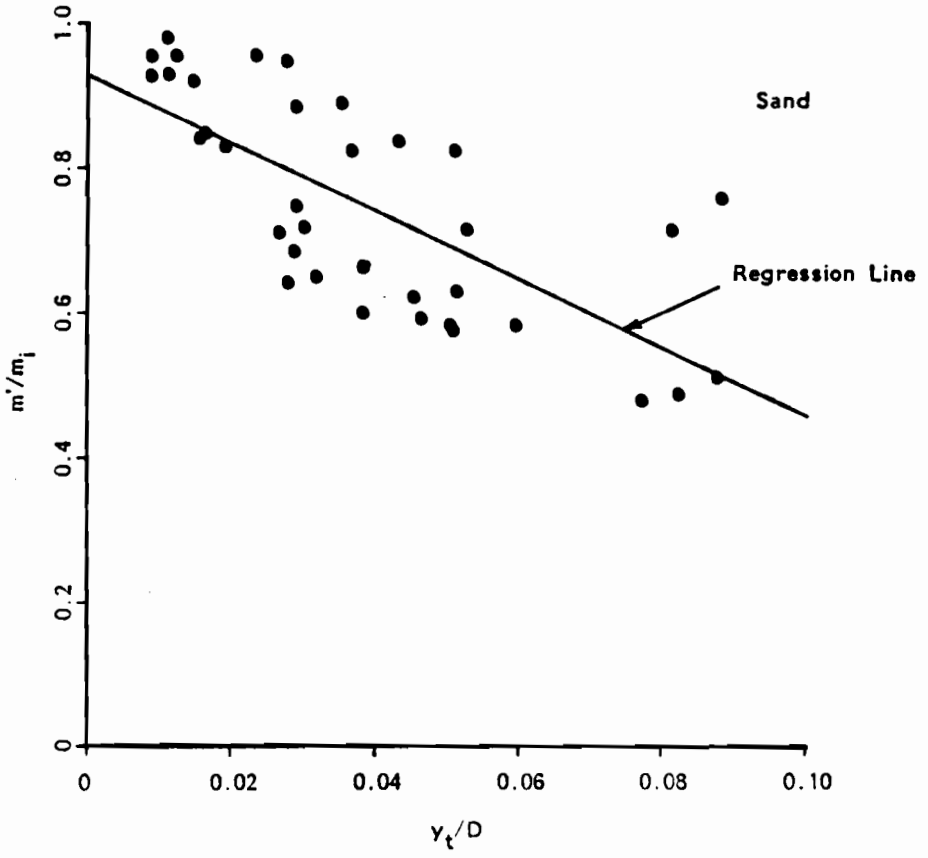

Figure 3.7: Plot of y_t/D versus m/m_i for Sand with Regression Line

3.3.5 Verification of the Simplified Procedure

Values of the length of drilled shaft required to achieve two points of zero deflection (L_e) were computed using the simplified procedures for comparison with the lengths calculated previously by the rigorous trial-and-error analyses employing COM624 and nonlinear p-y criteria. The lengths calculated using the simplified procedure and COM624 are presented in Table 3.5 for the analyses in stiff clay and in Table 3.6 for the analyses in sand. The two computed lengths are also compared for the stiff clay and sand in Figs. 3.8 and 3.9, respectively.

For drilled shafts in stiff clay, the lengths, L_e, calculated from the simplified procedure ranged from 85 per cent to 110 percent of the lengths computed by COM624. In addition, the average of the ratios of the simplified procedure-to-COM624 lengths, also presented in Table 3.5, was 0.99; the standard deviation was 0.07. For drilled shafts in sand, lengths, L_e, calculated from the simplified procedure ranged from 95 percent to 108 percent of the values computed by COM624. The average of the ratios of simplified-to-COM624 lengths for sand was 1.00; the standard deviation was 0.03. In general, the results from the simplified procedure are in excellent agreement with the results obtained from the rigorous analyses using COM624.

As further verification of the simplified procedure, eight sets of soil and drilled shaft parameters were selected in addition to those used to develop the simplified procedure. Four of these cases considered were for stiff clay and four were for sand. The drilled shaft and soil parameters used for these additional analyses are presented in Table 3.7. The values of the length of drilled shaft required to achieve two points of zero deflection computed using COM624 and the simplified procedure are presented in Table 3.8. Comparison between the lengths (Fig. 3.10) again demonstrates that the simplified procedure provides an excellent estimate of the length of drilled shaft required to achieve two points of zero deflection.

3.4 SUMMARY AND ADDITIONAL RESEARCH

The simplified procedure, developed for the p-y curve criteria for stiff-clay-below-the-water-table and sand, can aid in reducing both time and cost in the construction of laterally loaded drilled shafts. Though the

Table 3.5
Results From Analyses in Stiff Clay

Length of Drilled Shaft Required to Achieve Two Points of Zero Deflection COM624 and Simplified Procedure

Medium Stiff Clay m = 500 lb/in^3

Diameter (in)	L_e from COM624 (in)	L_e from Simp. Proc. (in)	Ratio of L_e Simp. Proc. to COM624
12	117	125.7	1.07
12	143	154.1	1.08
30	242	255.1	1.05
30	250	256.1	1.02
30	270	258.9	0.96
30	300	265.0	0.88
30	322	277.1	0.86
48	345	370.3	1.07
48	353	370.6	1.05
48	373	371.4	1.00
48	393	372.8	0.95
48	413	374.5	0.91
48	449	379.4	0.85
60	415	442.6	1.07
60	430	443.1	1.03
60	455	443.9	0.98
60	475	444.9	0.94
60	515	447.3	0.87

Table 3.5 cont.

Very Stiff Clay m = 2000 lb/in^3

Diameter (in)	L_e from COM624 (in)	L_e from Simp. Proc. (in)	Ratio of L_e Simp. Proc. to COM624
12	89	96.7	1.09
12	91	99.2	1.09
12	95	104.2	1.10
30	185	194.6	1.05
30	195	197.2	1.01
30	209	202.3	0.97
30	231	216.1	0.94
48	263	281.0	1.07
48	275	282.3	1.03
48	290	284.4	0.98
48	308	287.8	0.93
60	325	336.3	1.03
60	335	337.3	1.01
60	350	338.7	0.97
60	367	340.6	0.93
60	383	343.3	0.90

Table 3.6
Results From Analyses in Sand

Length of Drilled Shaft Required to Achieve
Two Points of Zero Deflection
COM624 and Simplified Procedure

Loose Sand m = 20 lb/in^3

Diameter (in)	L_e from COM624 (in)	L_e from Simp. Proc. (in)	Ratio of L_e Simp. Proc. to COM624
12	228	246.2	1.08
30	460	470.1	1.02
30	480	484.4	1.01
30	480	506.2	1.05
48	660	680.3	1.03
48	680	691.0	1.02
48	680	704.0	1.04
60	790	817.3	1.03
60	800	824.7	1.03
60	810	832.8	1.03

Table 3.6 cont.

Medium Dense Sand m = 60 lb/in^3

Diameter (in)	L_e from COM624 (in)	L_e from Simp. Proc. (in)	Ratio of L_e Simp. Proc. to COM624
12	190	186.5	0.98
30	373	371.7	1.00
30	385	377.8	0.98
30	400	385.6	0.96
30	412	410.9	1.00
48	530	539.4	1.02
48	545	543.4	1.00
48	570	555.8	0.98
48	585	571.9	0.98
60	627	644.0	1.03
60	638	646.5	1.01
60	665	657.0	0.99
60	690	670.4	0.97

Table 3.6 cont.

Very Dense Sand m = 125 lb/in^3

Diameter (in)	L_e from COM624 (in)	L_e from Simp. Proc. (in)	Ratio of L_e Simp. Proc. to COM624
12	163	157.0	0.96
30	314	318.6	1.01
30	340	325.3	0.96
30	359	351.5	0.98
48	460	465.2	1.01
48	489	474.4	0.97
48	505	487.6	0.97
48	525	507.4	0.97
60	550	555.1	1.01
60	560	559.2	1.00
60	580	565.7	0.98
60	600	573.6	0.96
60	605	583.2	0.96

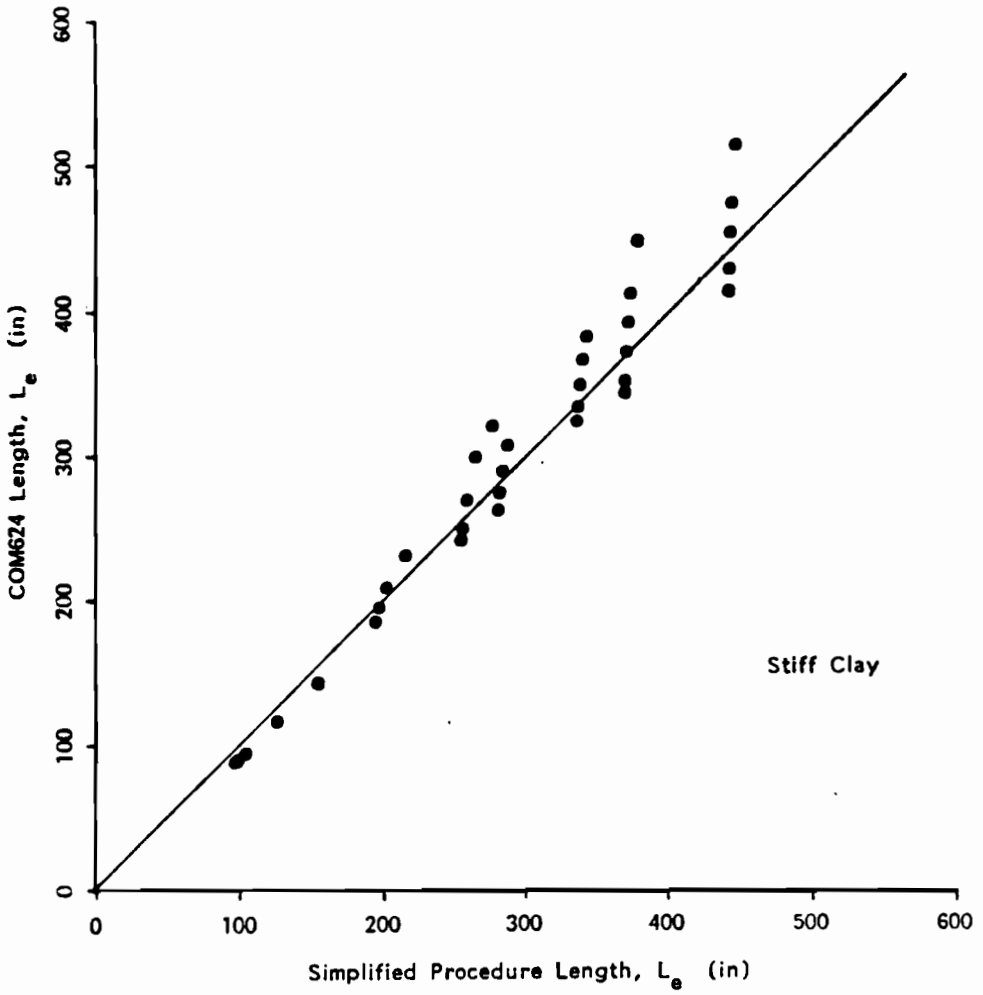

Figure 3.8: Simplified Procedures versus COM624 Lengths, L_e, for Stiff Clay

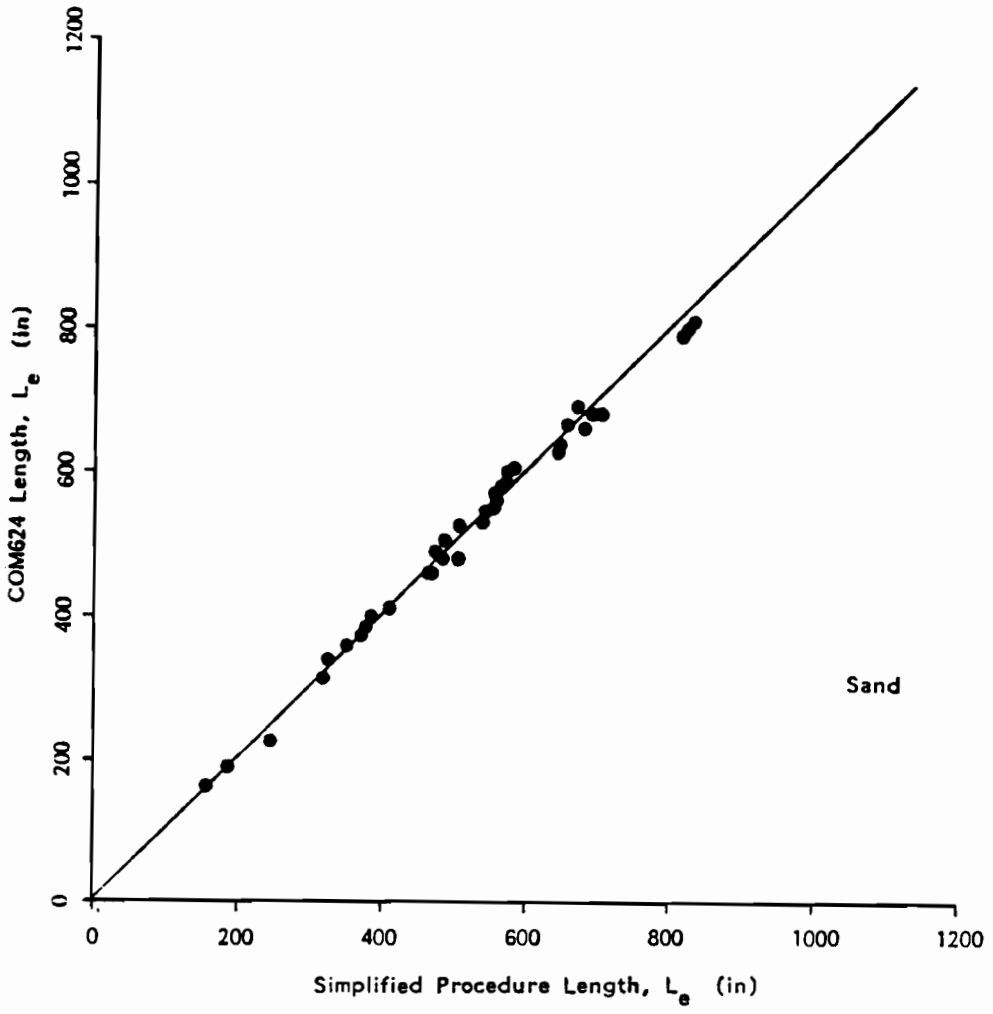

Figure 3.9: Simplified Procedures versus COM624 Lengths, L_e, for Sand

Table 3.7
Soil and Drilled Shaft Parameters Used
In Additional Analyses

Soil Parameters

Stiff Clay	Slightly Dense Sand
γ = 110 lb/ft^3	γ = 120 lb/ft^3
γ_w = 62.4 lb/ft^3	γ_w = 62.4 lb/ft^3
c = 3000 lb/ft^2	c = 0
ϕ = 0 deg.	ϕ = 34 deg.
m = 1000 lb/in^3	m = 40 lb/in^3
ε_{50} = 0.005	

Drilled Shaft Dimensions and Properties

Shaft Diameter (in)	Structural Stiffness $E_p I_p$ (lb-in^2)
24	5.87×10^{10}
36	2.97×10^{11}

Table 3.8
Results From Additional Analyses

Length of Drilled Shaft Required to Achieve
Two Points of Zero Deflection
COM624 and Simplified Procedure

Stiff Clay m = 1000 lb/in^3

Diameter (in)	L_e from COM624 (in)	L_e from Simp. Proc. (in)	Ratio of L_e Simp. Proc. to COM624
24	190	191.3	1.01
24	218	202.2	0.93
36	250	257.7	1.03
36	265	259.3	0.98

Slightly Dense Sand m = 40 lb/in^3

Diameter (in)	L_e from COM624 (in)	L_e from Simp. Proc. (in)	Ratio of L_e Simp. Proc. to COM624
24	350	345.7	0.99
24	360	352.1	0.98
36	470	467.0	0.99
36	485	482.6	1.00

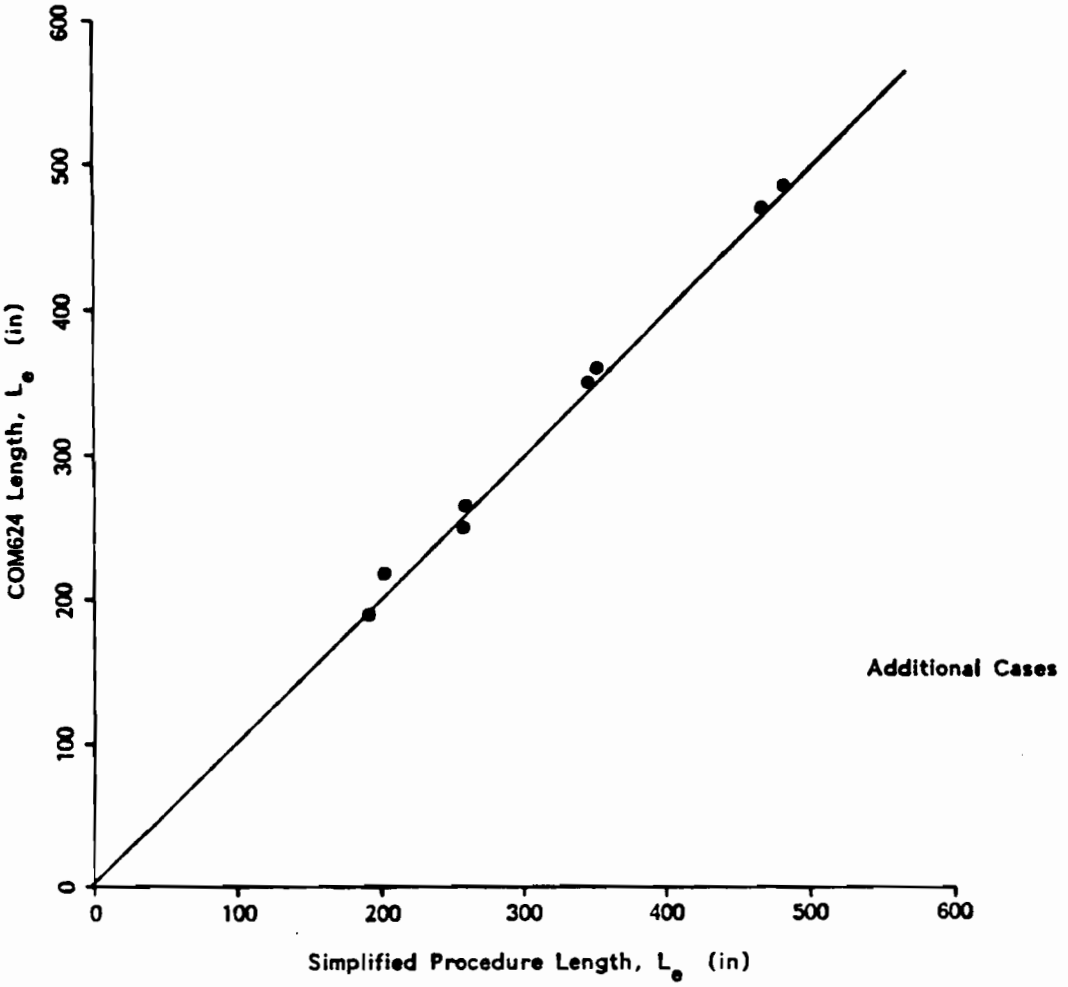

Figure 3.10: Simplified Procedures versus COM624 Lengths, L_e, for Additional Cases

simplified procedure is useful, it does not cover all soil or drilled shaft parameters possible for use in design. Additional research is needed to include other soil conditions and p-y criteria. In the case of other criteria, the p-y curves do not have initial, linear portions. Accordingly, relating the results obtained from analyses using such nonlinear p-y criteria to results of analyses using the procedure for the linear soil modulus may be somewhat more difficult.

CHAPTER 4. TEST DATA ON SHORT DRILLED SHAFTS

In the previous chapter, a simplified procedure to determine the length of drilled shaft required to achieve two points of zero deflection was developed. There are cases, however, where drilled shafts will be utilized which will have only a single point of zero deflection. For such "short" drilled shafts the conventional analytical procedures, used by COM624, have been found to be inadequate. In order to examine the behavior of "short" drilled shafts, data from a series of load tests, conducted under the auspices of the Electric Power Research Institute, EPRI, on "short" drilled shafts were examined. The load tests are described and the data are briefly reviewed in this chapter.

4.1 TEST DESCRIPTION

Data from the load tests were presented in a report by the Electric Power Research Institute (1982). The various tests were sponsored by a number of electric power companies and organizations (Table 4.1) and performed at various sites within the United States (Fig. 4.1). Although fourteen drilled shafts are shown in Table 4.1 as originally being tested, adequate data were available on only thirteen. Shaft No. 3 was not analyzed because of insufficient data.

4.1.1 Shaft Descriptions

The drilled shafts were cast-in-place concrete with lengths ranging from 155.0 to 264.0 in, diameters ranging from 54.0 to 78.0 in and flexural stiffnesses, E_pI_p, ranging from 1.37×10^{12} to 6.13×10^{12} lb-in^2. The distance between the top of the drilled shafts and the groundline ranged from nine to fourteen inches. The drilled shafts were tested at sites where the soil profiles consisted of various layers of sands, clays, silts, gravels and rock. The dimensions and properties of the drilled shafts are summarized in Table 4.2 along with the general soil profile at each testing site. The drilled shafts were structurally designed to have a moment capacity of at least

Table 4.1
Drilled Shaft Information
Sponsor and Site Location

Shaft No.	Sponsor	Test Site Location
1	Electric Power Research Institute	Springdale Township, PA
2	Virginia Electric and Power Company	12 miles west of Richmond, Virginia
3	Allegheny Power System	30 miles southwest of Greenburg, PA
4	Jersey Central Power and Light Company	10 miles east of Heightstown, NJ
5	Baltimore Gas and Electric Company	6 miles north-east of Baltimore ML
6	Carolina Power and Light Company	Southwest of Kinston, NC
7	Oklahoma Gas and Electric Company	Oklahoma City, OK
8	Union Electric Company	East of St. Charles, MO

Table 4.1 (cont.)

Shaft No.	Sponsor	Test Site Location
9	Dayton Power and Light Company	4 miles north-east of Farmerville,OH
10	Arizona Power Service Company	10 miles north-east of Phoenix,AZ
11	Southern California Edison Company	Garden Grove, CA
12	Utah Power and Light Company	Southwest of Salt Lake City, UT
13	Bonneville Power Administration	12 miles west of Portland,OR
14	Iowa Public Service Company Nebraska Public Power District Omaha Public Power District	West of Omaha,NE

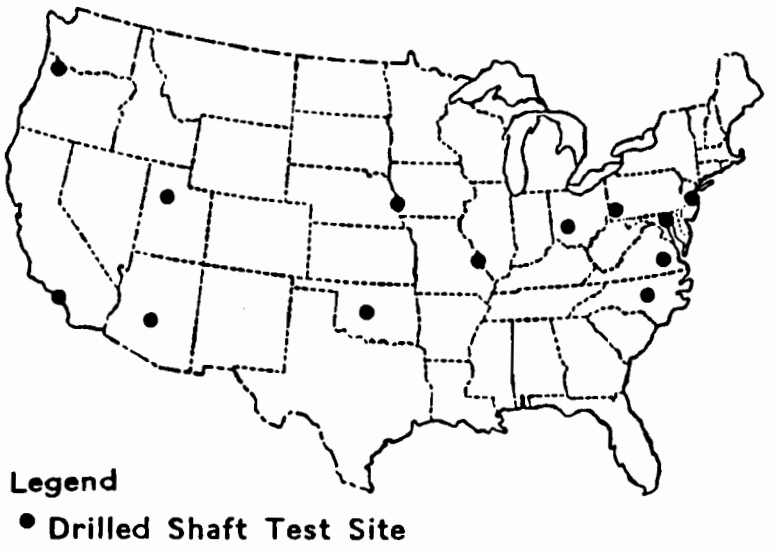

Figure 4.1: Location of EPRI Drilled Shafts (after EPRI, 1982)

Table 4.2
EPRI Drilled Shafts
Shaft Dimensions and Soil Profile

Shaft No.	Shaft Length (ft)	Shaft Diameter (in)	Stiffness, $E_p I_p$ ($\times 10^{12}$ lb-in^2)	Generalized Soil Profile
1	15.0	54.0	1.50	Stiff clay over medium dense silt
2	12.9	54.0	1.40	Stiff clay over rock
4	22.0	60.0	2.24	Loose silty sands
5	16.8	60.0	2.29	Dense silty sands
6	15.9	54.0	1.37	Loose over dense silty sands
7	13.5	60.0	2.25	Stiff clay over shale
8[1]	11.0	66.0	2.91	Loose silty sand
	6.2	60.0	1.99	over dense sand

[1]Test Pier 8 has two dimensions; one for the top 11.0 feet, the second for the bottom 6.2 feet.

Table 4.2 (cont.)

Shaft No.	Shaft Length (ft)	Shaft Diameter (in)	Stiffness, $E_p I_p$ ($\times 10^{12}$ lb-in^2)	Generalized Soil Profile
9	21.0	78.0	6.13	Clayey and sandy silts with gravel
10	17.0	57.8	1.72	Silty sand with some cemetation
11	21.3	60.0	2.60	Loose to medium dense silty sands
12	21.0	60.0	2.60	Soft to medium stiff clay over sand
13	18.5	54.0	1.39	Stiff clayey silt
14	16.0	54.0	1.50	Stiff clayey silt over stiff clay

54.6×10^6 in-lb. Such large capacities were employed to ensure that the failure occurred in the soil, rather than in the drilled shaft, during testing.

4.1.2 Testing Procedure

The drilled shafts were loaded using a steel pole, 80 feet in length, attached to the top of the drilled shaft. The top of the pole was pulled, at an oblique angle, by a cable connected to equipment on the ground, creating a large moment as well as lateral and axial forces. The typical loading configuration is illustrated in Fig. 4.2.

The drilled shafts were tested in stages by loading the shaft to a desired load and, then, releasing the load back to zero. This process was repeated, for increasing loads, until a suitable capacity, usually governed by the soil's ultimate resistance, had been reached. All drilled shafts, except No. 9, were loaded until the ultimate capacity of the soil was reached. Shaft No. 9 was used for a future transmission-pole structure, so loading was limited to restrict deformations to small amounts.

4.1.3 Data Measuring

The amount of measured data for each drilled shaft tested varied depending on the level of the test. Three levels were assigned to the testing. Level I tests; which included shafts No. 1, 2, 4, 6, 7, 8, 11, 12, and 13; were large-deformation tests with measurements of the deflection and rotation along the entire length of the drilled shafts. Dial gauges mounted on the exterior of the drilled shaft and slope indicators inside a casing embedded in the drilled shafts were used for measurement. The distribution of the soil pressure along the drilled shafts was measured with earth-pressure cells embedded around the exterior of the drilled shaft. Level II tests were large deformation tests where only the deflection and rotation at the top of the drilled shafts were measured. Level II tests were performed on shafts No. 5, 10, and 14. A Level III test was performed on drilled shaft No. 9 where the shaft was tested to only small deformations. Deflection and rotation at the top of the shaft were measured for this test. For the present study, only the deflection of the shafts will be considered. Dial gauges and/or linear variable differential transformers (LVDT's) were used to measure the top of

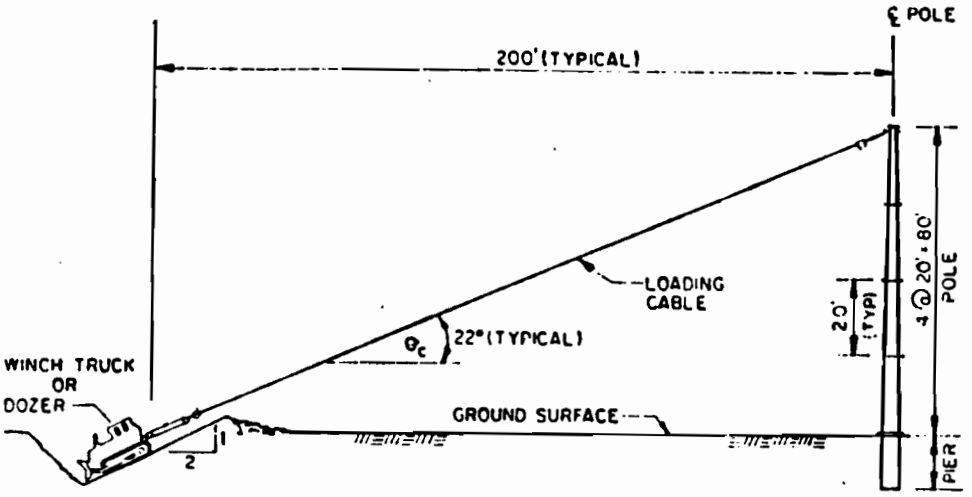

Figure 4.2: Typical Loading Configuration Used in Load Tests (after EPRI, 1982)

shaft deflections up to four inches. A graduated survey rod or metal tape, in conjunction with a surveying transit, were used to measure larger deflections.

4.2 SOIL CONDITIONS

Soil conditions varied widely from site to site with layered systems consisting of loose to very dense sands over, under and between soft to very stiff clays. Rock and hard shales were encountered at the sites of shafts No. 2 and 7, respectively. Slightly cemented materials were encountered at the sites of shafts No. 10 and 14. Many geological deposition systems including glacial, lucustrine, alluvial, and coastal were involved in the layering or stratigraphy of the testing sites.

Laboratory and in-situ soil tests were conducted on undisturbed and disturbed soil samples to obtain strength parameters. For primarily cohesive soils, it was assumed that the soil's undrained strength would be appropriate for analysis. The undrained shear strength, s_u, was obtained primarily from unconsolidated-undrained triaxial tests on undisturbed samples. Results from unconfined compression, consolidated-undrained triaxial and pocket penetrometer tests as well as correlations with Standard Penetration Tests were also used to define values of the undrained shear strength.

Drained strengths and effective stresses were used for analysis in primarily cohesionless soils. Consolidated-undrained triaxial tests with pore water pressure measurements were the primary means used to define effective stress angles of internal friction, ϕ, and cohesion values, c'. Correlation with Standard Penetration Tests and results from consolidated-drained triaxial tests were also used in the absence of results from consolidated-undrained triaxial tests. The cohesion values were assumed zero, a value confirmed by consolidated-undrained triaxial tests.

Index properties, including water content, grain-size distribution and plasticity index were determined for the classification of the soils. The effective unit weights, γ, of the soils were determined either directly from undisturbed soil samples or from empirical correlations with Standard Penetration Tests.

4.3 INPUT DATA FOR COM624

For the analyses, described subsequently in Chapter 5, each soil layer was idealized as either fully cohesive or cohesionless. Values of undrained shear strength, angles of internal friction and effective unit weights were obtained from the report by the Electric Power Research Institute. Values of the soil modulus variation with depth, m, and the strain, ε_{50}, were estimated based on representative values presented in Table 4.3 (Reese and Sullivan, 1980).

The soil parameters could vary widely along the the length of the shafts due to the many soil types and conditions possible at a test site. Weighted averages were used on portions of the soil's strength and effective unit weight distributions for shafts No. 6, 9, 11 and 12 to facilitate COM624's input limitations. Detailed drilled shaft dimensions and properties and soil parameters used for the analysis of each drilled shaft are presented in Figs. 4.3 through 4.15.

Table 4.3
Representative Values of the Soil Modulus Variation With Depth, m, and the Strain, ε_{50}

Values of ε_{50} for Clays

c_u (lb/ft²)	ε_{50} (%)
250 - 500	2.0
500 - 1000	1.0
1000 - 2000	0.7
2000 - 4000	0.5
4000 - 8000	0.4

Values of the Soil Modulus Variation With Depth for Clays

c_u (lb/ft²)	m (lb/in³)
250 - 500	30
500 - 1000	100
1000 - 2000	300
2000 - 4000	1000
4000 - 8000	3000

Values of the Soil Modulus Variation with Depth for Sands

Relative Density	Sand Below Water Table (lb/in³)	Sand Above Water Table (lb/in³)
Loose	20	25
Medium	60	90
Dense	125	225

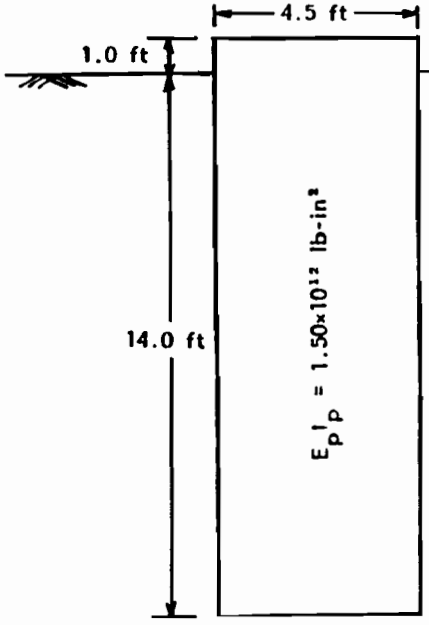

Depth, x (ft)	s_u (lb/ft²)	ϕ' (deg.)	ε_{50} (%)	m (lb/in³)	γ' (lb/ft³)
0	1900	--	0.7	600	131
5.0	700	--	1.0	100	131
6.5	--	35	--	90	126
11.5	--	35	--	90	123
14.0					

Figure 4.3: Soil and Drilled Shaft Data Used for COM624 Input, Shaft No. 1

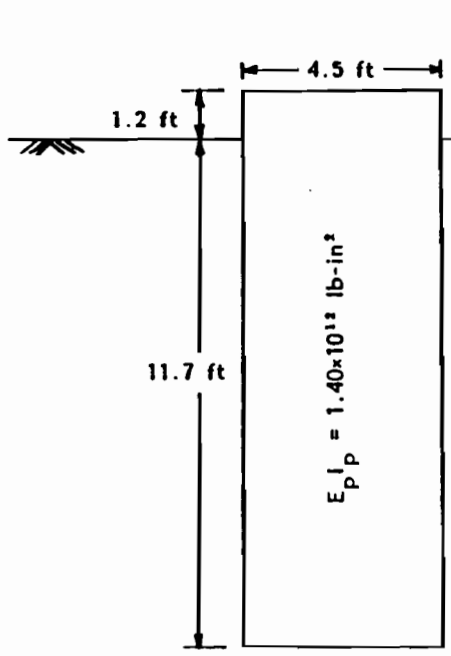

Depth, x (ft)	s_u (lb/ft^2)	ϕ' (deg.)	ε_{50} (%)	m (lb/in^3)	γ' (lb/ft^3)
0	1900	--	0.7	400	119
5.0	3500	--	0.5	1100	130
6.0	4500	--	0.35	2500	140
7.3	4500	--	0.35	3000	140
10.5	4500	--	0.35	3000	131
12.0					

Figure 4.4: Soil and Drilled Shaft Data Used for COM624 Input, Shaft No. 2.

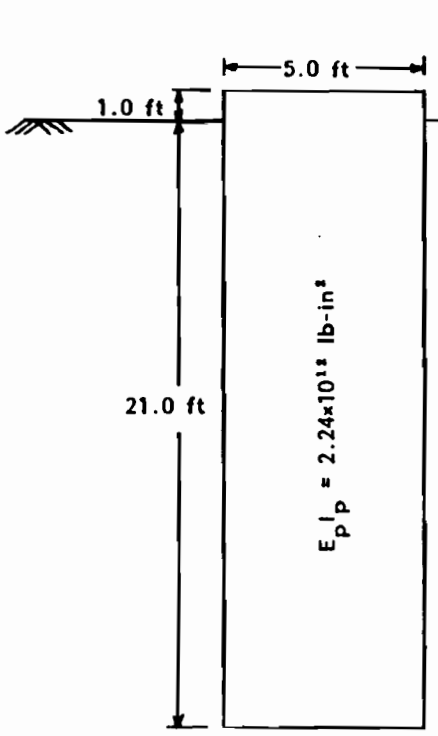

Depth, x (ft)	s_u (lb/ft^2)	ϕ' (deg.)	ε_{50} (%)	m (lb/in^3)	γ' (lb/ft^3)
0	--	28	--	25	110
2.0	--	29	--	30	110
9.5	--	30	--	40	110
11.0 ▽	--	30	--	25	62
18.0	--	28	--	20	62
22.0					

Figure 4.5: Soil and Drilled Shaft Data Used for COM624 Input, Shaft No. 4.

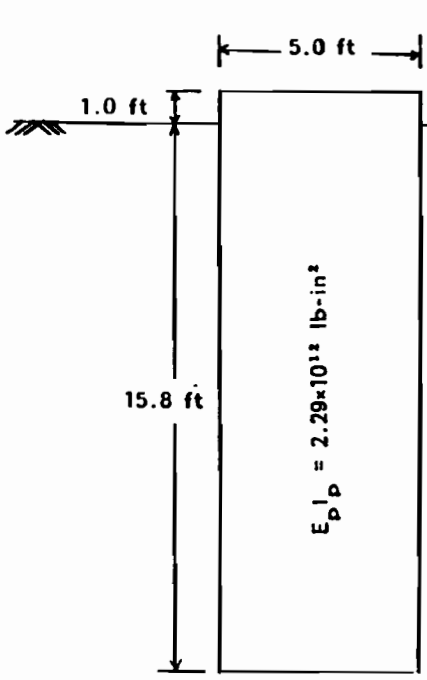

Depth, x (ft)	s_u (lb/ft²)	ϕ' (deg.)	ε_{50} (%)	m (lb/in³)	γ' (lb/ft³)
0	--	45	--	225	140
1.5	700	--	1.0	100	135
5.0	--	46	--	225	131
10.5	--	42	--	160	131
12.0	--	39	--	90	131
12.5 ▽	--	39	--	60	69
17.5					

Figure 4.6: Soil and Drilled Shaft Data Used for COM624 Input, Shaft No. 5.

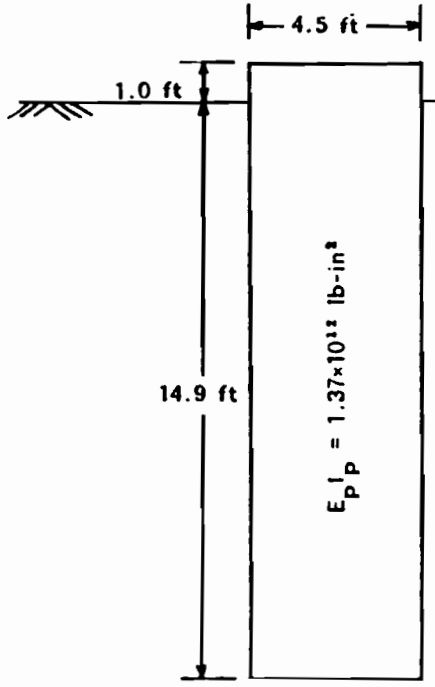

Depth, x (ft)	s_u (lb/ft²)	ϕ' (deg.)	ε_{50} (%)	m (lb/in³)	γ' (lb/ft³)
0					
	--	34.5	--	35	133
3.5 ▽					
	--	39	--	60	60
7.3					
	2300	--	0.5	1000	60
10.5					
	900	--	1.0	500	60
12.5					
	--	45	--	125	66
16.0					

Figure 4.7: Soil and Drilled Shaft Data Used for COM624 Input, Shaft No. 6.

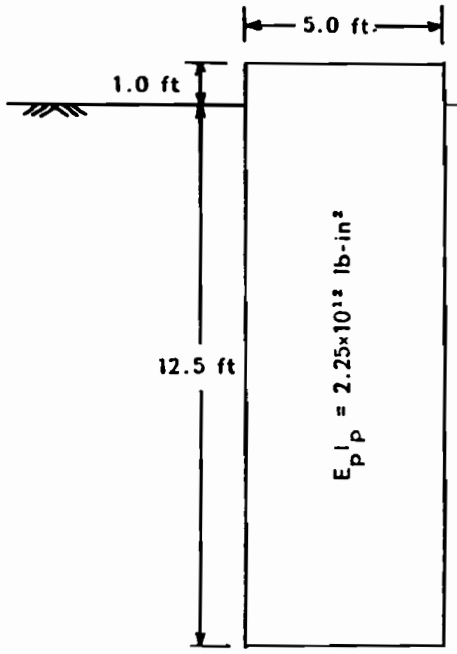

Depth, x (ft)	s_u (lb/ft²)	ϕ' (deg.)	ε_{50} (%)	m (lb/in³)	γ' (lb/ft³)
0	1500	--	0.7	1000	130
5.5	2000	--	0.5	1200	137
8.5	3750	--	0.4	2500	137
10.0	9000	--	0.1	4000	137
13.0					

Figure 4.8: Soil and Drilled Shaft Data Used for COM624 Input, Shaft No. 7.

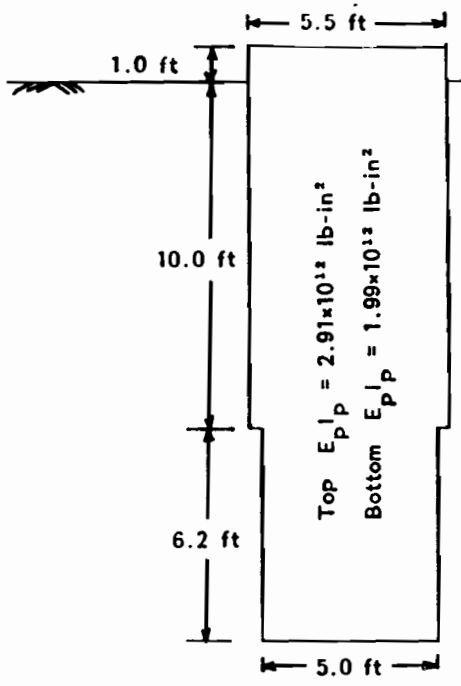

Depth, x (ft)	s_u (lb/ft²)	ϕ' (deg.)	ε_{50} (%)	m (lb/in³)	γ' (lb/ft³)
0	--	32	--	35	111
4.5	--	38	--	90	111
6.0	--	36	--	75	111
7.5 ▽	--	36	--	50	48
12.0	--	45	--	125	48
13.5	--	36	--	50	48
17.5					

Figure 4.9: Soil and Drilled Shaft Data Used for COM624 Input, Shaft No. 8.

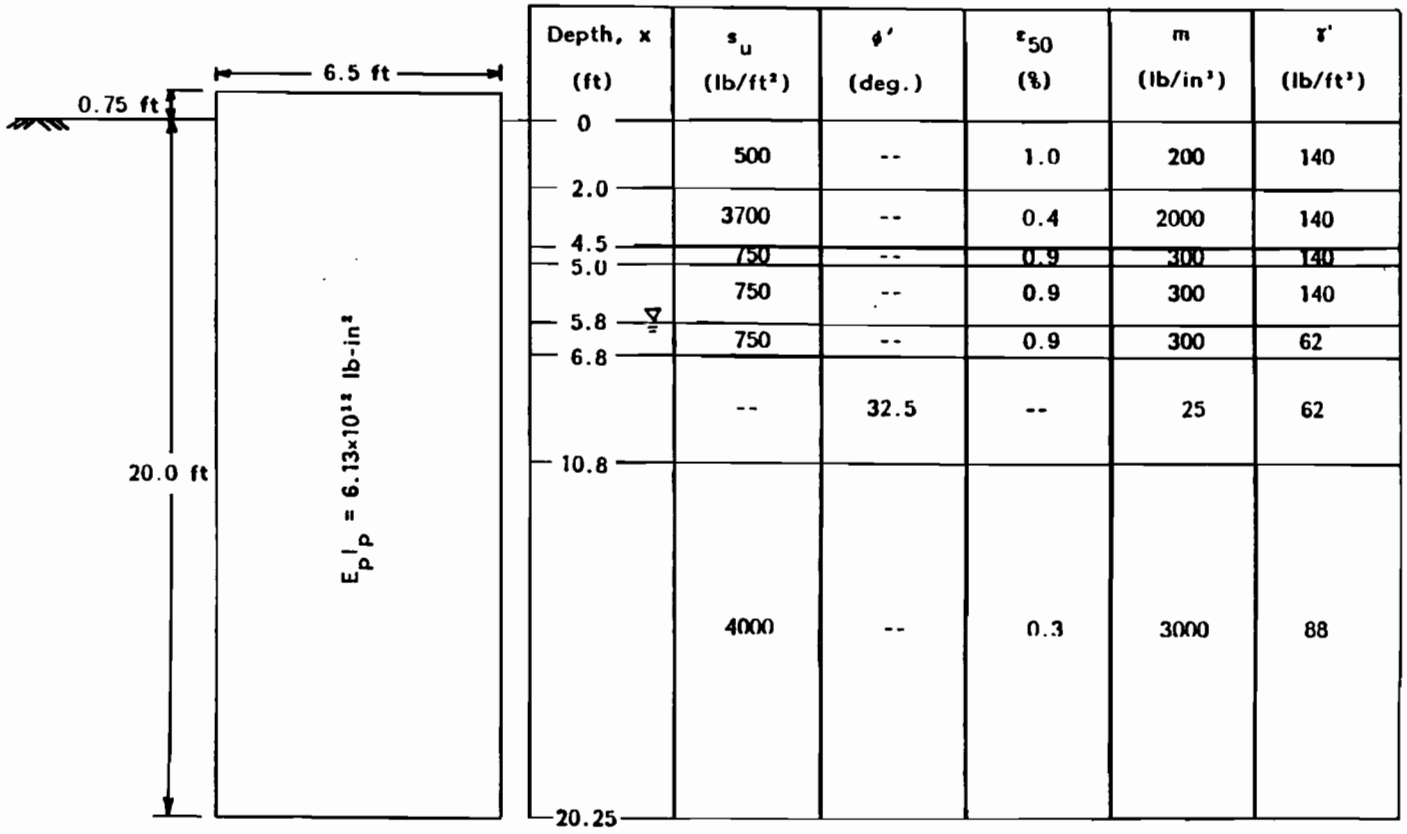

Depth, x (ft)	s_u (lb/ft^2)	ϕ' (deg.)	ε_{50} (%)	m (lb/in^3)	γ' (lb/ft^3)
0					
	500	--	1.0	200	140
2.0					
	3700	--	0.4	2000	140
4.5					
5.0	750	--	0.9	300	140
	750	--	0.9	300	140
5.8 ▽					
	750	--	0.9	300	62
6.8					
	--	32.5	--	25	62
10.8					
	4000	--	0.3	3000	88
20.25					

Figure 4.10: Soil and Drilled Shaft Data Used for COM624 Input, Shaft No. 9.

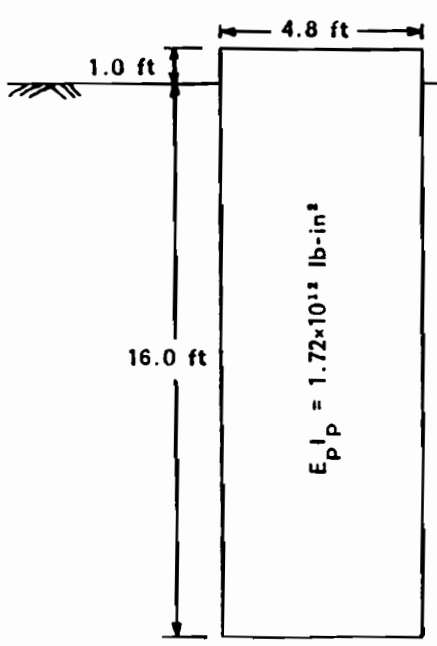

Depth, x (ft)	s_u (lb/ft²)	ϕ' (deg.)	ε_{50} (%)	m (lb/in³)	γ' (lb/ft³)
0					
	--	30	--	25	119
3.5					
	--	32.5	--	30	119
7.0					
	--	43	--	180	130
10.0					
	--	38	--	90	130
15.0					
	--	45	--	225	130
17.0					

Figure 4.11: Soil and Drilled Shaft Data Used for COM624 Input, Shaft No. 10.

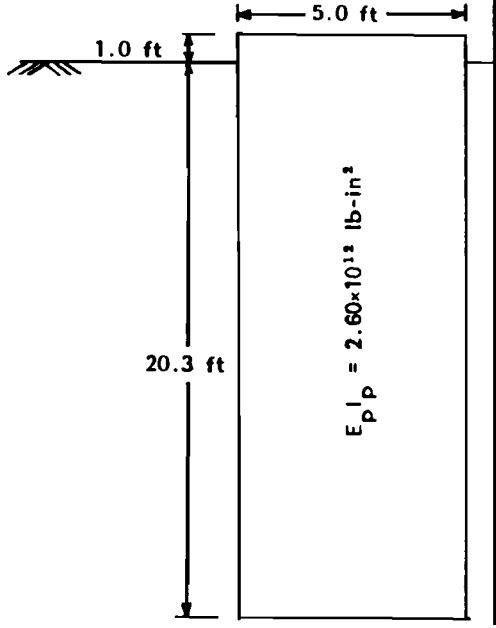

Depth, x (ft)	s_u (lb/ft²)	ϕ' (deg.)	ε_{50} (%)	m (lb/in³)	γ' (lb/ft³)
0	--	28	--	25	110
2.0	--	35.5	--	70	110
6.0	--	30	--	35	110
10.0 ▽	1700	--	0.7	1050	62
12.0	--	36	--	50	62
20.5					

Figure 4.12: Soil and Drilled Shaft Data Used for COM624 Input, Shaft No. 11.

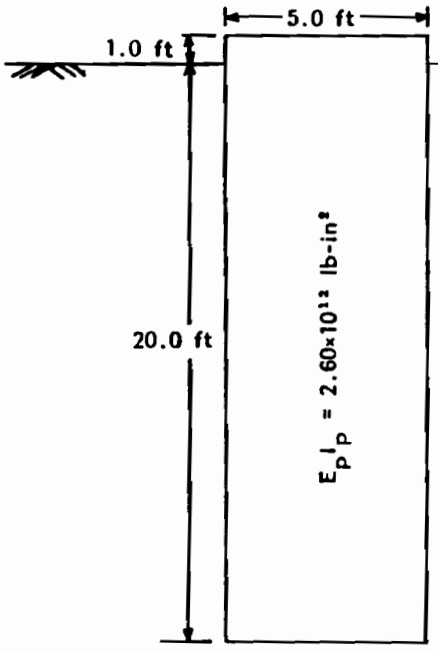

Depth, x (ft)	s_u (lb/ft^2)	ϕ' (deg.)	ε_{50} (%)	m (lb/in^3)	γ' (lb/ft^3)
0	1000	--	0.8	300	66
4.0	500	--	1.0	150	69
5.5	200	--	2.0	30	69
7.5	200	--	2.0	30	40
13.5	--	29	--	20	60
18.5	--	35	--	50	62
21.0					

Figure 4.13: Soil and Drilled Shaft Data Used for COM624 Input, Shaft No. 12.

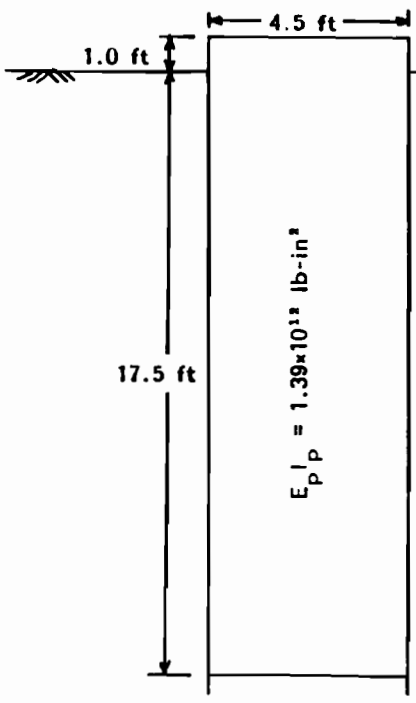

Depth, x (ft)	s_u (lb/ft²)	ϕ' (deg.)	ε_{50} (%)	m (lb/in³)	γ' (lb/ft³)
0	1500	--	0.7	500	119
5.5	1500	--	0.7	500	112
9.5	1500	--	0.7	500	112
13.0 ▽	2600	--	0.4	1200	55
16.5	--	37	--	55	59
18.0					

Figure 4.14: Soil and Drilled Shaft Data Used for COM624 Input, Shaft No. 13.

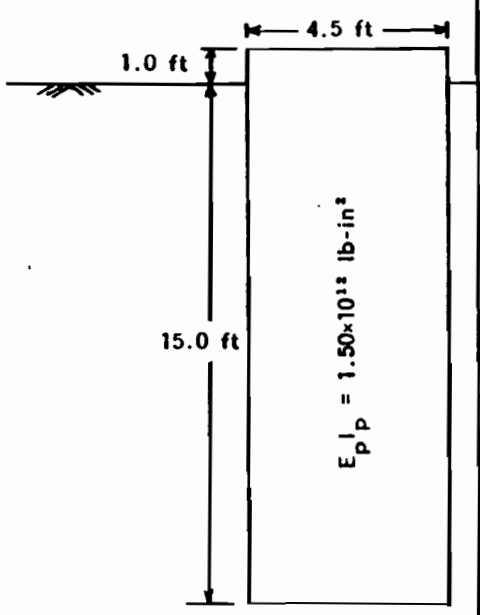

Depth, x (ft)	s_u (lb/ft²)	ϕ' (deg.)	ε_{50} (%)	m (lb/in³)	γ' (lb/ft³)
0					
	1000	--	0.8	300	104
3.0					
	1000	--	0.8	300	109
6.5					
	2000	--	0.5	800	112
9.0					
	2000	--	0.7	500	112
12.0					
	2700	--	0.4	1200	112
15.5					

Figure 4.15: Soil and Drilled Shaft Data Used for COM624 Input, Shaft No. 14.

CHAPTER 5. INITIAL ANALYSES OF DRILLED SHAFTS

An initial series of computer analyses was performed on the drilled shafts described in Chapter 4 using the conventional analytical procedures. As discussed in Chapters 1 and 2, the conventional procedures were derived principally from load tests on "long" drilled shafts and piles, but the shafts described in Chapter 4 would be considered "short" drilled shafts. Accordingly, deficiencies in the analyses of "short" drilled shafts using the conventional procedures are possible. The deficiencies are revealed by the analyses described in this chapter. For each drilled shaft, the deflections at the top of the shaft, y_t, were computed for four, incremental loads. The computed deflections were then compared to measured values from the load tests.

5.1 DESCRIPTION OF ANALYSIS

The soil and drilled shaft parameters presented in Chapter 4 were used in the analyses of the "short" drilled shafts. With layerings of cohesive and cohesionless soils present at each test site, various p-y relationships are required to define the soil responses along the length of the drilled shafts. Accordingly, appropriate p-y curve criteria were employed to describe the various p-y relationships (curves) along each shaft. The p-y curves were generated internally by the computer program, COM624, using the four, widely-used p-y criteria discussed in Chapter 2. Shaft No. 2 was embedded in decomposed granite; a material for which none of the four, current p-y criteria is applicable. Accordingly, no analysis was performed for shaft No. 2.

Computations for each drilled shaft were performed for four, incremental loads applied to the top of the shaft. Each load consisted of three components: an applied moment (M_t), an axial force (A_t) and a lateral force (P_t). As described in Chapter 4, the method used to load the drilled shafts

during the load tests created moments which were relatively large when compared to the axial and lateral forces. Therefore, it was decided that for computations, the loads would be based on applied moments (M_t) with the axial and lateral forces determined from statics and the geometry of the loading apparatus used in the load tests (Fig. 5.1).

Values of the four, incremental loads used in the analysis of each shaft were based on a maximum load which, initially, was at least 50 percent of the ultimate load applied to the shaft during the load tests. However, convergence to a stable solution was not possible for some of the higher loads used in six of the twelve shafts. Consequently, for these six shafts, the four loads were proportionally reduced until stable results were obtained for all four. The final four loads (applied moments, axial and lateral forces) used for the analysis of each drilled shaft are presented in Table 5.1.

5.2 RESULTS OF COMPUTER ANALYSES

The measured and predicted deflections were related to the applied moments used in the computer analyses. The predicted values of the top of shaft deflection, y_t, from the computer analyses and the corresponding measured values are presented in Table 5.2. Plots of the predicted and measured deflections versus the applied moment are presented in Figs. 5.2 through 5.13.

5.2.1 Shaft No. 11 - A Special Case

Shaft No. 11 was considered a special case during the computer analyses because of the behavior noted in the report by the Electric Power Research Institute, EPRI (1982). In the load test on shaft No. 11, analysis with slope indicators suggested that a point along the drilled shaft was developing a sharper curvature than its adjacent points as the load increased. The increased curvature signalled that the drilled shaft had experienced a reduction of structural stiffness (E_pI_p) at this point. The reduction in structural stiffness caused the measured deflections of the shaft to increase beyond what would normally occur if the stiffness had remained constant. Possible reasons for the reduction could include improper construction and faulty materials. Predicted deflections for shaft No. 11 were larger than the

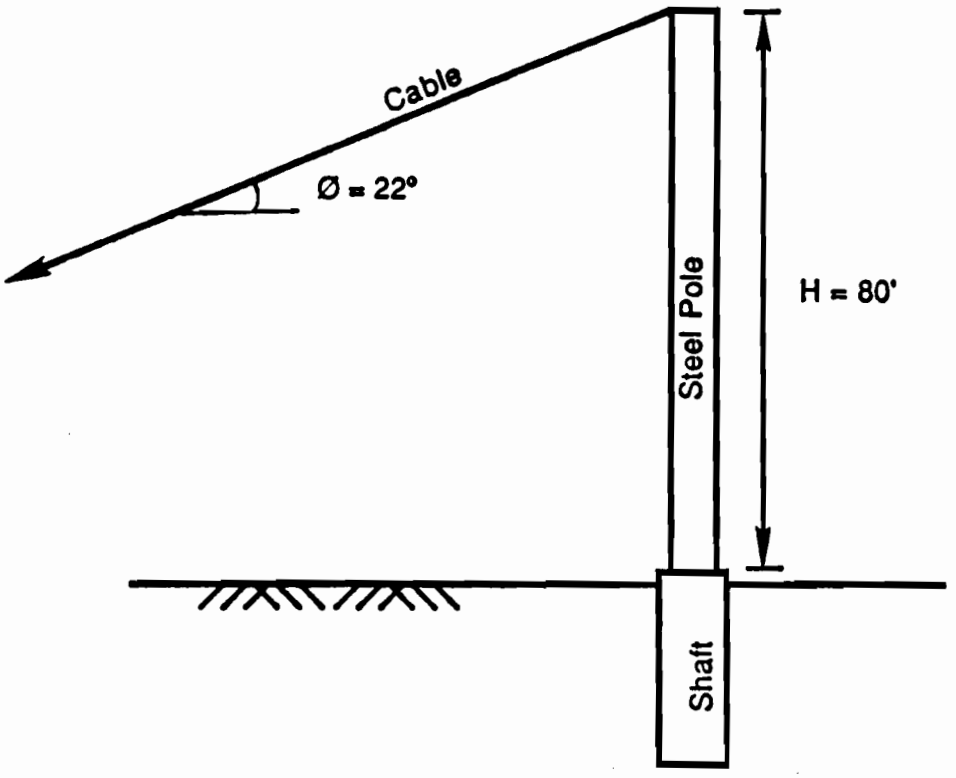

$$\text{Lateral Force, } P_t = \frac{M_t}{H} \cos \emptyset$$

$$\text{Axial Force, } A_t = \frac{M_t}{H} \sin \emptyset$$

Figure 5.1: Geometry of Loading Apparatus Used to Compute Axial and Lateral Forces

Table 5.1
Maximum Loads Including
Applied Moment, Axial and Lateral Force
Used in Computer Analyses

Shaft No.	Applied Moment M_t ($\times 10^6$ lb-in)	Lateral Force P_t ($\times 10^3$ lb)	Axial Force A_t ($\times 10^3$ lb)
1			
	6.0	5.7	2.3
	12.0	11.6	4.7
	18.0	17.4	7.0
	24.0	23.4	9.4
4			
	6.0	5.7	2.3
	12.0	11.6	4.7
	18.0	17.4	7.0
	24.0	23.4	9.4
5			
	9.0	8.7	3.5
	18.0	17.4	7.0
	27.0	26.1	10.5
	36.0	34.8	14.1
6			
	4.5	4.3	1.8
	9.0	8.7	3.5
	13.5	13.0	5.3
	18.0	17.4	7.0

Table 5.1 (cont.)

Shaft No.	Applied Moment M_t ($\times 10^6$ lb-in)	Lateral Force P_t ($\times 10^3$ lb)	Axial Force A_t ($\times 10^3$ lb)
7			
	3.0	2.9	1.2
	6.0	5.8	2.3
	9.0	8.7	3.5
	12.0	11.6	4.7
8			
	6.0	5.7	2.3
	12.0	11.6	4.7
	18.0	17.4	7.0
	24.0	23.4	9.4
9			
	3.0	2.9	1.2
	6.0	5.8	2.3
	9.0	8.7	3.5
	12.0	11.6	4.7
10			
	6.0	5.7	2.3
	12.0	11.6	4.7
	18.0	17.4	7.0
	24.0	23.4	9.4
11			
	6.0	5.7	2.3
	12.0	11.6	4.7
	18.0	17.4	7.0
	24.0	23.4	9.4

Table 5.1 (cont.)

Shaft No.	Applied Moment M_t ($\times 10^6$ lb-in)	Lateral Force P_t ($\times 10^3$ lb)	Axial Force A_t ($\times 10^3$ lb)
12			
	2.3	2.2	0.88
	4.5	4.3	1.8
	6.8	6.5	2.6
	9.0	8.7	3.5
13			
	3.0	2.9	1.2
	6.0	5.8	2.3
	9.0	8.7	3.5
	12.0	11.6	4.7
14			
	3.0	2.9	1.2
	6.0	5.8	2.3
	9.0	8.7	3.5
	12.0	11.6	4.7

Table 5.2
Results From Drilled Shaft Analyses
Top of Shaft Deflections

Shaft No.	M_t ($\times 10^6$ lb-in)	Measured y_t (in)	Predicted y_t (in)	Predicted to Measured y_t Ratios
1				
	6	0.02	0.27	13.5
	12	0.74	1.35	1.82
	18	2.40	4.50	1.88
	24	4.50	14.5	3.22
4				
	6	0.05	0.45	8.92
	12	0.20	0.89	4.47
	18	0.43	1.44	3.35
	24	1.08	2.29	2.12
5				
	9	0.10	0.49	4.87
	18	0.36	1.07	2.97
	27	0.70	1.98	2.83
	36	1.16	3.69	3.18
6				
	4.5	0.03	0.49	14.0
	9	0.16	0.87	5.44
	13.5	0.41	1.38	3.36
	18	0.68	2.67	3.93

Table 5.2 cont.

Shaft No.	M_t ($\times 10^6$ lb-in)	Measured y_t (in)	Predicted y_t (in)	Predicted to Measured y_t Ratios
7				
	3	0.09	0.031	0.34
	6	0.16	0.43	2.70
	9	0.30	2.16	7.20
	12	0.50	6.88	13.8
8				
	6	0.16	0.46	2.86
	12	0.40	0.94	2.35
	18	0.70	1.91	2.72
	24	1.21	3.68	3.04
9				
	3	0.008	0.011	1.35
	6	0.015	0.038	2.55
	9	0.027	0.094	3.48
	12	0.045	0.177	3.93
10				
	6	0.05	0.35	6.98
	12	0.18	0.71	3.94
	18	0.30	1.20	4.00
	24	0.72	1.91	2.65

Table 5.2 cont.

Shaft No.	M_t ($\times 10^6$ lb-in)	Measured y_t (in)	Predicted y_t (in)	Predicted to Measured y_t Ratios
11				
	6	0.05	0.27	5.44
	12	0.32	0.56	1.73
	18	1.52	0.96	0.63
	24	2.89	1.55	0.54
12				
	2.25	0.01	0.07	6.37
	4.5	0.04	0.22	5.37
	6.75	0.08	11.5	144
	9	0.16	38.5	241
13				
	3	0.04	0.022	0.54
	6	0.09	0.11	1.22
	9	0.18	0.32	1.78
	12	0.35	0.68	1.95
14				
	3	0.02	0.07	3.49
	6	0.07	1.00	14.2
	9	0.16	5.03	31.4
	12	0.31	16.2	52.3

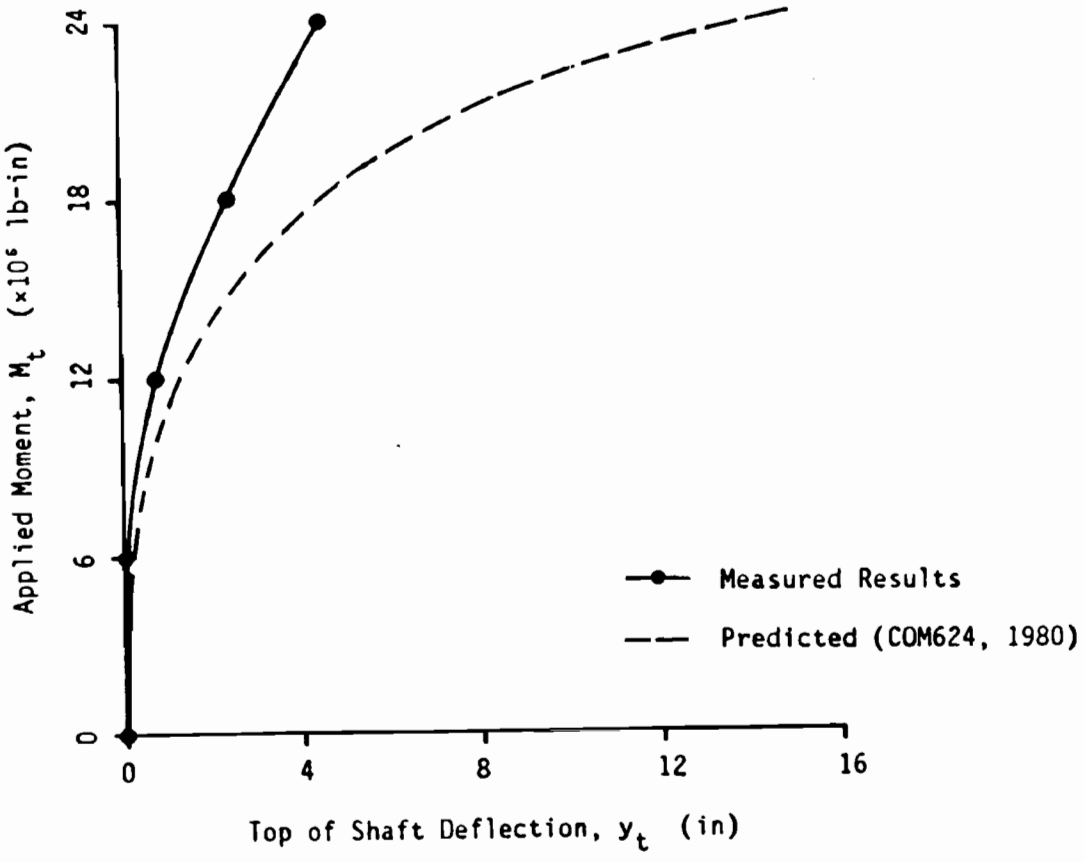

Figure 5.2: Top of Shaft Deflection versus Applied Moment for Shaft No. 1.

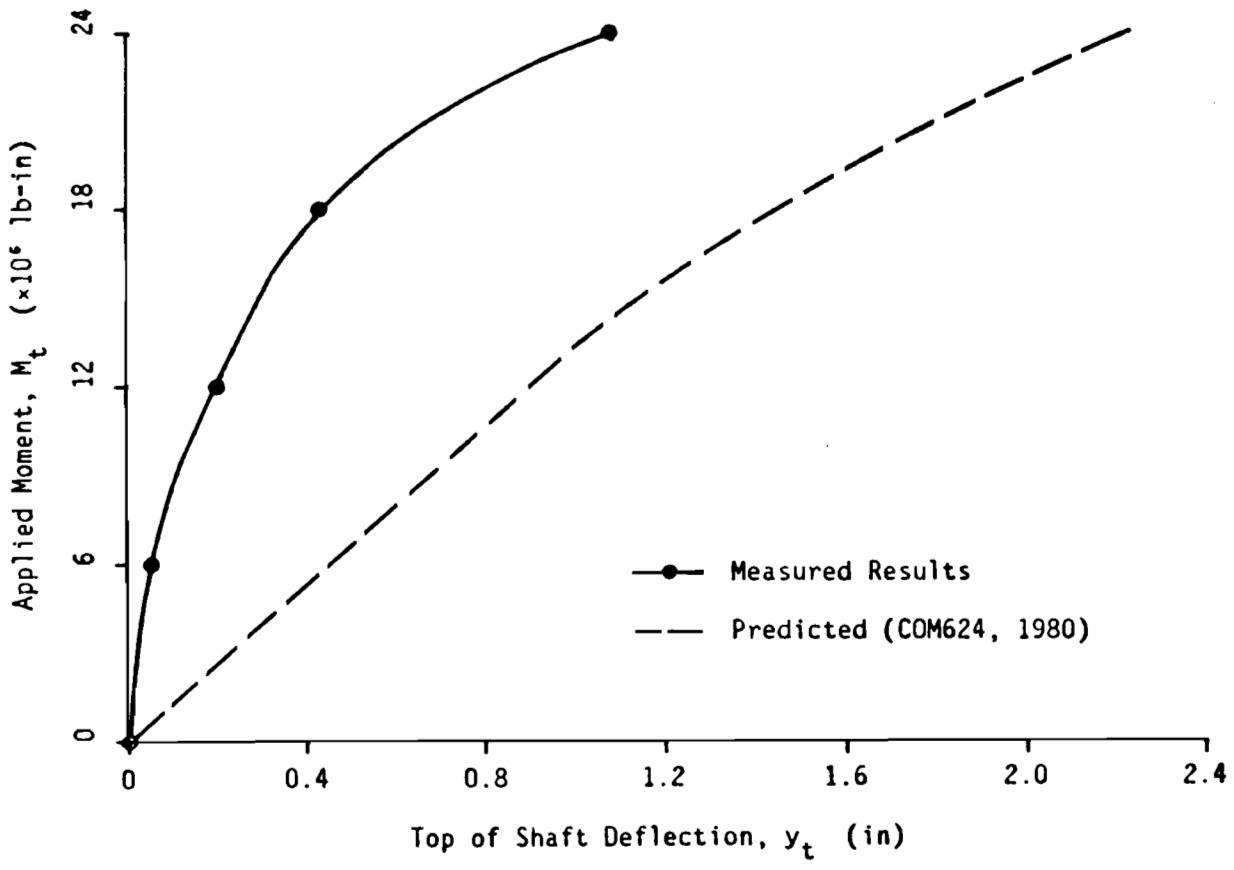

Figure 5.3: Top of Shaft Deflection versus Applied Moment for Shaft No. 4.

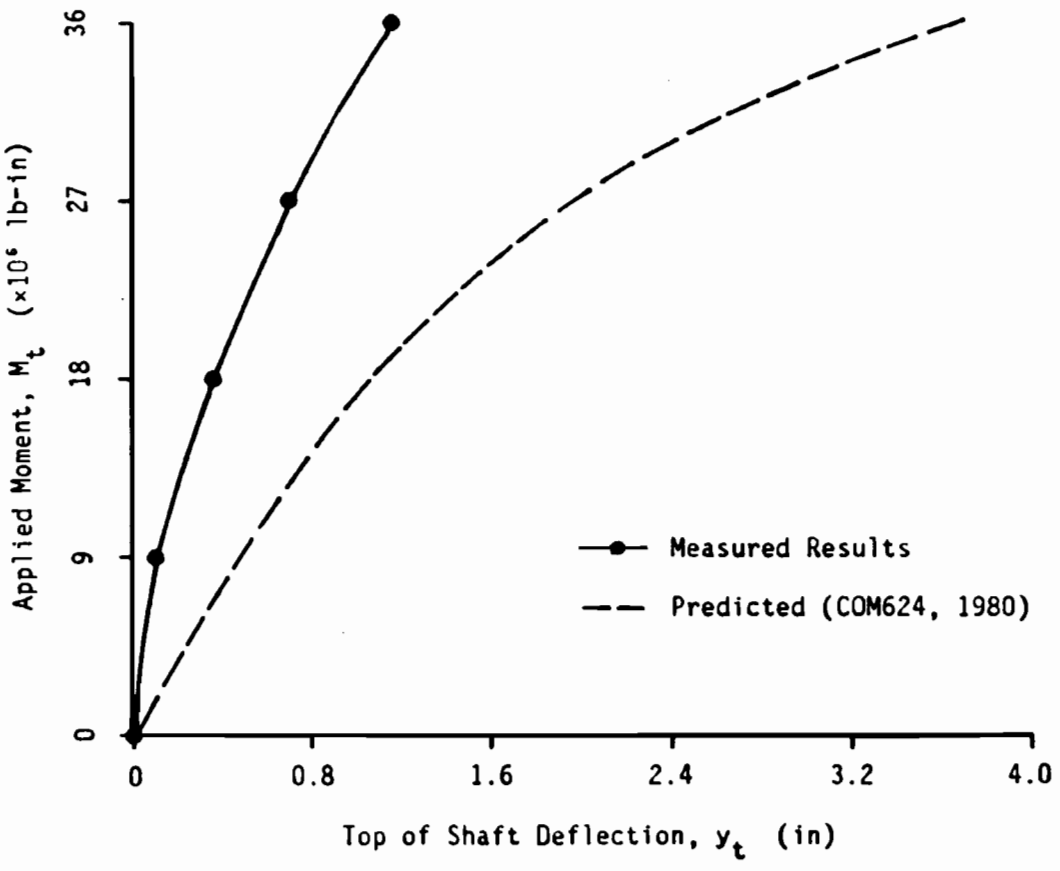

Figure 5.4: Top of Shaft Deflection versus Applied Moment for Shaft No. 5.

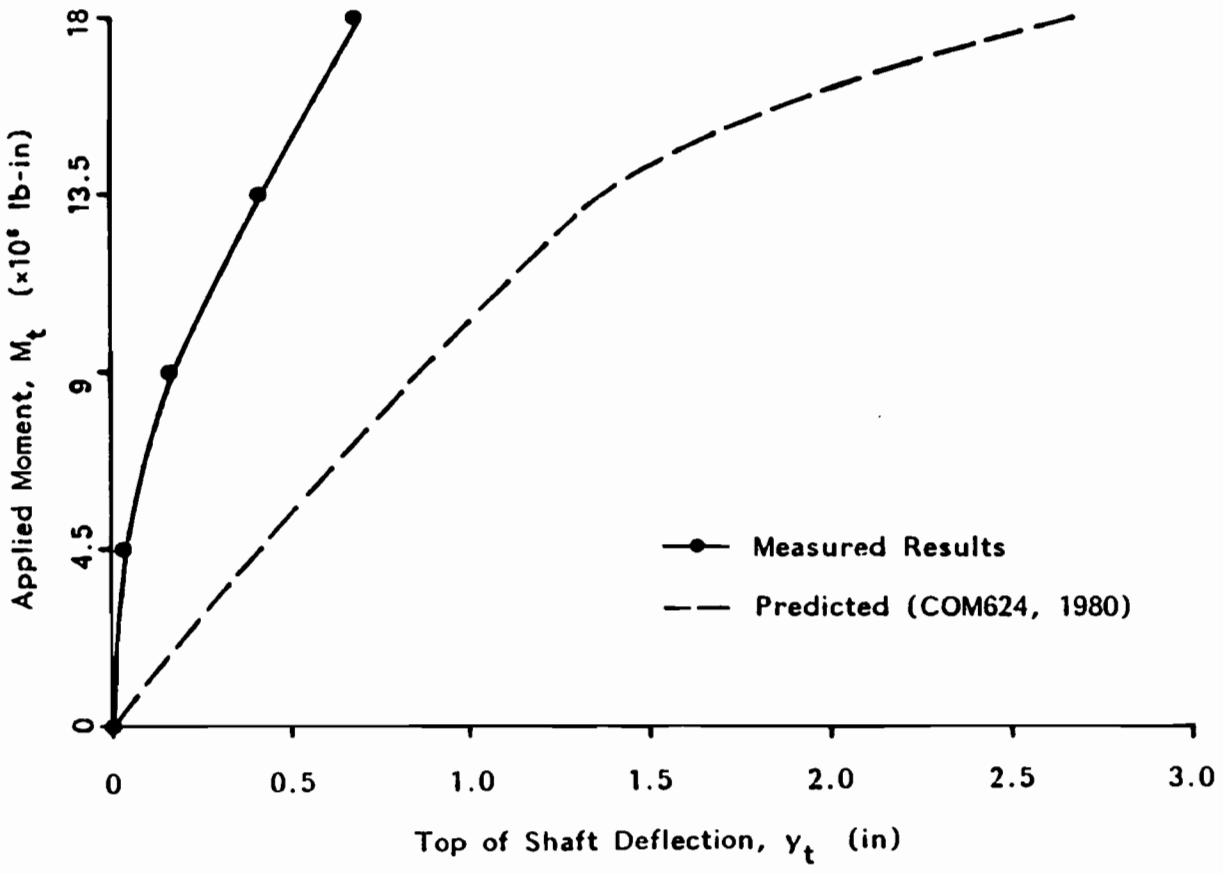

Figure 5.5: Top of Shaft Deflection versus Applied Moment for Shaft No. 6.

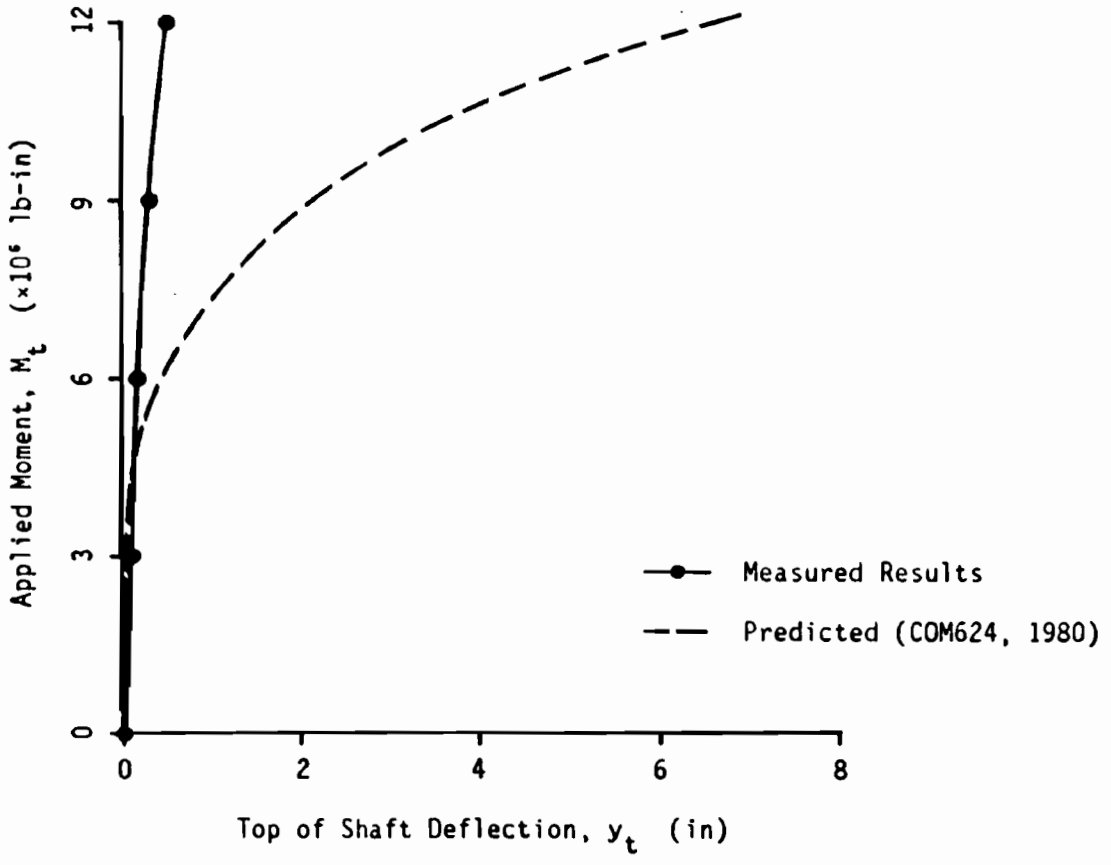

Figure 5.6: Top of Shaft Deflection versus Applied Moment for Shaft No. 7.

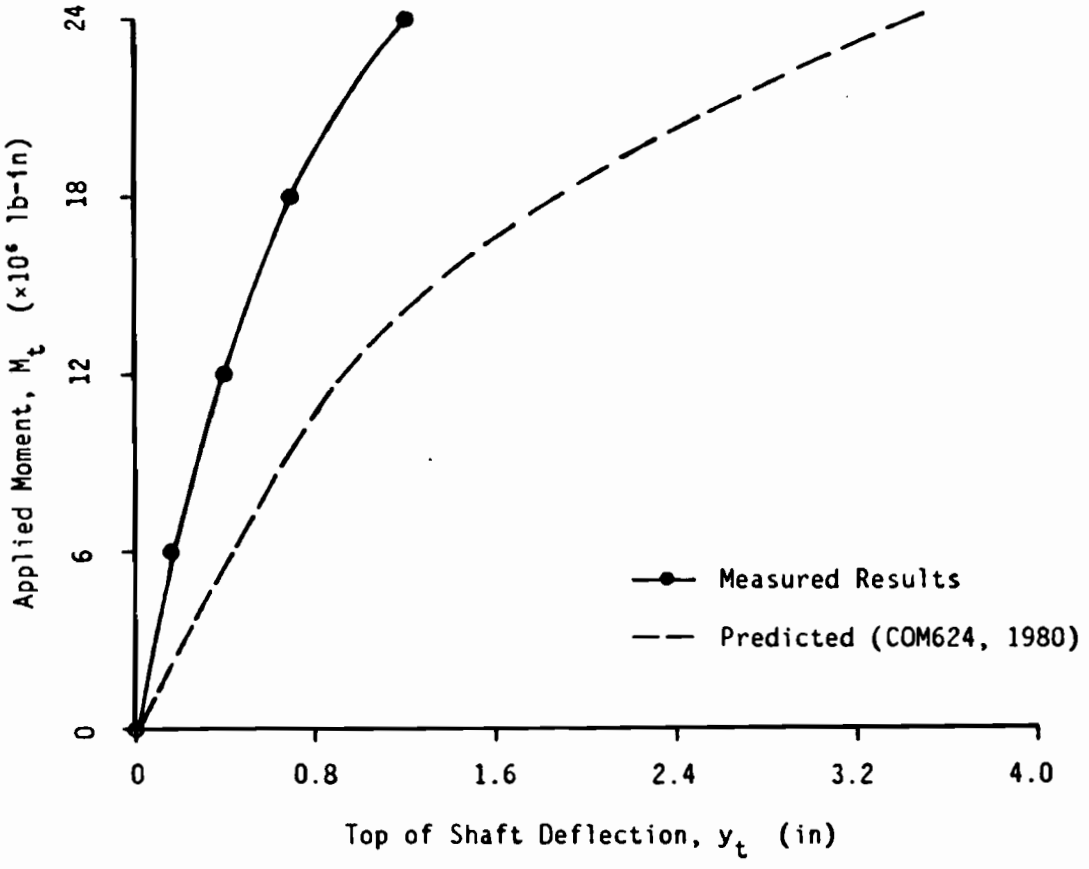

Figure 5.7: Top of Shaft Deflection versus Applied Moment for Shaft No. 8.

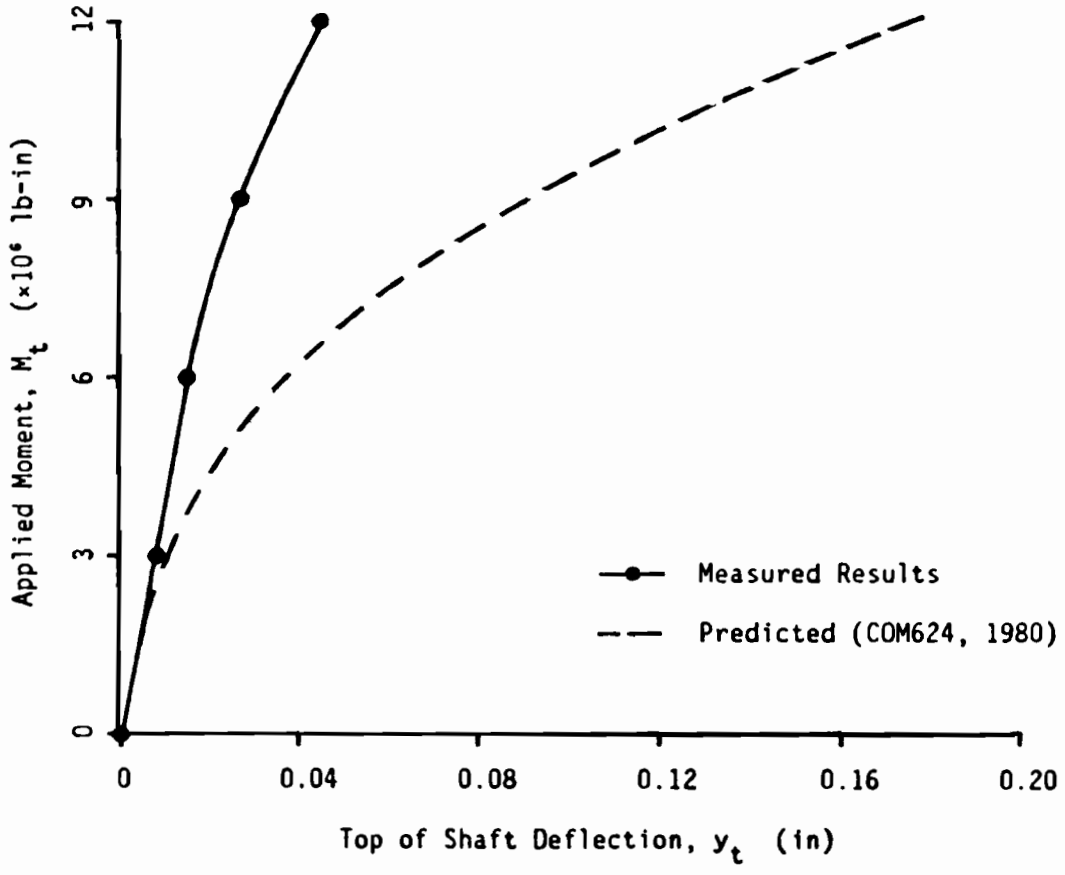

Figure 5.8: Top of Shaft Deflection versus Applied Moment for Shaft No. 9.

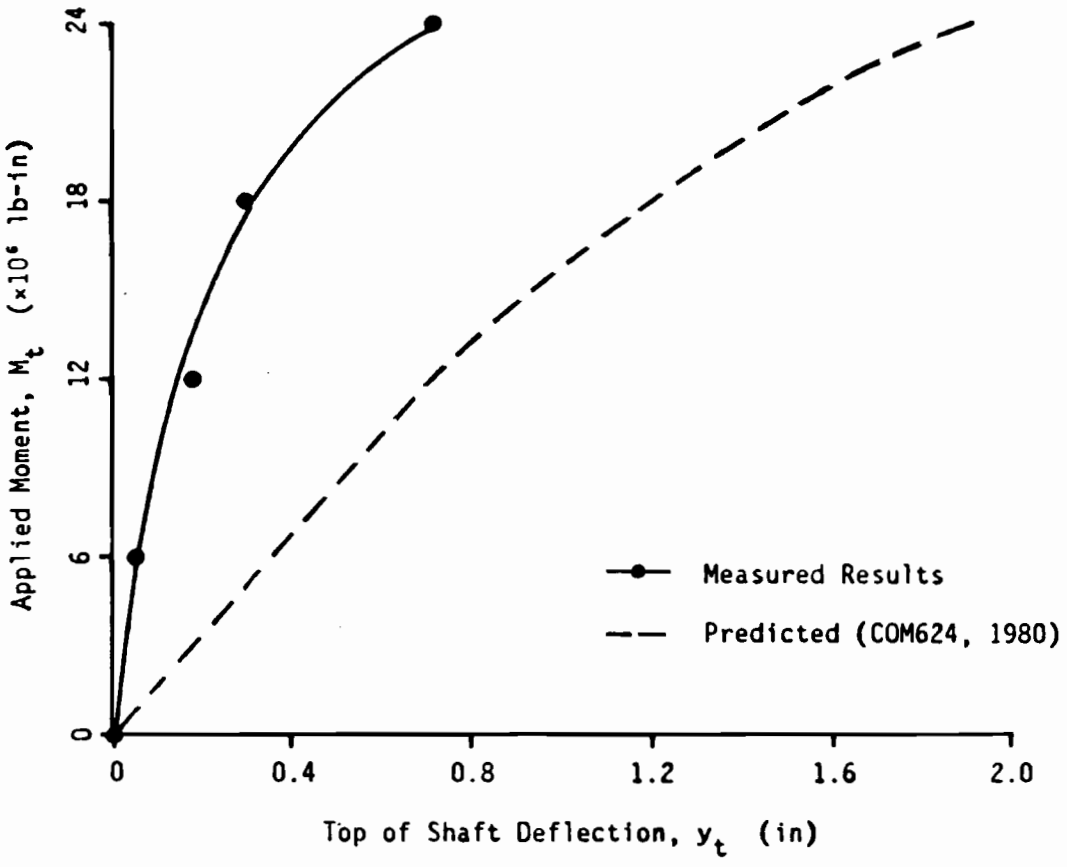

Figure 5.9: Top of Shaft Deflection versus Applied Moment for Shaft No. 10.

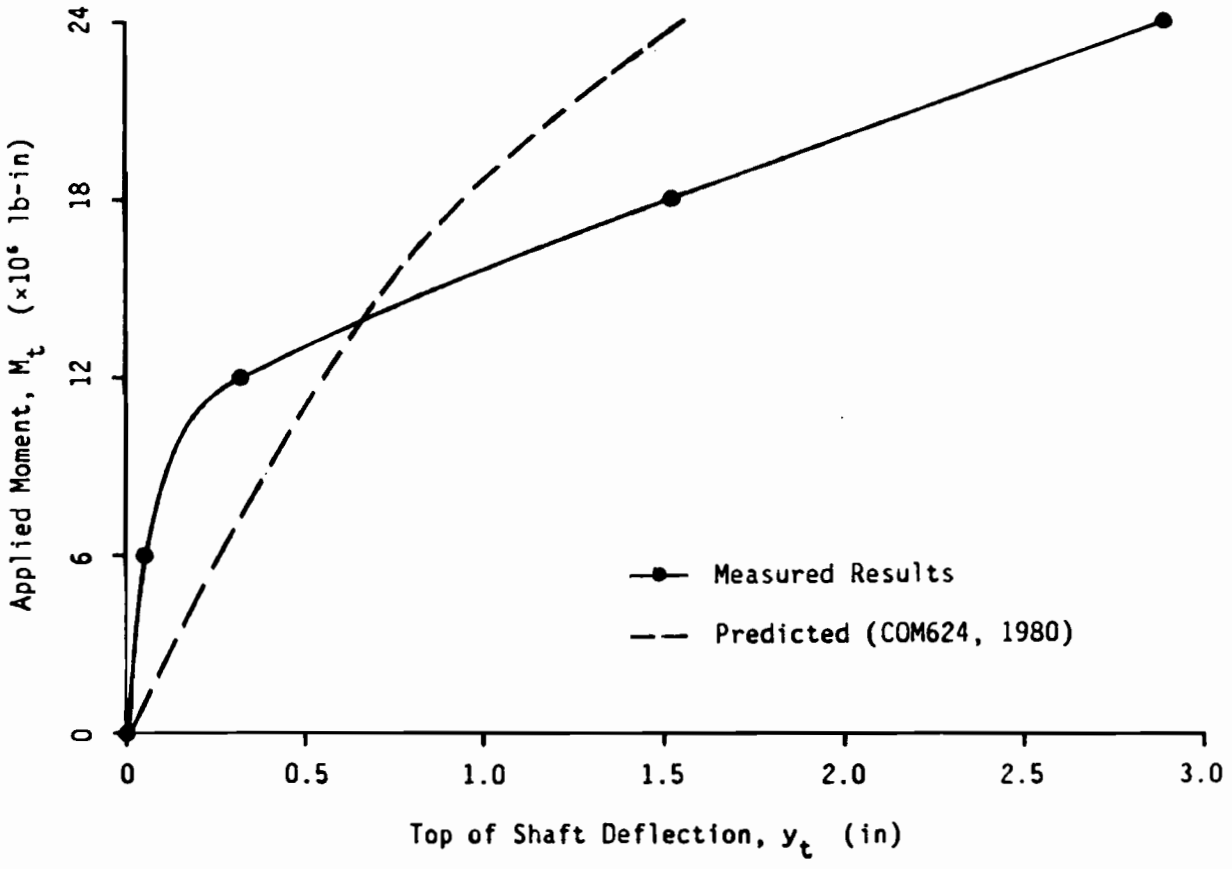

Figure 5.10: Top of Shaft Deflection versus Applied Moment for Shaft No. 11.

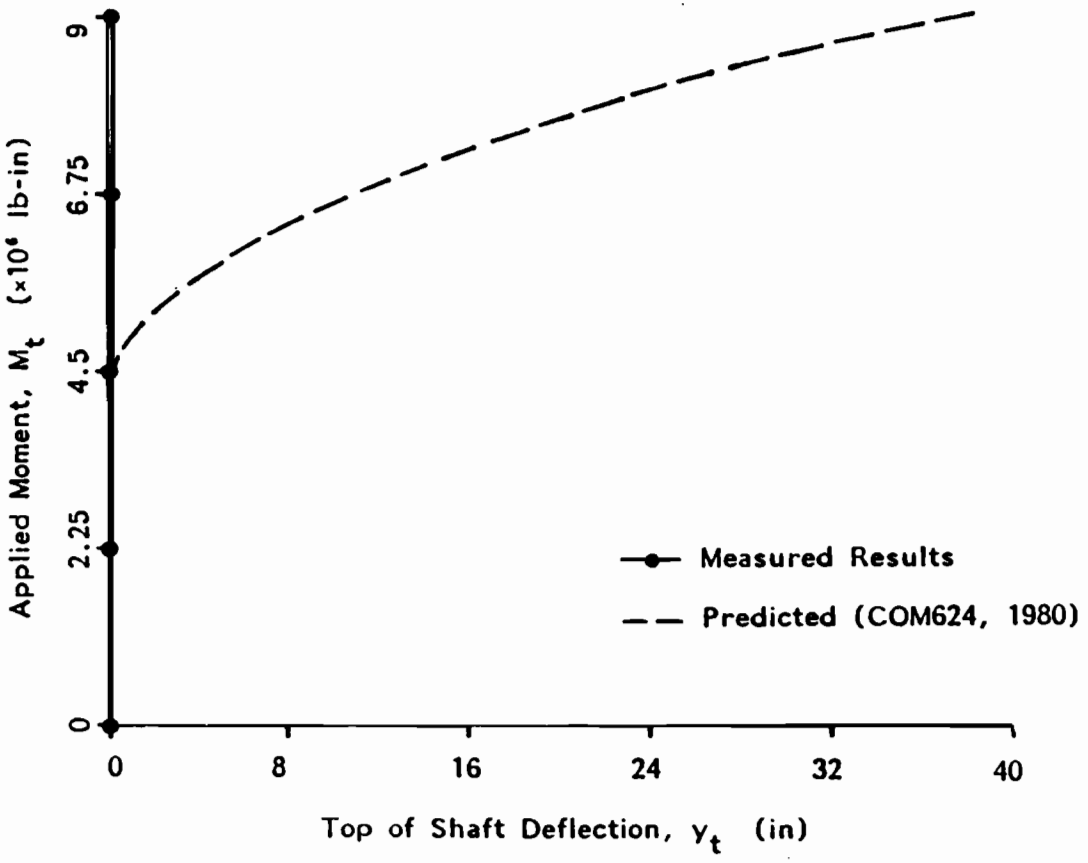

Figure 5.11: Top of Shaft Deflection versus Applied Moment for Shaft No. 12.

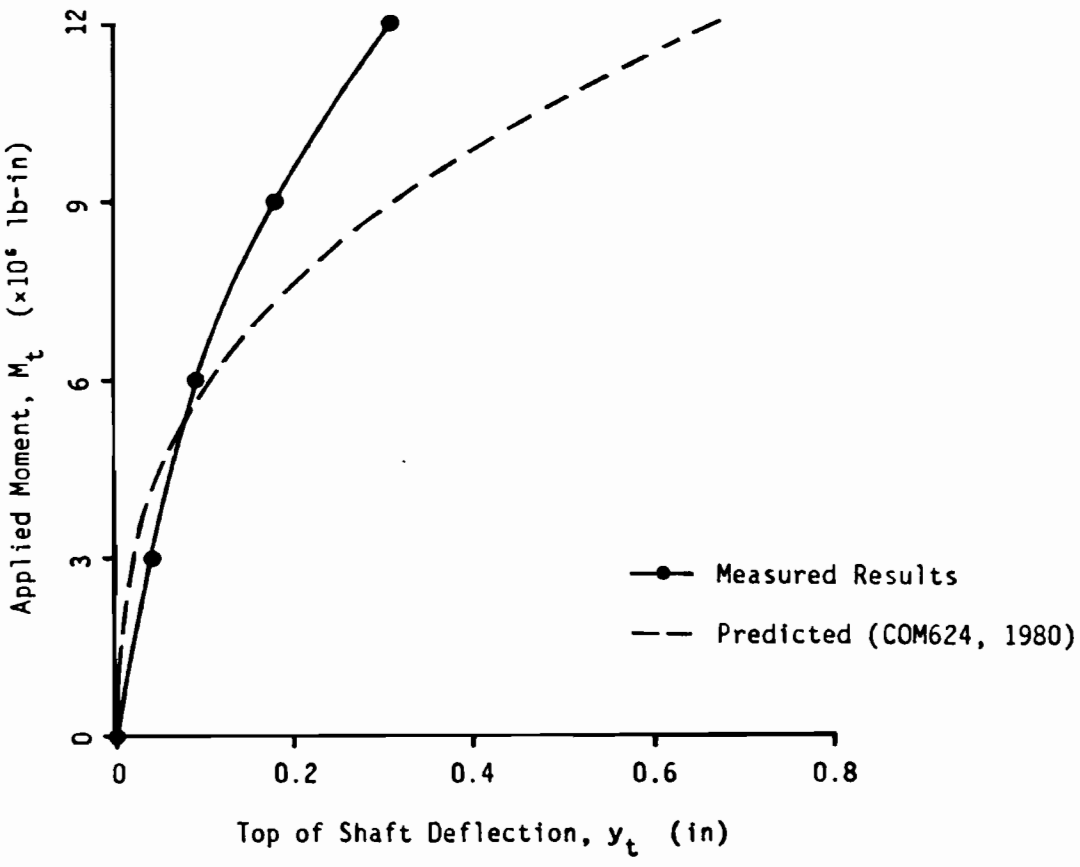

Figure 5.12: Top of Shaft Deflection versus Applied Moment for Shaft No. 13.

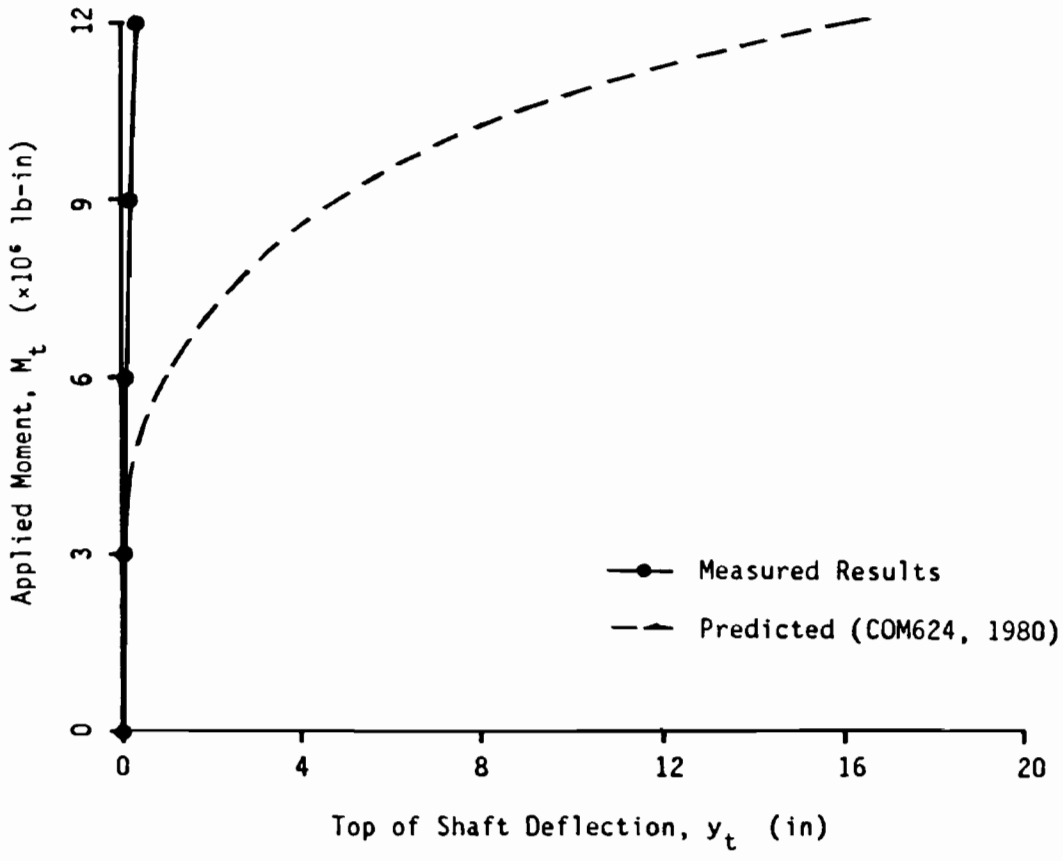

Figure 5.13: Top of Shaft Deflection versus Applied Moment for Shaft No. 14.

measured values for the smaller loads, but the reverse was true for the larger loads (Fig. 5.10). This would seem to confirm the suspicions that were noted in the EPRI report. Based on these findings it was concluded that shaft No. 11 would be excluded from further consideration.

5.2.2 Predicted Versus Measured Top of Shaft Deflection

For the remaining eleven drilled shafts, the predicted deflections exceeded measured values for all but two loads: the lowest load for shafts No. 7 and 13. For these two loads, predicted deflections were less than the measured values.

The ratios between predicted and measured deflections at the top of the shaft are presented in Table 5.2. The average value of the ratios was 14.7; the standard deviation was 41.6. For eight of the 44 loads analyzed, the ratio between the predicted and measured top of shaft deflection was greater than 10. If these extreme cases are excluded, the average value of the ratios was reduced to 3.42; the standard deviation to 1.86.

5.2.3 Deflected Shaft

The drilled shafts acted essentially rigid, as illustrated in Fig. 5.14 for shaft No. 1. The shafts rotated about a single point of zero deflection located down the shaft a distance, L_z, ranging from 53 percent to 86 percent of the total length of the shaft. An extreme range in movements were noted at the base of the shafts, ranging from 0.002 in to 7.76 in. Distances to the point of zero deflection (L_z) and movements at the base of the shafts are presented in Table 5.3.

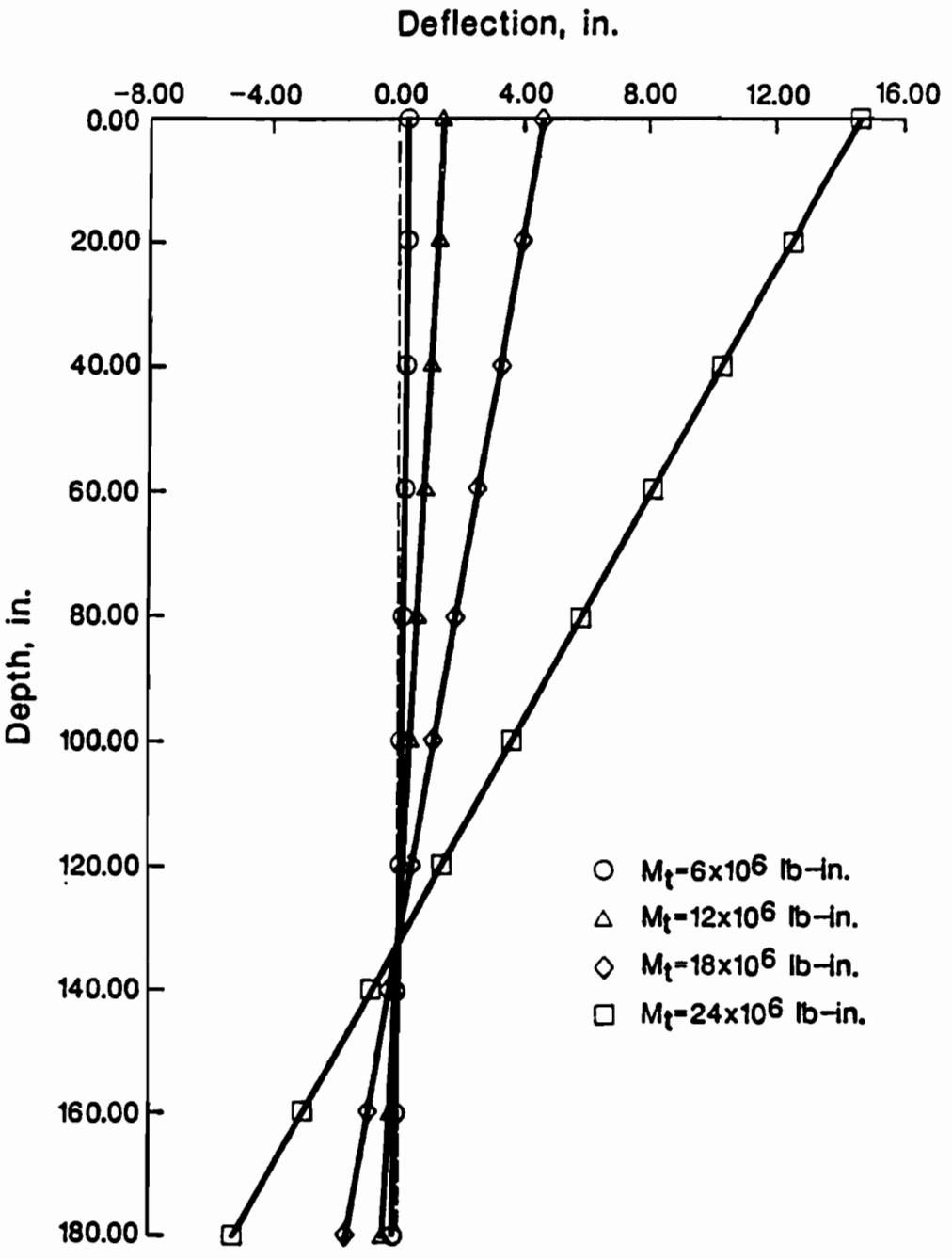

Figure 5.14: Deflected Shapes of Shaft No. 1 for All Loads Applied in Analysis

Table 5.3

Base of Shaft Deflections and

Distance to Point of Zero Deflection, L_z

Shaft No.	M_t ($\times 10^6$ lb-in)	Distance L_z (in)	Ratio of L_z to Length, L	Base of Shaft Deflection (in)
1				
	6	115.6	0.64	0.137
	12	129.1	0.72	0.511
	18	131.3	0.73	1.64
	24	131.0	0.73	5.37
4				
	6	170.2	0.64	0.204
	12	170.3	0.65	0.411
	18	171.6	0.65	0.672
	24	174.2	0.66	1.09
5				
	9	129.4	0.64	0.254
	18	130.8	0.65	0.54
	27	134.2	0.66	0.94
	36	137.2	0.68	1.67
6				
	4.5	147.5	0.77	0.12
	9	148.5	0.78	0.23
	13.5	147.0	0.77	0.39
	18	148.8	0.78	0.73

Table 5.3 cont.

Shaft No.	M_t ($\times 10^6$ lb-in)	Distance L_z (in)	Ratio of L_z to Length, L	Base of Shaft Deflection (in)
7				
	3	120.6	0.74	0.008
	6	121.3	0.75	0.14
	9	121.4	0.75	0.72
	12	121.4	0.75	2.29
8				
	6	144.1	0.70	0.19
	12	144.0	0.70	0.39
	18	145.7	0.71	0.78
	24	145.0	0.70	1.53
9				
	3	175.4	0.70	0.002
	6	190.2	0.75	0.008
	9	193.6	0.75	0.022
	12	194.8	0.77	0.044
10				
	6	153.2	0.78	0.09
	12	152.7	0.78	0.18
	18	150.2	0.77	0.33
	24	150.0	0.77	0.54

Table 5.3 cont.

Shaft No.	M_t ($\times 10^6$ lb-in)	Distance L_z (in)	Ratio of L_z to Length, L	Base of Shaft Deflection (in)
12				
	2.25	150.0	0.60	0.06
	4.5	171.0	0.68	0.18
	6.75	216.0	0.86	1.91
	9	217.0	0.86	6.20
13				
	3	118.1	0.53	0.005
	6	147.3	0.66	0.03
	9	157.6	0.71	0.11
	12	163.4	0.74	0.21
14				
	3	128.7	0.67	0.03
	6	129.6	0.68	0.47
	9	129.7	0.68	2.39
	12	129.7	0.68	7.76

CHAPTER 6. MODIFICATIONS TO EXISTING PROCEDURES

In Chapter 5, the agreement between the predicted and measured responses of "short" drilled shafts was shown to be relatively poor; revealing the deficiencies involved with using the conventional procedures in analysis. In order to improve the predictions of the behavior of "short" shafts, three modifications to the conventional procedures were developed and implemented. The first two modifications involve changes to the p-y curves; specifically, reducing the characteristic deflection (y_{50}) used in the p-y curve criteria for clays and increasing the ultimate soil resistance (p_{ult}) at depths below the first point of zero deflection. The third modification consists of introducing a shear force to the base of the drilled shafts.

6.1 CHANGES TO THE p-y CURVES

The four p-y curve criteria, currently employed in COM624, use an ultimate soil resistance, p_{ult}, whose value is based on one of two assumed failure modes; wedge-type failure and flow-around failure. In addition, three of the criteria use a characteristic deflection, y_{50}, in the construction of their p-y curves. Both of these quantities (p_{ult} and y_{50}), in their current forms, were developed for "long" drilled shafts. For the analysis of "short" drilled shafts, the current methods to compute the characteristic deflection and the ultimate soil resistance need to be modified.

6.1.1 Characteristic Deflection

The characteristic deflection, y_{50}, for the p-y curve criteria for soft clay (Matlock, 1970) and for stiff clay above the water table (Welch and Reese, 1972), is calculated from

$$y_{50} = 2.5\varepsilon 50^{b} \tag{6.1}$$

where b is the shaft diameter and ε_{50} is the strain at 50 percent of the principal stress difference at failure, $(\sigma_1-\sigma_3)_{failure}$.

The above equation for y_{50} was derived from an equation developed by Skempton (1951) for the deflection of a footing on clay. Skempton's equation involved the product of the footing's width, the strain in the supporting soil, and a dimensionless coefficient. The value of the dimensionless coefficient depended on the length-to-width ratio of the footing with a value of 2.5 corresponding to a length-to-width ratio of 10 or more. Values of the coefficients developed by Skempton are presented in Table 6.1.

When the p-y curve criteria were originally developed, Skempton's equation for footings was adapted for use with drilled shafts or piles. The current p-y curve criteria were developed using data from actual load tests on instrumented piles with embedded length of shaft to diameter (width) ratios greater than 10. Accordingly, a dimensionless coefficient of 2.5 was employed in Eq. 6.1. However, for the "short" drilled shafts analyzed in Chapter 5, the embedded length-to-diameter ratios are between 2.6 and 4.2. Based on the coefficients summarized in Table 6.1, the smaller values of the length-to-diameter ratio will reduce the dimensionless coefficient in Eq. 6.1 to values approximately from 2.1 to 2.3, thus reducing the value of y_{50} and causing the p-y curve to become steeper than if the value of y_{50} was calculated from Eq. 6.1 (Fig.6.1).

In the case of the p-y curve for the stiff clay below the water table, the characteristic deflection is calculated as

$$y_{50} = \varepsilon_{50} b \tag{6.2}$$

with ε_{50} and b being the same as in Eq. 6.1 and the value of the coefficient being unity. However, this p-y curve criteria was also developed using data from a load test on an instrumented pile which had an length-to-diameter ratio greater than 10. If Skempton's work is followed, the dimensionless coefficient in Eq. 6.2 should also be reduced with a reduction of the length-to-diameter ratio. For the current study, it was reasoned that the reduction in the dimensionless coefficient of unity in Eq. 6.2 should be proportionally the same as the reduction of the coefficient, 2.5, in Eq. 6.1. Accordingly, the dimensionless coefficient of unity in Eq. 6.2 should be reduced to a value between 0.84 (= 2.1 ÷ 2.5) and 0.92 (= 2.3 ÷ 2.5) for length-to-diameter ratios between 2.6 and 4.2. This modification causes the

Table 6.1
Values of Skempton's Dimensionless Coefficients

Length-to-Width Ratios	Values of Coefficients
circle	1.7
1:1	1.9
2:1	2.1
5:1	2.4
10:1	2.5

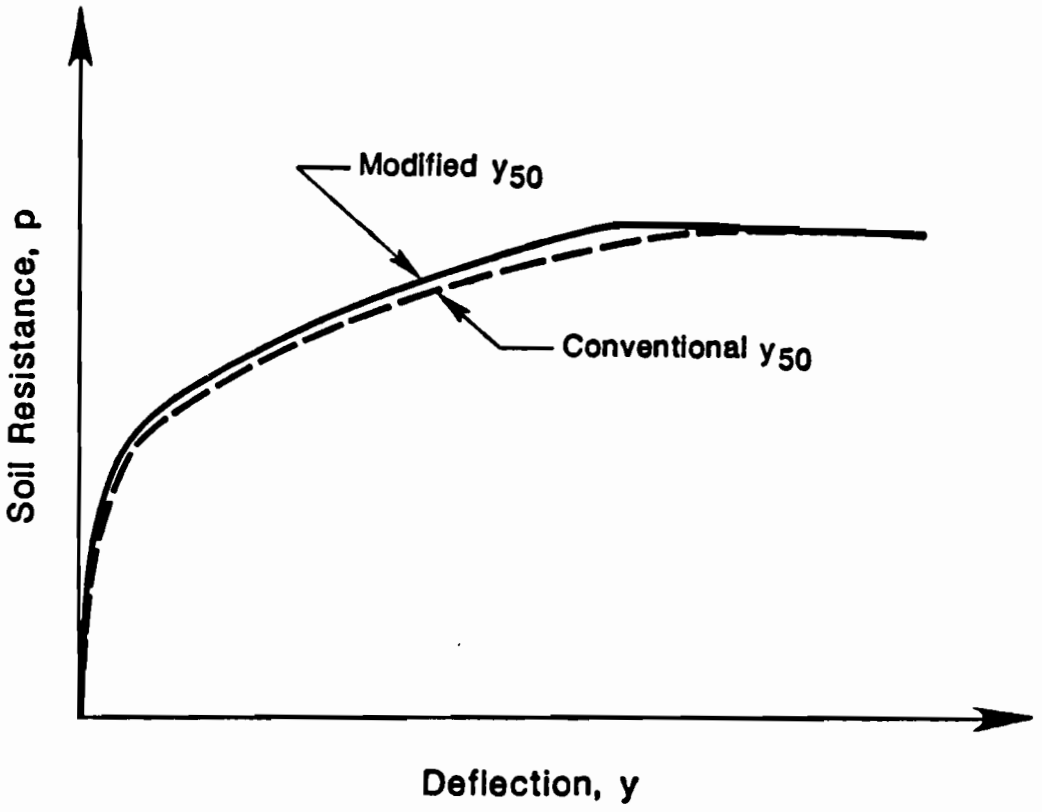

Figure 6.1: Shift in p-y Curve for Soft Clay and Stiff Clay Above the Water Tables with Change in y_{50}

p-y curve for the stiff clay below the water table to shift to the left as illustrated in Fig. 6.2.

6.1.2 Ultimate Soil Resistance

The value of the ultimate soil resistance, p_{ult}, depends on how the soil is idealized to fail along the length of the shaft. The soil is assumed to fail in one of two idealized failure modes; wedge-type failure or flow-around failure.

Wedge-type failure is considered to occur when the soil moves forward and pushes a wedge of soil upward. The soil behind the shaft tends to form an active wedge, flowing in a downward direction behind the drilled shaft (Fig. 6.3a). Flow-around failure occurs when the resistance to a wedgetype failure is higher and the soil tends to flow laterally around the shaft in a horizontal plane (Fig. 6.3b).

Equations have been derived for each of the four p-y curve criteria to calculate the ultimate soil resistance for the two failure modes. Values of the ultimate soil resistance are calculated for both failure modes and compared at the depths where a p-y curve is to be formed. At each depth, the lowest calculated value of p_{ult} is considered to govern and is used to construct the p-y curve for that depth. For the drilled shafts analyzed in Chapter 5, the ultimate soil resistances were governed by the equations for a wedge-type failure for the entire length of the shafts.

However, the rational of using these ultimate soil resistances becomes questionable when the deflected shapes of the drilled shafts are examined. As noted in Chapter 5, the drilled shafts remained essentially straight with the shafts rotating about a single point of zero deflection (Fig. 6.4). The soil above the point of zero deflection should follow the pattern of a wedge-type failure; however, it is questionable whether the soil below the point of zero deflection should follow the pattern of a wedge-type failure. To do so, a second, upward moving, passive wedge would form in direct opposition to the downward moving, active wedge which developed for the soil above the point of zero deflection (Fig. 6.4).

As an approximation for the ultimate soil resistances below the point of zero deflection for drilled shafts like the one shown in Fig. 6.4, it was decided that the ultimate soil resistances would be calculated using equations

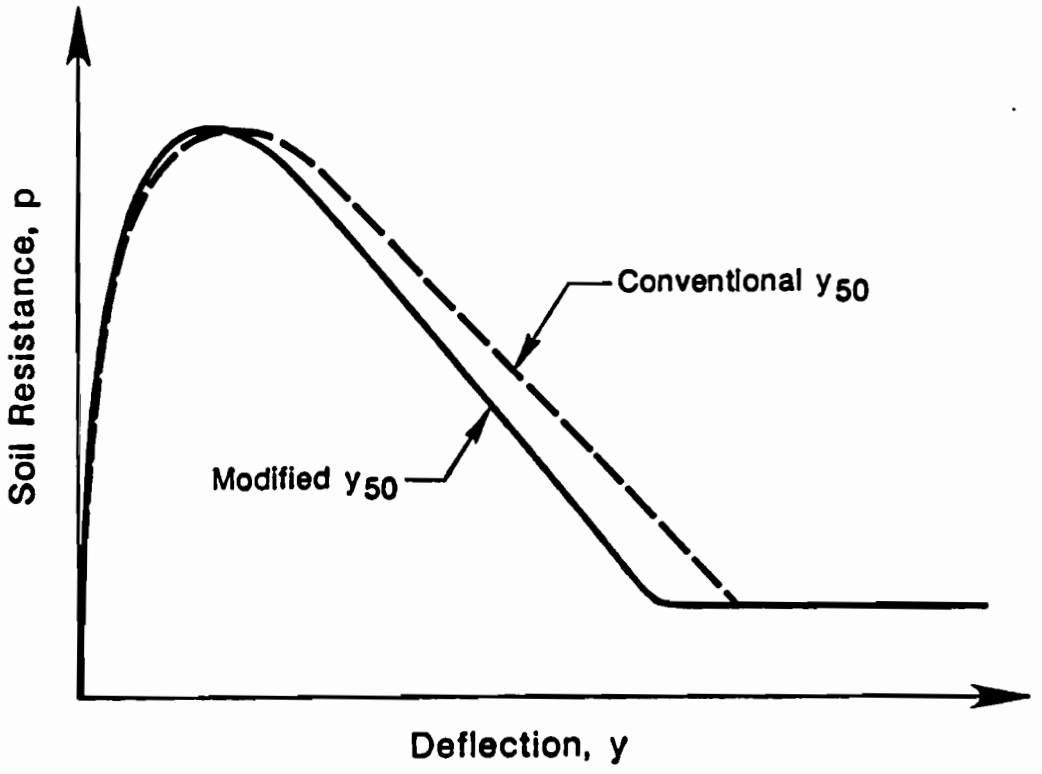

Figure 6.2: Shift in p-y Curve for Stiff Clay Below the Water Table with Change in y_{50}

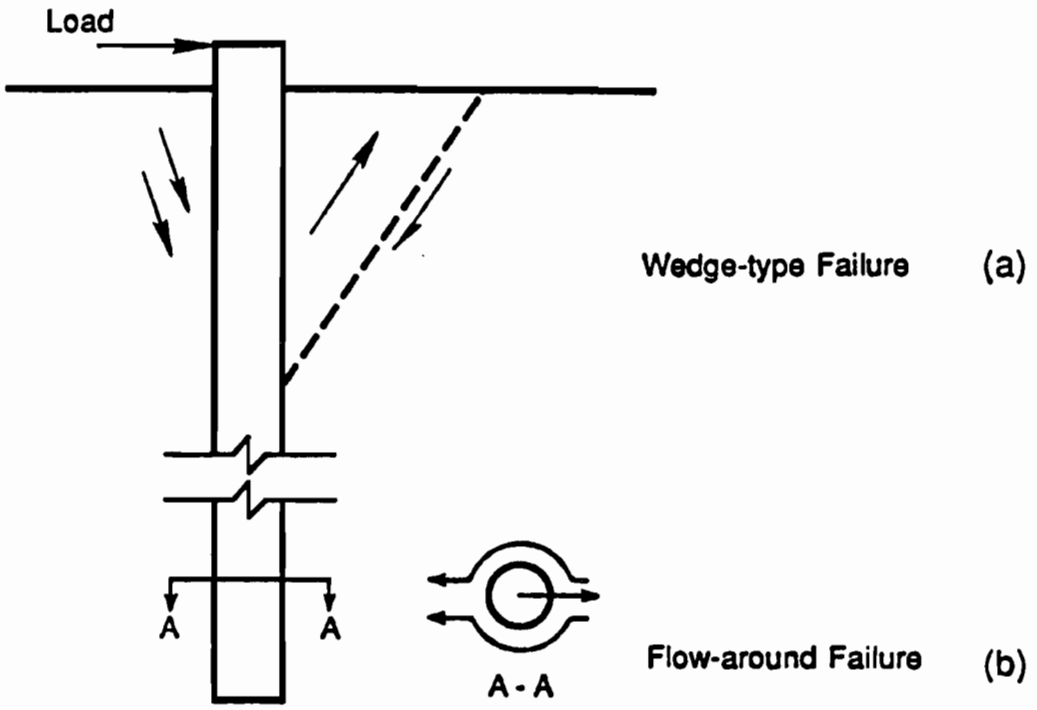

Figure 6.3: Modes of Failure: (a) Wedge-Type Failure, (b) Flow-Around Failure

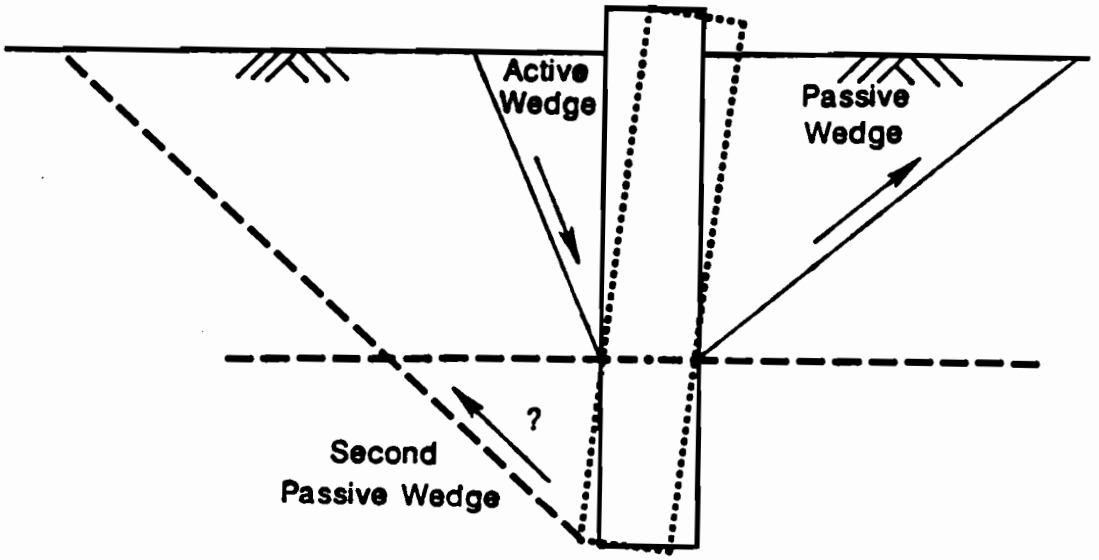

Figure 6.4: Assumed Modes of Failure for "Short" Shafts

for a flowaround failure. Consequently, the soil resistance, for a given deflection, increases as illustrated in Fig. 6.5. For the drilled shafts in the current study, the depths below which this modification would be applied were assumed to be the depths to the points of zero deflection noted in Chapter 5.

6.2 BASE RESISTANCE

The conventional procedures for analysis of laterally loaded drilled shafts consider the shear and moment at the base of the shaft to be zero. In the case of "long" drilled shafts, this is reasonable because the base of the shaft undergoes little if any movement during loading. However, as noted in Chapter 5, significant movements may occur at the base of "short" drilled shafts. Such movements are likely to produce a shear stress between the base of the drilled shaft and the soil.

As a modification to the conventional procedures, a shear force was introduced along the base of the shaft in the form of a force-deflection (F_B-y) curve. The proposed force-deflection curve, as shown in Fig. 6.6, is bi-linear, beginning at the origin and increasing linearly to an ultimate force $F_{B,max}$) at a deflection of 0.1 inch; a value synonymous to the "quake" used in load-transfer curves for the analysis of axially loaded drilled shafts (Coyle, Bartoskewitz and Berger, 1973). The curve becomes horizontal at the ultimate force for all deflections greater than 0.1 inch.

The ultimate force is calculated using the product of the shear strength of the soil at the base of the shaft and the shaft's cross-sectional area. For cohesive soils, the shear strength was taken as the undrained shear strength. For cohesionless soils, the shear strength was computed by multiplying the effective overburden pressure by the tangent of the effective angle of internal friction. The full shear strength was used and was not adjusted to account for any reduction in resistance at the soil-concrete interface.

The modifications; reducing the characteristic deflection, increasing the ultimate soil resistance and introducing a shear force to the base of the shaft, were incorporated into new analyses of the drilled shafts described in

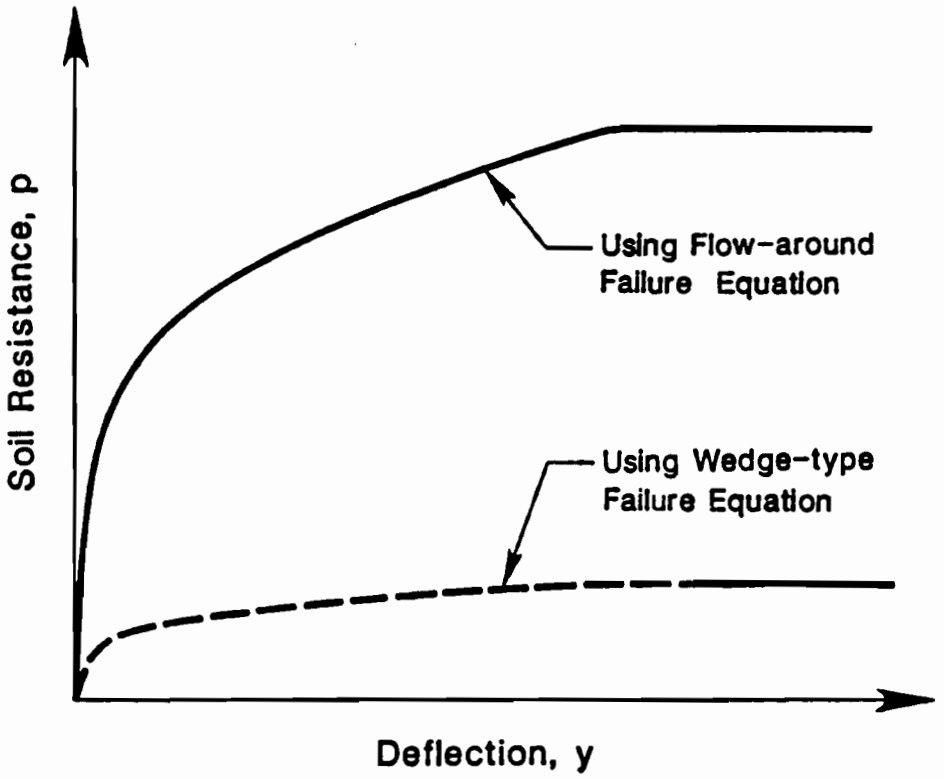

Figure 6.5: Effect in p-y Curve with Increase in Ultimate Soil Resistance, p_{ult}

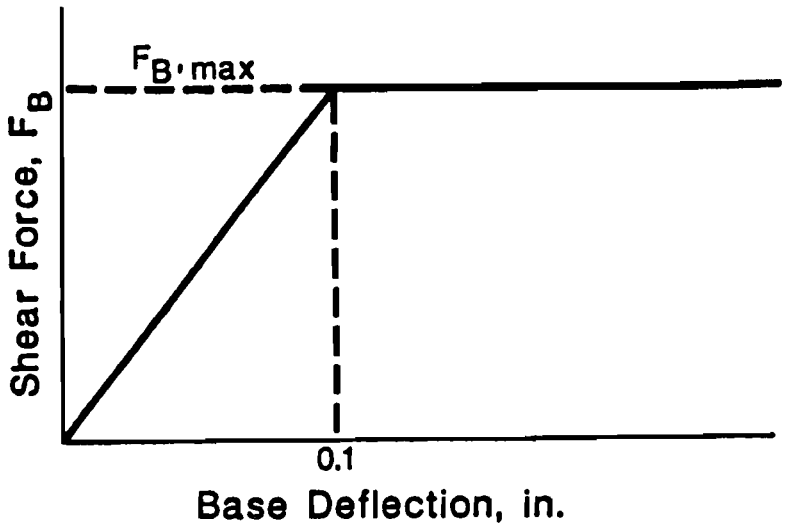

Figure 6.6: Form of Force-Deflection Curve, F_B - y

Chapter 4 and 5. The results of the new analyses are presented in the following chapter, Chapter 7.

CHAPTER 7. RESULTS OF ANALYSES USING MODIFIED PROCEDURES

New analyses on the eleven drilled shafts presented in Chapters 4 and 5; shafts No. 1, 4, 5, 6, 7, 8, 9, 10, 12, 13 and 14, were performed using the modified procedures presented in Chapter 6. Except for the modifications to the conventional procedures, the soil and shaft parameters as well as the loads used in the new analyses were identical to those used previously in Chapter 5.

7.1 APPLYING THE MODIFIED PROCEDURES TO THE DRILLED SHAFTS

Both the input parameters and the computer program COM624 were modified to accommodate the modified procedures described in Chapter 6. The first modification involved the reduction of the characteristic deflection, y_{50}, which is computed using the strain, ε_{50}, the shaft's diameter, D, and a dimensionless coefficient. The values of the coefficient will vary for the analysis of each shaft due to the various length-to-diameter ratios, L/D, involved. The values of y_{50} are computed internally by COM624 using Eqs. 6.1 and 6.2 and input values of the diameter and the strain (ε_{50}). It would be simpler to alter input values of the strain rather than modify COM624 to alter the coefficient for each new analysis. For example, if the coefficient in Eq. 6.1 needed to be reduced from 2.5 to 2.1, the strain, input into COM624, would be reduced to an equivalent strain, ε_{50}', which satisfied the following relationship:

$$y_{50} = 2.1\varepsilon_{50}D = 2.5\varepsilon_{50}'D \qquad (7.1)$$

For each shaft, values of the equivalent strain (ε_{50}') were computed based on the shaft's length-to-diameter ratio. Equivalent strains considered in the analyses are presented in Table 7.1 for corresponding values of the length-to-diameter ratios.

The second modification consisted of utilizing ultimate soil resistances, p_{ult}, calculated from equations for a flow-around failure, for depths below

Table 7.1
Correction for y_{50}
Equivalent ε_{50} Values

	Length-to-Diameter Ratio			
	$2 < L/D < 3$	$3 < L/D < 4$	$4 < L/D < 5$	$L/D \geq 5$
ε_{50} =	1.68	1.76	1.84	2.0
	0.84	0.88	0.92	1.0
	0.756	0.792	0.828	0.9
	0.672	0.704	0.736	0.8
	0.588	0.616	0.644	0.7
	0.420	0.440	0.460	0.5
	0.336	0.352	0.368	0.4
	0.252	0.264	0.276	0.3
	0.168	0.176	0.184	0.2
	0.084	0.088	0.092	0.1

Note: ε_{50}'s are in percent

the point of zero deflection. This was achieved by first constructing p-y curves, separately from COM624, and then introducing them into the computer program as part of the input data.

The final modification consisted of introducing a shear force at the base of the shaft. This was accomplished by modifying COM624 so that a force-deflection (F_B - y) curve for the base of the shaft could be included as input data. The values of the ultimate force, $F_{B,max}$ used in the analysis for each drilled shaft are presented in Table 7.2.

7.2 RESULTS OF ANALYSES

The predicted deflections at the top of the shaft, y_t, from the analyses using the modified procedures are presented in Table 7.3 along with the measured top of shaft deflections. Plots of the top of shaft deflection versus the applied moment are presented in Figs. 7.1 through 7.11. Three sets of deflections are presented in each figure: deflections measured in the load tests, those computed using the conventional procedures and those computed using the modified procedures.

7.2.1 Predicted Top of Shaft Deflection

The deflections at the top of the shaft computed using the modified procedures generally agreed more closely with the measured values than the values computed using the conventional procedures. In the analyses using the conventional procedures, two loads, one each for shafts No. 7 and 13, produced predicted deflections lower than the measured values; the analyses using the modified procedures predicted slightly lower deflections.

The ratios of the predicted-to-measured deflections at the top of the shaft are summarized in Table 7.3. The average value of the ratios based on the modified procedures was 5.19; the standard deviation was 12.0. These values are significantly better than those based on the conventional procedures where the average and standard deviation were 14.7 and 41.6, respectively (Chapter 5). The number of instances where the predicted-to-measured ratio was greater than ten was only three using the modified procedures compared to the eight cases which occurred using the conventional procedures. If the three ratios greater than 10 are excluded,

Table 7.2
Ultimate Shear Force at Base of Shaft

Shaft No.	$F_{B,max}$ ($\times 10^3$ lb)
1	19.9
4	19.1
5	29.7
6	18.6
7	176.7
8	17.7
9	49.8
10	36.7
12	15.6
13	18.4
14	42.9

Table 7.3

Results from Analyses Using Modified Procedures
Top of Shaft Deflections and Predicted-to-Measured Ratios

Shaft No.	M_t ($\times 10^6$ lb-in)	Measured y_t (in)	Predicted y_t (in)	Predicted to Measured y_t Ratios
1				
	6	0.02	0.20	9.75
	12	0.74	1.04	1.41
	18	2.40	2.56	1.07
	24	4.50	5.26	1.17
4				
	6	0.05	0.33	6.64
	12	0.20	0.74	3.71
	18	0.43	1.22	2.84
	24	1.08	1.93	1.79
5				
	9	0.10	0.39	3.93
	18	0.36	0.95	2.64
	27	0.70	1.78	2.54
	36	1.16	2.96	2.55
6				
	4.5	0.03	0.38	12.6
	9	0.16	0.82	5.12
	13.5	0.41	1.28	3.12
	18	0.68	2.22	3.26

Table 7.3 (cont).

Shaft No.	M_t ($\times 10^6$ lb-in)	Measured y_t (in)	Predicted y_t (in)	Predicted to Measured y_t Ratios
7				
	3	0.09	0.014	0.16
	6	0.16	0.13	0.79
	9	0.30	0.54	1.78
	12	0.50	1.41	2.82
8				
	6	0.16	0.40	2.50
	12	0.40	0.86	2.16
	18	0.70	1.57	2.24
	24	1.21	2.65	2.19
9				
	3	0.008	0.010	1.28
	6	0.015	0.034	2.27
	9	0.027	0.072	2.66
	12	0.045	0.132	2.93
10				
	6	0.05	0.31	6.10
	12	0.18	0.65	3.62
	18	0.30	1.04	3.46
	24	0.72	1.54	2.14

Table 7.3 (cont.)

Shaft No.	M_t ($\times 10^6$ lb-in)	Measured y_t (in)	Predicted y_t (in)	Predicted to Measured y_t Ratios
12				
	2.25	0.01	0.051	5.11
	4.5	0.04	0.17	4.28
	6.75	0.08	0.51	6.40
	9	0.16	12.9	80.6
13				
	3	0.04	0.021	0.52
	6	0.09	0.09	1.00
	9	0.18	0.25	1.38
	12	0.35	0.52	1.48
14				
	3	0.02	0.03	1.54
	6	0.07	0.27	3.84
	9	0.16	1.08	6.75
	12	0.31	3.80	12.3

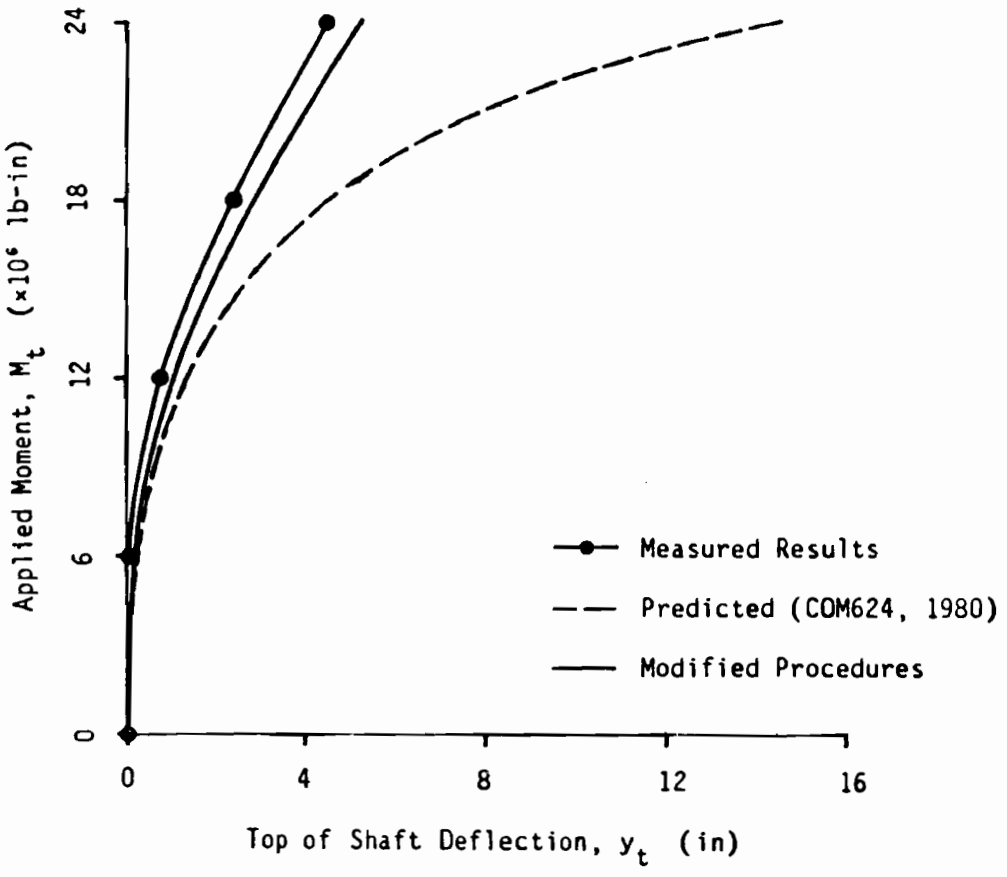

Figure 7.1: Top of Shaft Deflection versus Applied Moment for Shaft No. 1. - Conventional and Modified Procedures

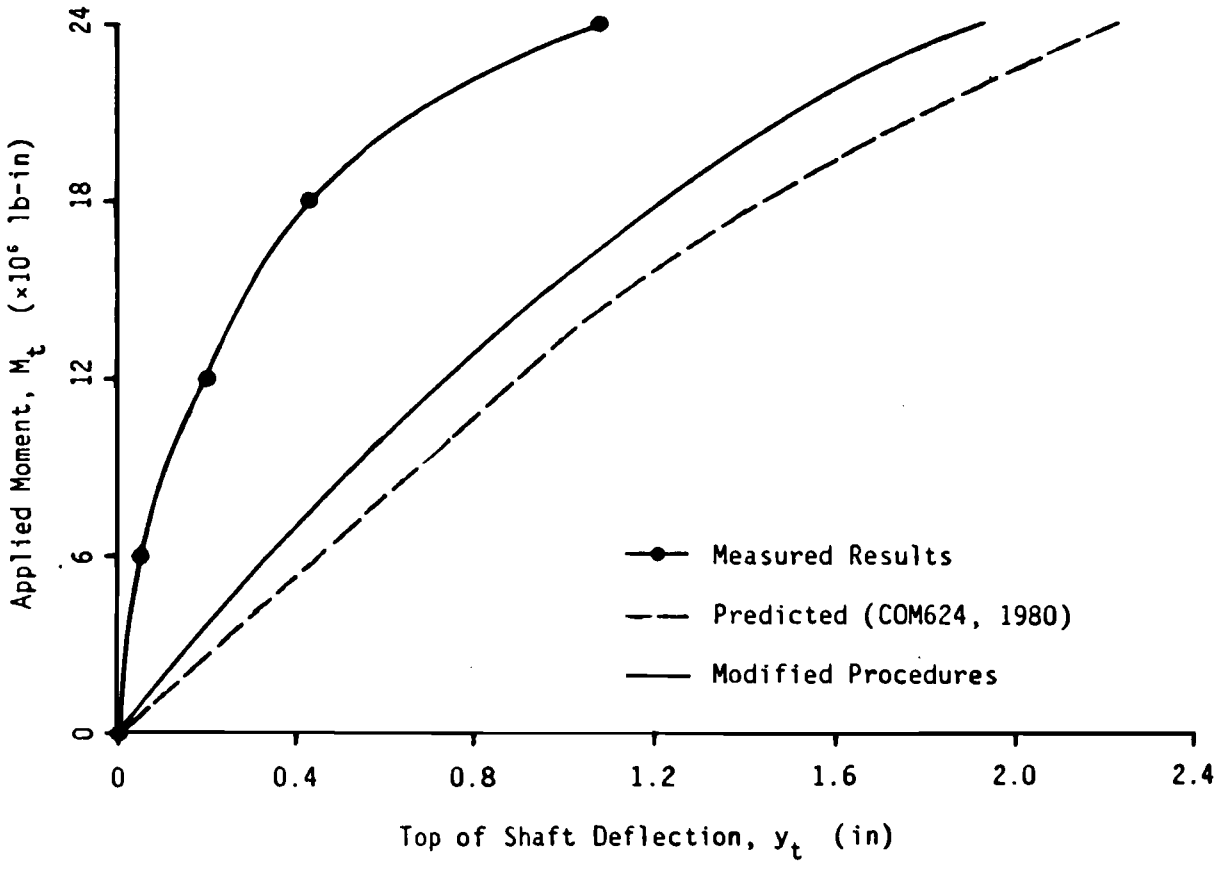

Figure 7.2: Top of Shaft Deflection versus Applied Moment for Shaft No. 4. - Conventional and Modified Procedures

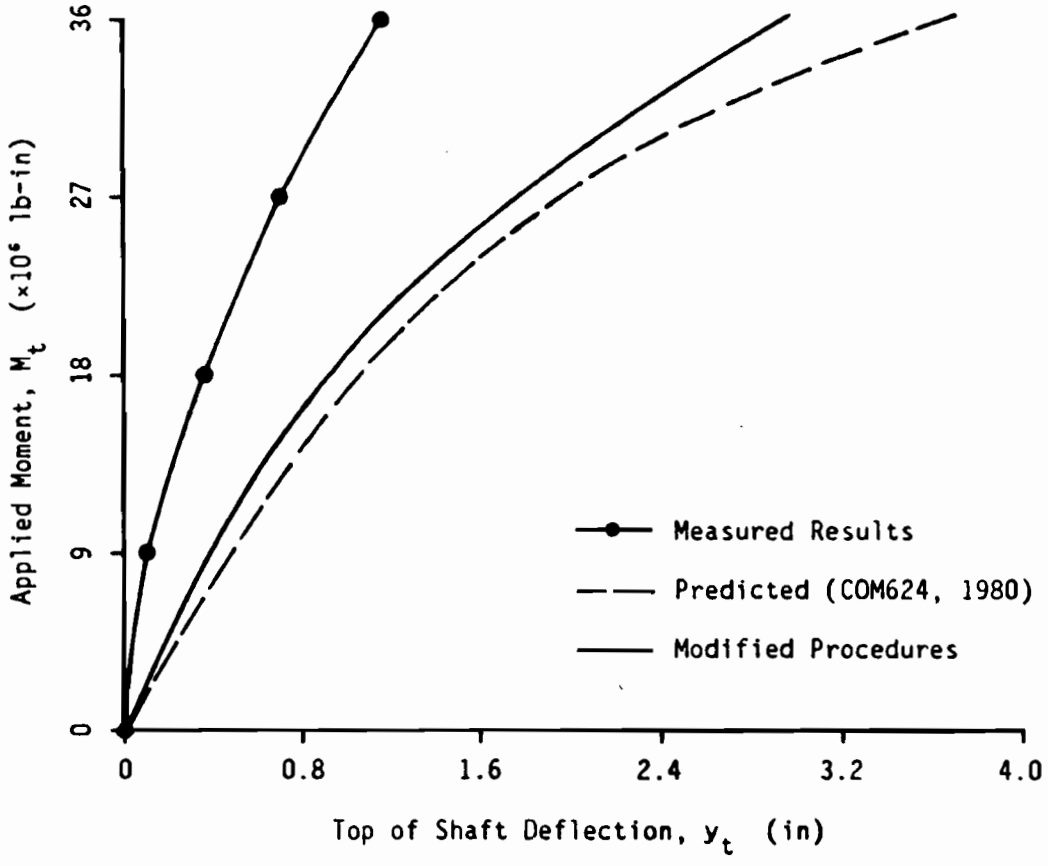

Figure 7.3: Top of Shaft Deflection versus Applied Moment for Shaft No. 5. - Conventional and Modified Procedures

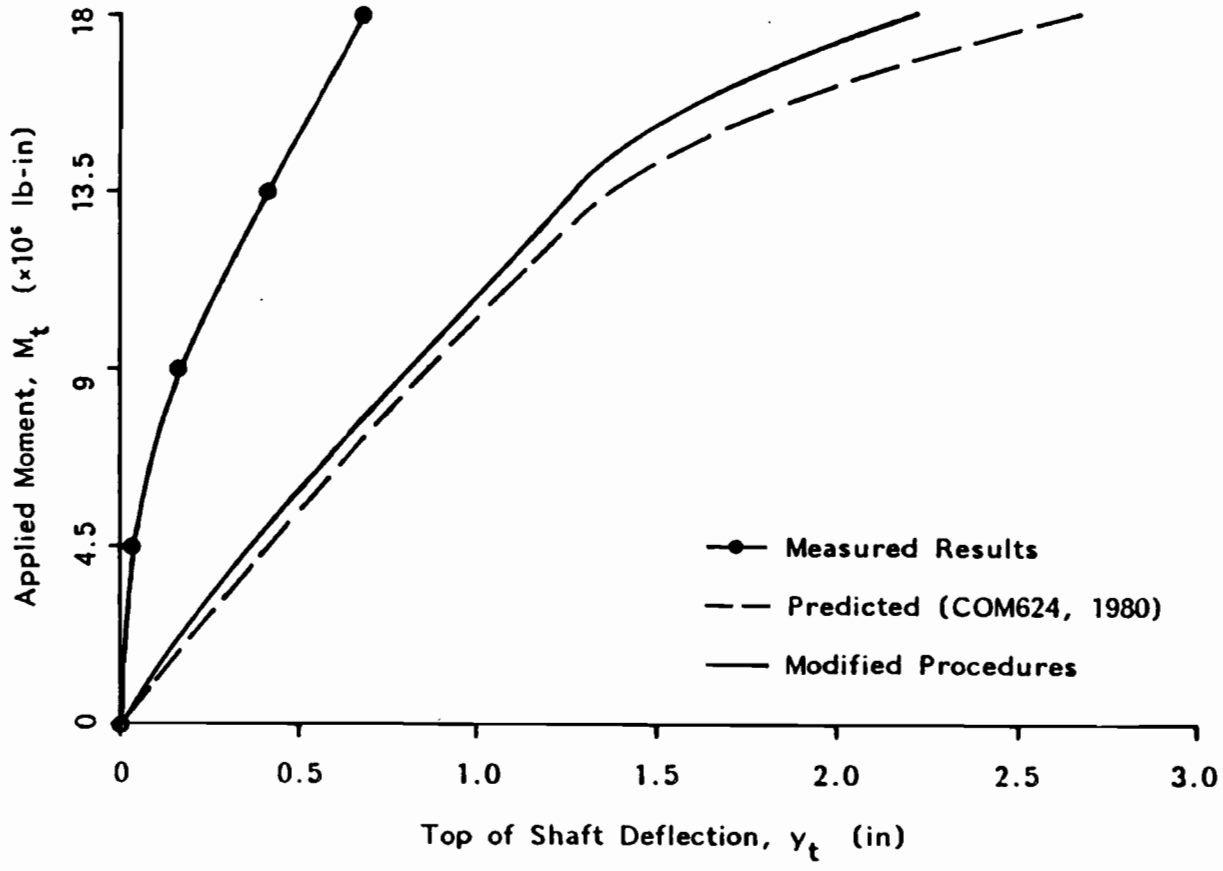

Figure 7.4: Top of Shaft Deflection versus Applied Moment for Shaft No. 6. - Conventional and Modified Procedures

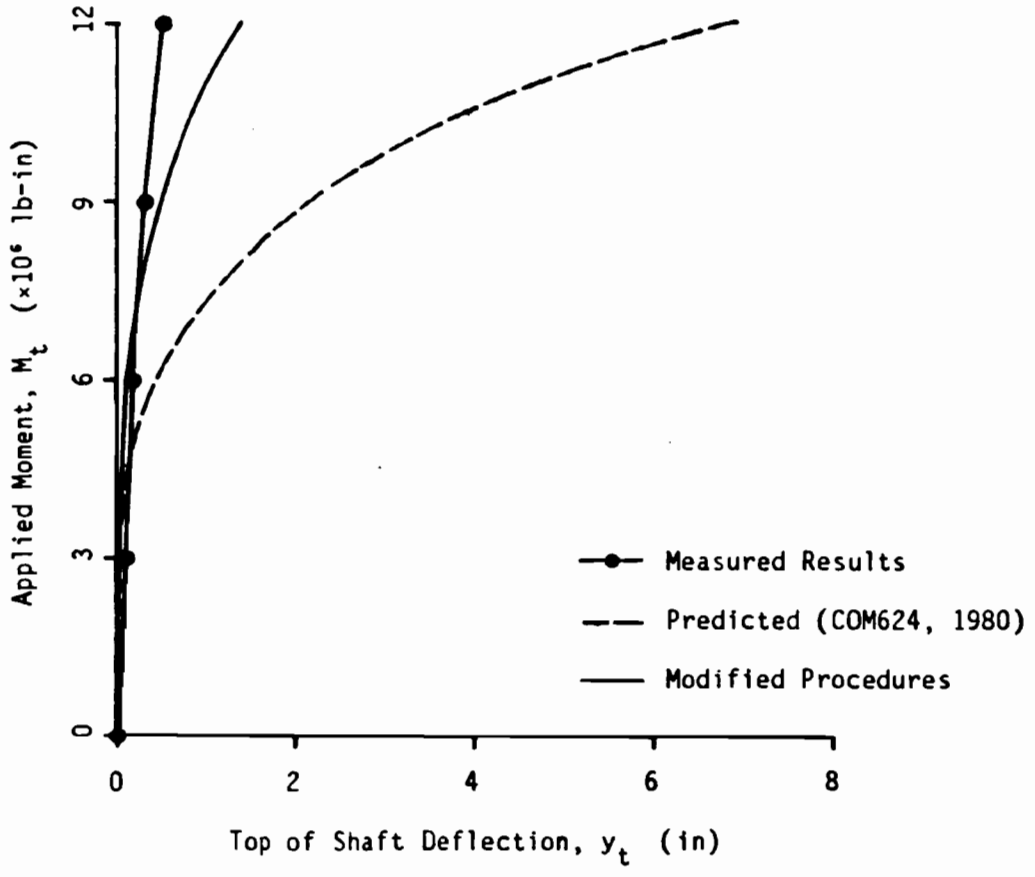

Figure 7.5: Top of Shaft Deflection versus Applied Moment for Shaft No. 7. - Conventional and Modified Procedures

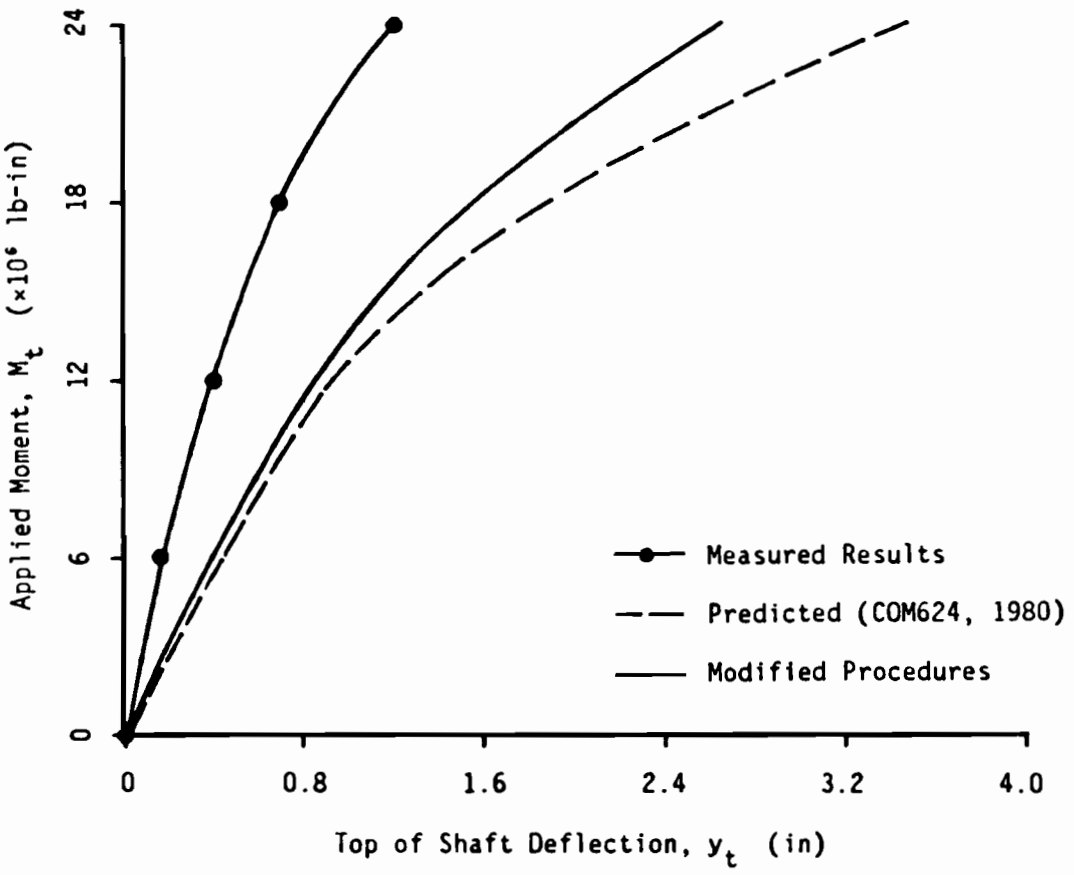

Figure 7.6: Top of Shaft Deflection versus Applied Moment for Shaft No. 8. - Conventional and Modified Procedures

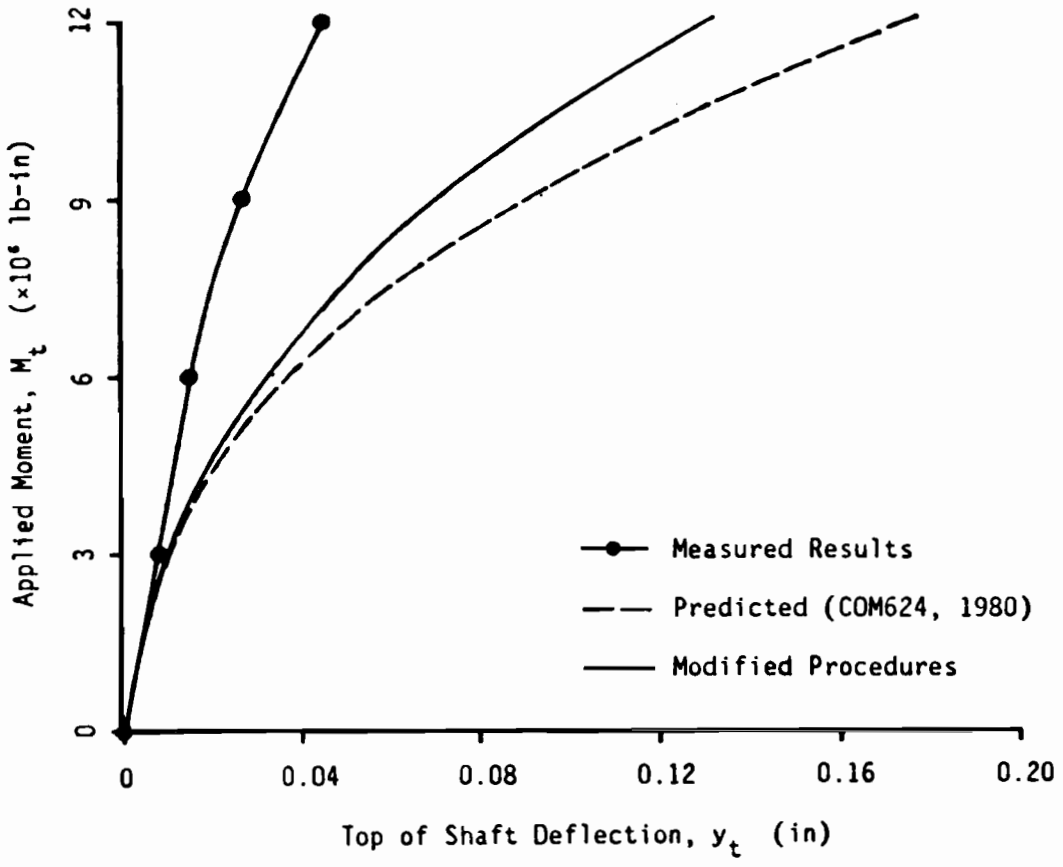

Figure 7.7: Top of Shaft Deflection versus Applied Moment for Shaft No. 9. - Conventional and Modified Procedures

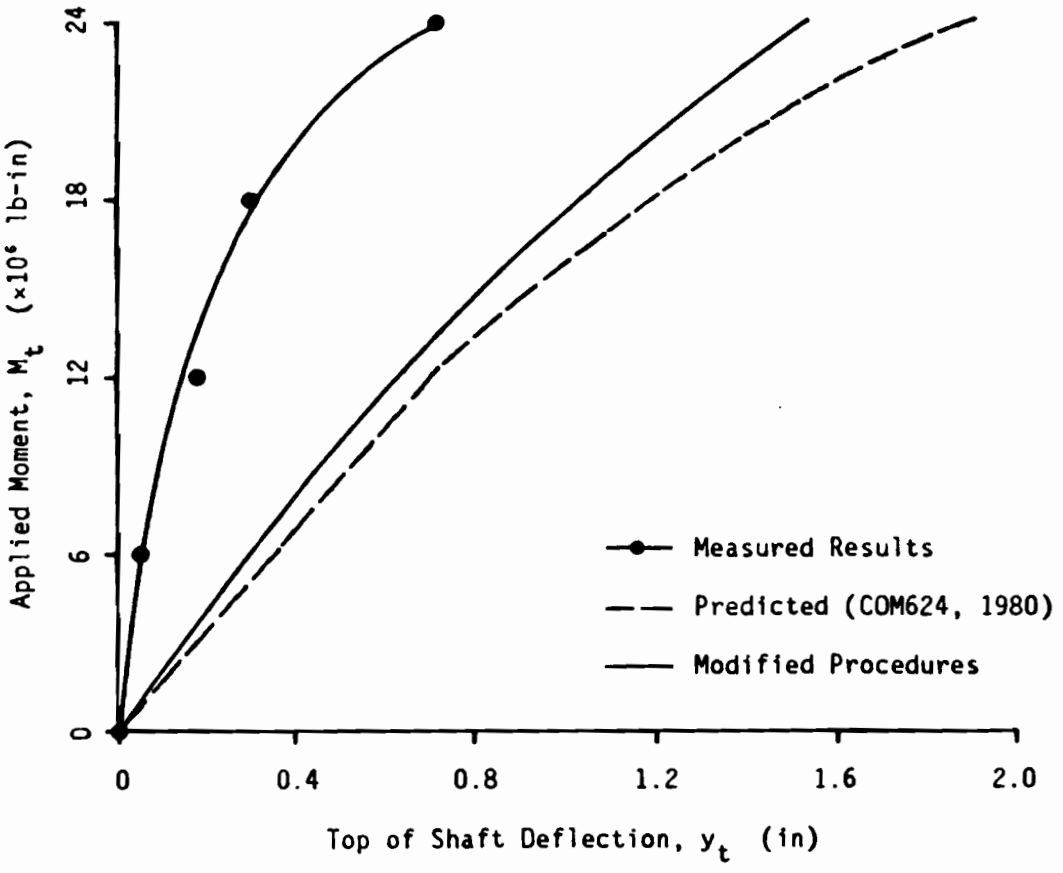

Figure 7.8: Top of Shaft Deflection versus Applied Moment for Shaft No. 10. - Conventional and Modified Procedures

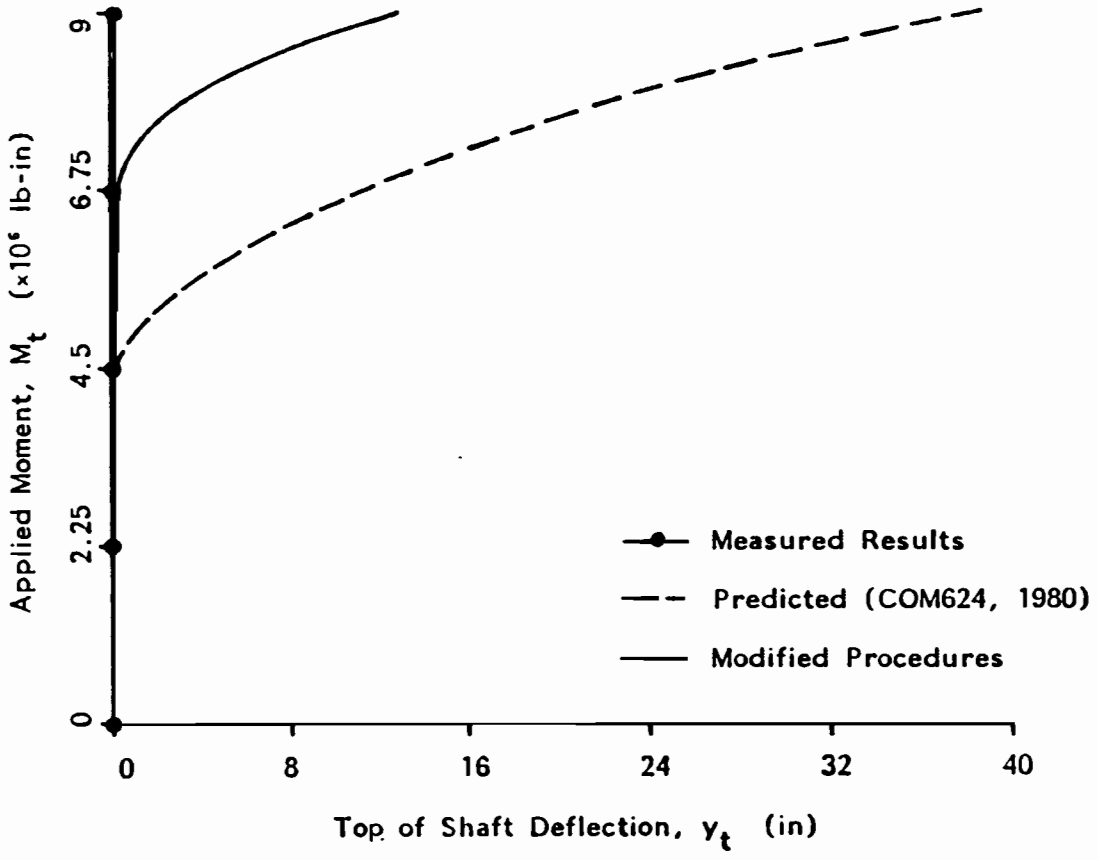

Figure 7.9: Top of Shaft Deflection versus Applied Moment for Shaft No. 12. - Conventional and Modified Procedures

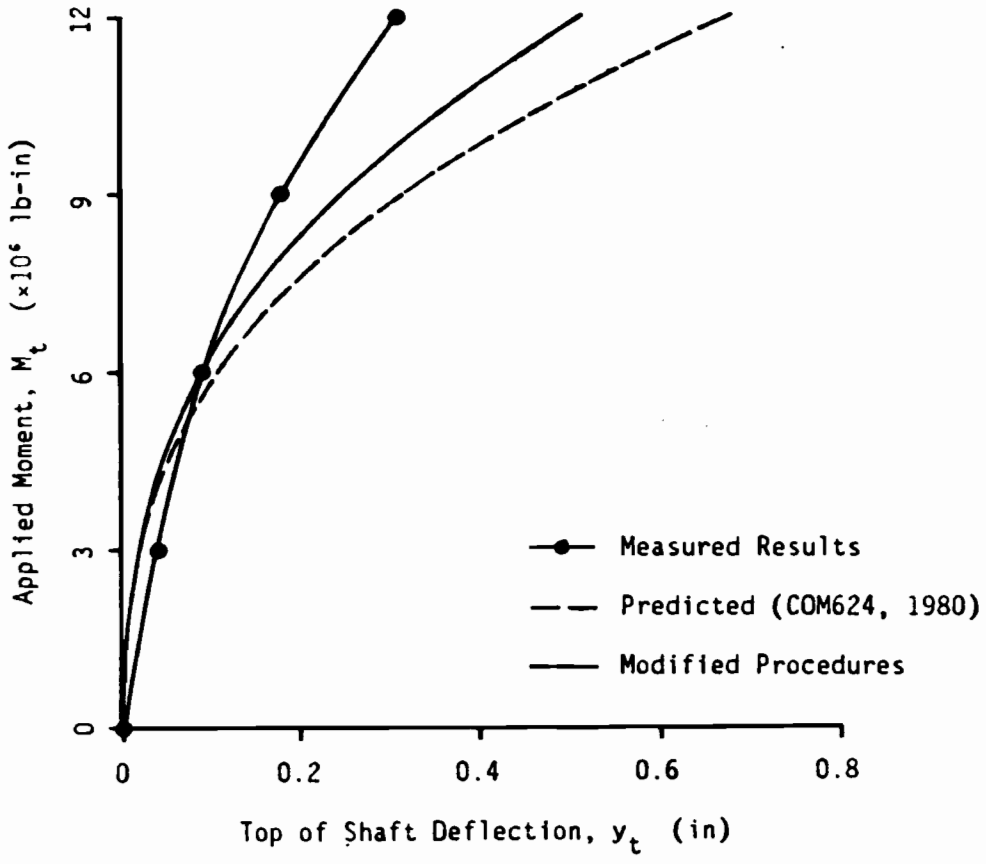

Figure 7.10: Top of Shaft Deflection versus Applied Moment for Shaft No. 13. - Conventional and Modified Procedures

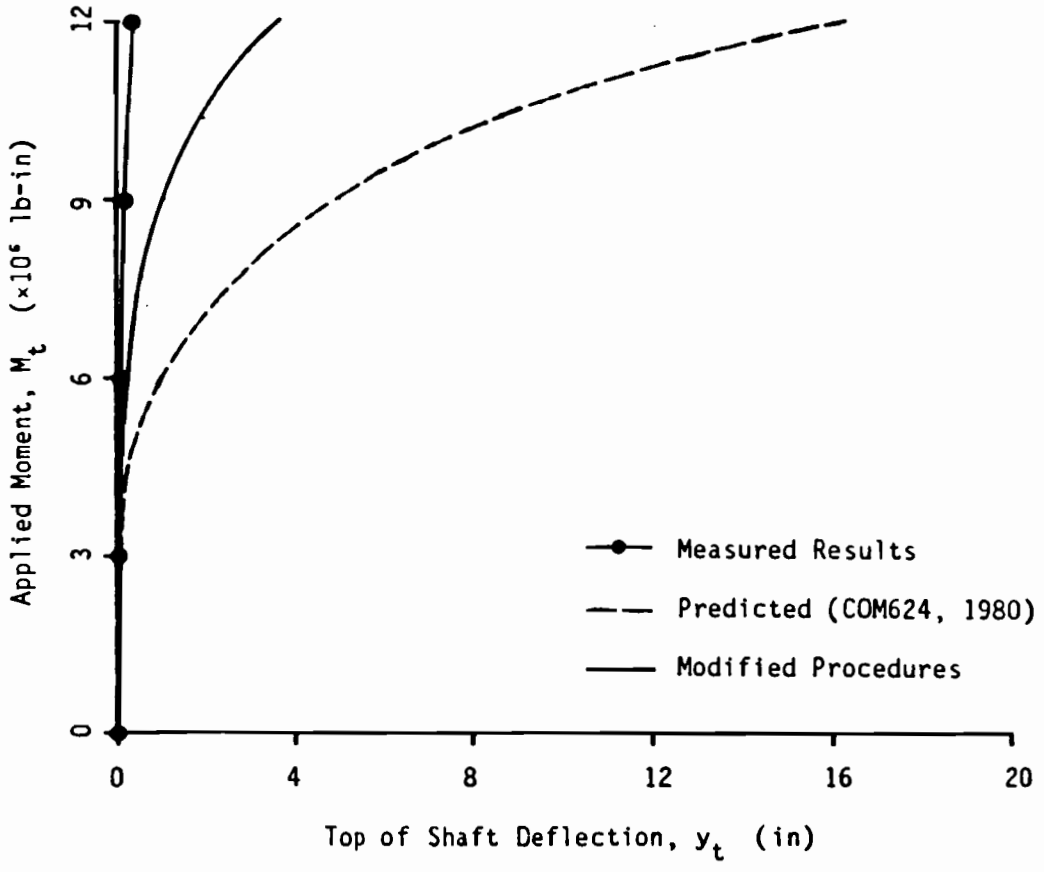

Figure 7.11: Top of Shaft Deflection versus Applied Moment for Shaft No. 14. - Conventional and Modified Procedures

the average of the ratios of the predicted-to-measured deflections and the standard deviation reduced to 3.00 and 1.86, respectively for the modified procedures.

7.2.2 Deflected Shapes of Drilled Shafts

Computations with the modified procedures still indicate that the drilled shafts would deflect as essentially rigid members. However, as shown in Fig. 7.12 for shaft No. 7, the computed points of zero deflection were further down the drilled shaft than the points computed using the conventional procedures. Consequently, the deflections at the base of the shaft decreased from those computed in the analyses using the conventional procedures. The ratios between the distance to the point of zero deflection, L_z, and the total length of the shaft, L, are presented in Table 7.4. The deflections at the base of the shaft are presented in Table 7.5.

7.3 CONCLUSION

The modified procedures, described in Chapter 6, appear to reduce the discrepancies between the computed and measured responses of "short" drilled shafts. To confirm this observation, further analyses were performed on nine additional drilled shafts. The results from these additional analyses are presented in the following chapter, Chapter 8.

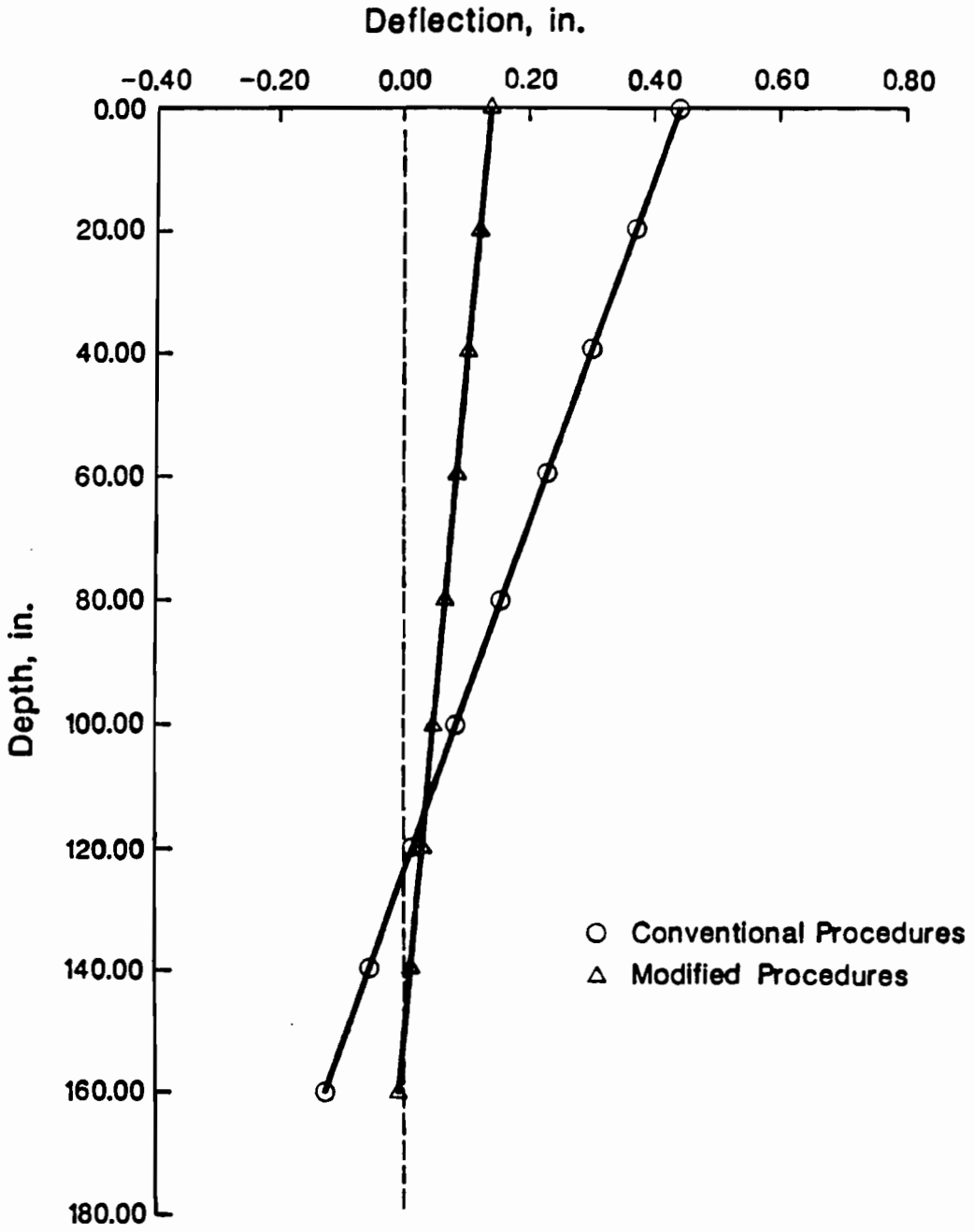

Figure 7.12: Deflected Shape of Shaft No. 7 at an Applied Moment = 6 $\times 10^6$ lb-in

Table 7.4
Ratio of Distance to Point of Zero Deflection, L_z to Total Length, L

Shaft No.	M_t ($\times 10^6$ lb-in)	Ratios from Conventional Procedures	Ratios from Modified Procedures
1			
	6	0.64	0.66
	12	0.72	0.77
	18	0.73	0.77
	24	0.73	0.81
4			
	6	0.64	0.70
	12	0.65	0.67
	18	0.65	0.67
	24	0.66	0.68
5			
	9	0.64	0.66
	18	0.65	0.66
	27	0.66	0.67
	36	0.68	0.69
6			
	4.5	0.77	0.80
	9	0.78	0.80
	13.5	0.77	0.79
	18	0.68	0.82

Table 7.4 cont.

Shaft No.	M_t ($\times 10^6$ lb-in)	Ratios from Conventional Procedures	Ratios from Modified Procedures
7			
	3	0.74	0.87
	6	0.75	0.92
	9	0.75	0.94
	12	0.75	0.95
8			
	6	0.70	0.73
	12	0.70	0.71
	18	0.71	0.72
	24	0.70	0.74
9			
	3	0.70	0.69
	6	0.75	0.76
	9	0.77	0.79
	12	0.77	0.81
10			
	6	0.78	0.81
	12	0.78	0.80
	18	0.77	0.79
	24	0.77	0.80

Table 7.4 cont.

Shaft No.	M_t ($\times 10^6$ lb-in)	Ratios from Conventional Procedures	Ratios from Modified Procedures
12			
	2.25	0.60	0.63
	4.5	0.68	0.72
	6.75	0.86	0.80
	9	0.86	0.92
13			
	3	0.53	0.53
	6	0.66	0.68
	9	0.71	0.73
	12	0.77	0.76
14			
	3	0.67	0.81
	6	0.68	0.84
	9	0.68	0.86
	12	0.68	0.84

Table 7.5
Results of Drilled Shaft Analyses
Base of Shaft Deflections

Shaft No.	M_t ($\times 10^6$ lb-in)	Deflection from Conventional Proc. (in)	Deflection from Modified Proc. (in)
1			
	6	0.14	0.089
	12	0.51	0.35
	18	1.64	0.73
	24	5.37	1.24
4			
	6	0.20	0.12
	12	0.41	0.33
	18	0.67	0.55
	24	1.09	0.84
5			
	9	0.25	0.18
	18	0.54	0.46
	27	0.94	0.82
	36	1.67	1.27
6			
	4.5	0.12	0.086
	9	0.23	0.20
	13.5	0.39	0.31
	18	0.73	0.47

Table 7.5 cont.

Shaft No.	M_t ($\times 10^6$ lb-in)	Deflection from Conventional Proc. (in)	Deflection from Modified Proc. (in)
7			
	3	0.008	0.0008
	6	0.14	0.009
	9	0.72	0.031
	12	2.29	0.075
8			
	6	0.19	0.14
	12	0.39	0.34
	18	0.78	0.59
	24	1.53	0.91
9			
	3	0.002	0.002
	6	0.008	0.006
	9	0.022	0.013
	12	0.044	0.024
10			
	6	0.087	0.061
	12	0.18	0.15
	18	0.33	0.24
	24	0.54	0.35

Table 7.5 cont.

Shaft No.	M_t ($\times 10^6$ lb-in)	Deflection from Conventional Proc. (in)	Deflection from Modified Proc. (in)
12			
	2.25	0.043	0.029
	4.5	0.10	0.065
	6.75	1.91	0.13
	9	6.20	1.17
13			
	3	0.005	0.004
	6	0.036	0.023
	9	0.11	0.067
	12	0.21	0.13
14			
	3	0.027	0.003
	6	0.47	0.049
	9	2.39	0.17
	12	7.76	0.73

CHAPTER 8. ADDITIONAL ANALYSES ON DRILLED SHAFTS

To establish further the validity of the modifications described in Chapter 6, data were obtained for nine additional load tests performed on "short" drilled shafts. Analyses were performed for each of these additional drilled shafts using both the conventional procedures, currently employed by COM624, and the modified procedures developed as part of the current study.

8.1 DESCRIPTION OF DRILLED SHAFTS

The nine additional drilled shafts are designated by the numbers 15 through 23 for reference and to distinguish them from the fourteen shafts considered previously. Data for the drilled shafts were obtained from the report by the Electric Power Research Institute, EPRI, (1982); however, the load tests were sponsored and conducted, independent of EPRI, by three power companies (Table 8.1). The drilled shafts were cast-in-place concrete ranging in diameters from 24 to 96 inches, lengths ranging from 108 to 240 inches and structural stiffnesses (E_pI_p) ranging from 5.08×10^{10} to 1.30×10^{13} lb-in^2. Soil profiles of the test sites varied from layers of sands, silts and clays to a uniform layer of hard, sandy clay. The diameter, length, structural stiffness and general soil profile for each drilled shaft are presented in Table 8.2.

8.1.1 Loading of Drilled Shafts

The drilled shafts were loaded in various ways. Shafts 15 and 16 were loaded using a long steel pole, 90 feet in length. The pole was attached to the top of the drilled shafts and a horizontal force applied to the top of the pole, thus applying a moment to the drilled shafts along with the lateral force. Shafts 17 though 20 were loaded horizontally by a system of two jacks. The jacks were located to create a moment-to-shear (lateral) force ratio equivalent to a moment arm of 80 feet, thus eliminating the need of a long steel pole to simulate an electrical transmission tower. Shafts 21 though 23

Table 8.1
Sponsors and Additional References for Additional Drilled Shafts

Shaft No.	Sponsor	Reference
15	Pennsylvania Power and Light Company	Huang and Chen (1977)
16	Pennsylvania Power and Light Company	Huang and Chen (1977)
17	Ontario Hydro	Adams and Radhakrishna (1978)
18	Ontario Hydro	Adams and Radhakrishna (1978)
19	Ontario Hydro	Adams and Radhakrishna (1978)
20	Ontario Hydro	Adams and Radhakrishna (1978)
21	Southern California Edision	Bhushan, Haley and Fong (1979)
22	Southern California Edision	Bhushan, Haley and Fong (1979)
23	Southern California Edision	Bhushan, Haley and Fong (1979)

Table 8.2
Additional Drilled Shafts
Shaft Dimensions and Soil Profile

Shaft Number	Shaft Length (in)	Shaft Diameter (ft)	Stiffness, $E_p I_p$ ($\times 10^{11}$ lb-in^2)	Generalized Soil Profile
15	17.0	96.0	130	Stiff clayey silt
16	17.0	66.0	29	Stiff clayey silt
17	20.0	60.0	20	Silty sands over medium dense sand
18	20.0	60.0	20	Sands over glacial till
19	20.0	36.0	2.6	Silty sands over medium dense sand
20	20.0	36.0	2.6	Sands over glacial till
21	16.25	48.0	8.2	Hard stiff clay
22	13.25	48.0	8.2	Hard stiff clay
23	9.0	24.0	0.51	Hard stiff clay

were loaded using a jack which applied only a lateral force to the drilled shafts; no moments were induced.

Appropriate components of the lateral force and/or moment comprised the loads used in the computer analysis of each drilled shaft. Four, incremental loads, used for the computations on each shaft, were based on a maximum load which was at least 60 percent of the largest load applied in the load test. Unlike the analyses on the previously considered shafts, the loads were not reduced because convergence was obtained for all loads used in the analyses with either the conventional or modified procedures. The loads used in the analysis of each shaft are presented in Table 8.3.

8.1.2 Input Data for Analyses

The strength parameters (s_u and ϕ) and the effective unit weights (γ') for the various soils were obtained directly from the EPRI report. Values of the soil modulus variation with depth, m, and the strain, ε_{50}, were estimated base on values suggested by Reese and Sullivan (1980), presented previously in Chapter 4. The soil and shaft parameters used in the analyses are presented in Figs. 8.1 through 8.9.

For the analyses using the modified procedures, the modifications were applied in the same manner as for the previously analyzed drilled shafts (Chapter 7). The length-to-diameter ratios, for determining the values of the equivalent strain, ε_{50}', and the ultimate shear forces at the base of the shaft, $F_{B,max}$, for each drilled shaft are presented in Table 8.4.

8.2 RESULTS OF ANALYSES

The application of a lateral force was common in all load tests, thus deflections at the top of the shaft, y_t, are presented in terms of lateral forces, P_t. Deflections of the top of shaft, predicted by both conventional and modified procedures are presented in Table 8.5 along with measured values. Plots of the predicted and measured top of shaft deflections versus the lateral force are presented in Figs. 8.10 through 8.18.

Table 8.3

Applied Moment, Axial and Lateral Force Components Used in Analyses of Shafts No. 15 through 23

Shaft No.	Applied Moment M_t ($\times 10^6$ lb-in)	Lateral Force P_t ($\times 10^3$ lb)
15		
	6.0	5.56
	12.0	11.1
	18.0	16.7
	24.0	22.2
16		
	4.5	4.17
	9.0	8.33
	13.5	12.5
	18.0	16.7
17		
	4.5	4.69
	9.0	9.38
	13.5	14.1
	18.0	18.8
18		
	6.0	6.25
	12.0	12.5
	18.0	18.8
	24.0	25.0

Table 8.3 (cont.)

Shaft No.	Applied Moment M_t ($\times 10^6$ lb-in)	Lateral Force P_t ($\times 10^3$ lb)
19		
	4.5	4.69
	9.0	9.38
	13.5	14.1
	18.0	18.8
20		
	6.0	6.25
	12.0	12.5
	18.0	18.8
	24.0	25.0
21		
	NA	100
	NA	200
	NA	300
	NA	400
22		
	NA	75
	NA	150
	NA	225
	NA	300
23		
	NA	25
	NA	50
	NA	75
	NA	100

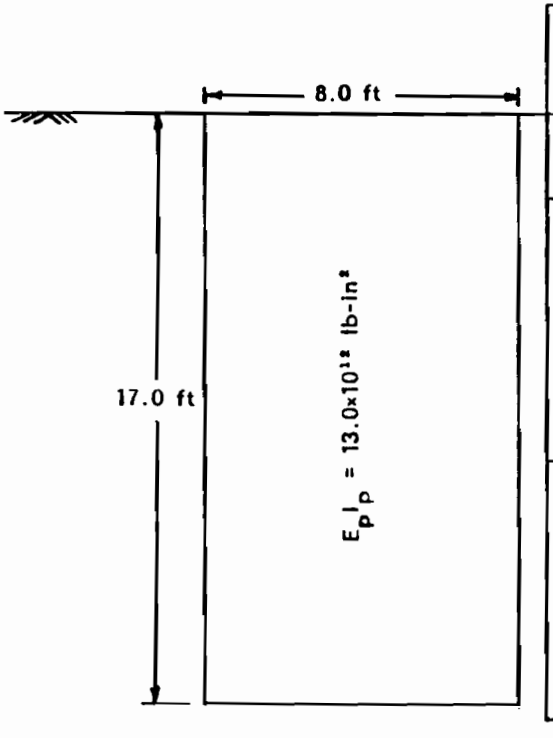

Depth, x (ft)	s_u (lb/ft^2)	ϕ' (deg.)	ε_{50} (%)	m (lb/in^3)	γ' (lb/ft^3)
0	500	--	2.0	30	119
2.5	2800	--	0.7	1000	130
10.0 ▽	3300	--	0.5	1250	67
17.5					

Figure 8.1: Soil and Drilled Shaft Data Used for COM624 Input, Shaft No. 15.

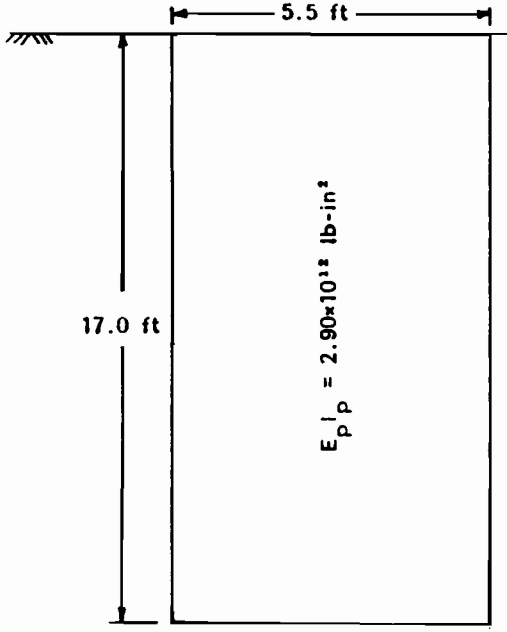

Depth, x (ft)	s_u (lb/ft²)	ϕ' (deg.)	ε_{50} (%)	m (lb/in³)	γ' (lb/ft³)
0	750	--	2.0	30	119
2.5	1600	--	1.0	750	124
5.0	3700	--	0.5	1000	130
10.0	2600	--	0.7	1250	67
17.5					

Figure 8.2: Soil and Drilled Shaft Data Used for COM624 Input, Shaft No. 16.

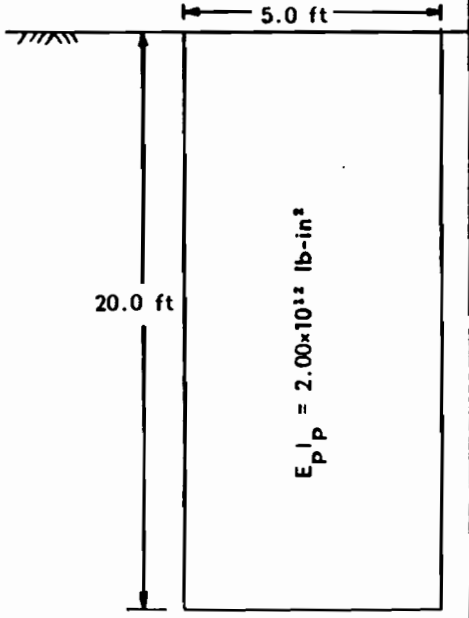

Depth, x (ft)	s_u (lb/ft²)	ϕ' (deg.)	ε_{50} (%)	m (lb/in³)	γ' (lb/ft³)
0					
	--	29	--	25	100
5.0					
	--	36	--	90	119
8.0					
	--	33	--	70	119
12.0					
	--	36	--	90	119
16.0 ▽					
	--	33	--	70	59
21.0					

Figure 8.3: Soil and Drilled Shaft Data Used for COM624 Input, Shaft No. 17.

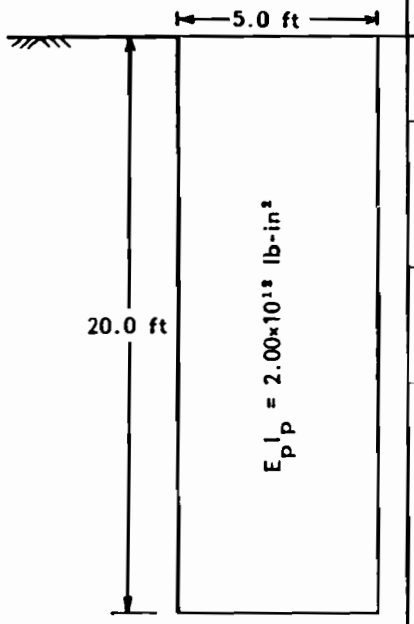

Depth, x (ft)	s_u (lb/ft²)	ϕ' (deg.)	ε_{50} (%)	m (lb/in³)	γ' (lb/ft³)
0	--	34	--	90	120
3.0	4700	--	0.4	2000	145
8.0	7200	--	0.4	2000	145
12.0	10000	--	0.4	2000	145
21.0					

Figure 8.4: Soil and Drilled Shaft Data Used for COM624 Input, Shaft No. 18.

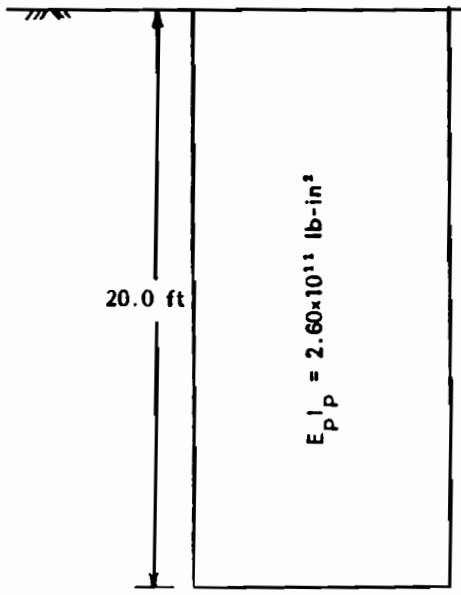

Depth, x (ft)	s_u (lb/ft²)	ϕ' (deg.)	ε_{50} (%)	m (lb/in³)	γ' (lb/ft³)
0	--	29	--	25	100
5.0	--	36	--	90	119
8.0	--	33	--	70	119
12.0	--	36	--	90	119
16.0 ▽	--	33	--	70	59
21.0					

Figure 8.5: Soil and Drilled Shaft Data Used for COM624 Input, Shaft No. 19.

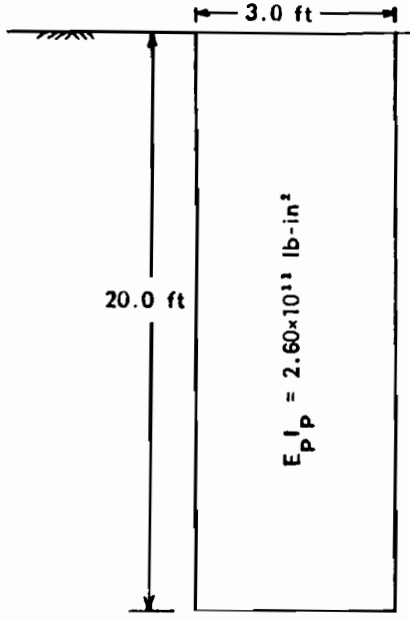

Depth, x (ft)	s_u (lb/ft²)	ϕ' (deg.)	ε_{50} (%)	m (lb/in³)	γ' (lb/ft³)
0					
	--	34	--	90	120
3.0					
	4700	--	0.4	2000	145
8.0					
	7200	--	0.4	2000	145
12.0					
	10000	--	0.4	2000	145
21.0					

Figure 8.6: Soil and Drilled Shaft Data Used for COM624 Input, Shaft No. 20.

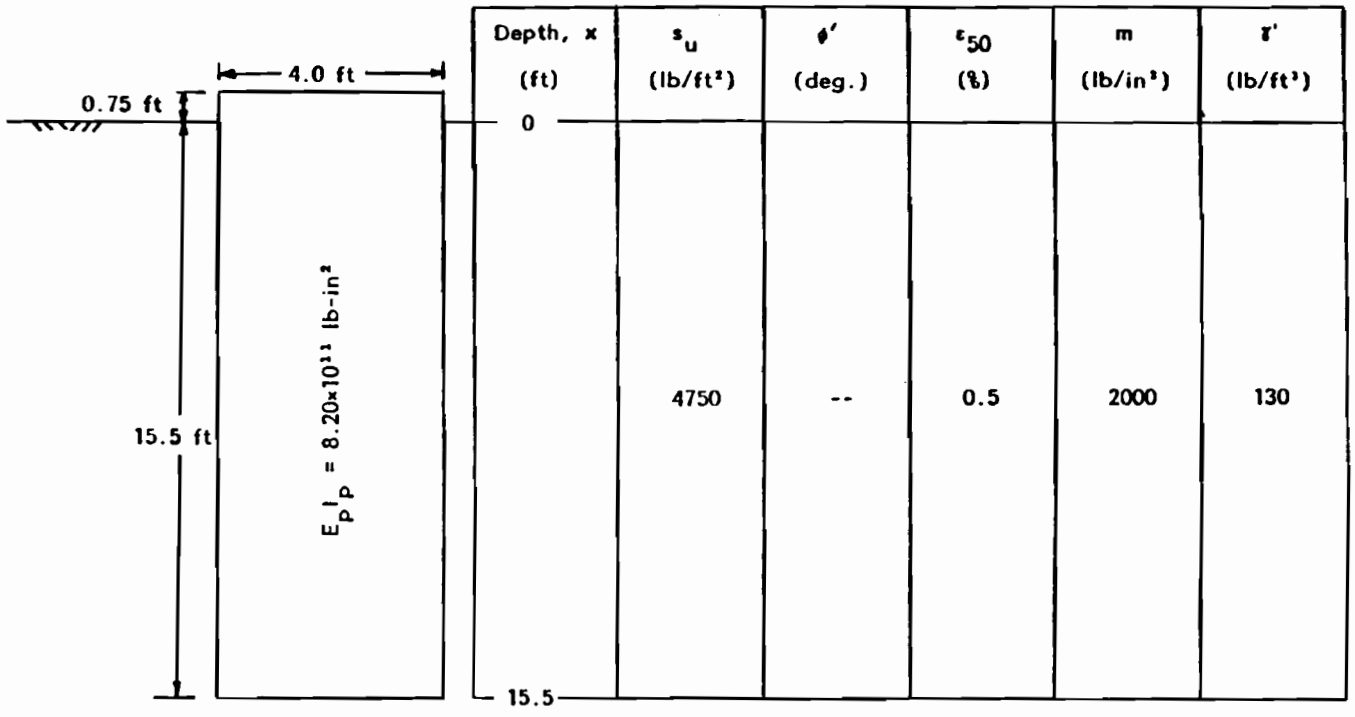

Depth, x (ft)	s_u (lb/ft²)	ϕ' (deg.)	ε_{50} (%)	m (lb/in³)	γ' (lb/ft³)
0					
	4750	--	0.5	2000	130
15.5					

Figure 8.7: Soil and Drilled Shaft Data Used for COM624 Input, Shaft No. 21.

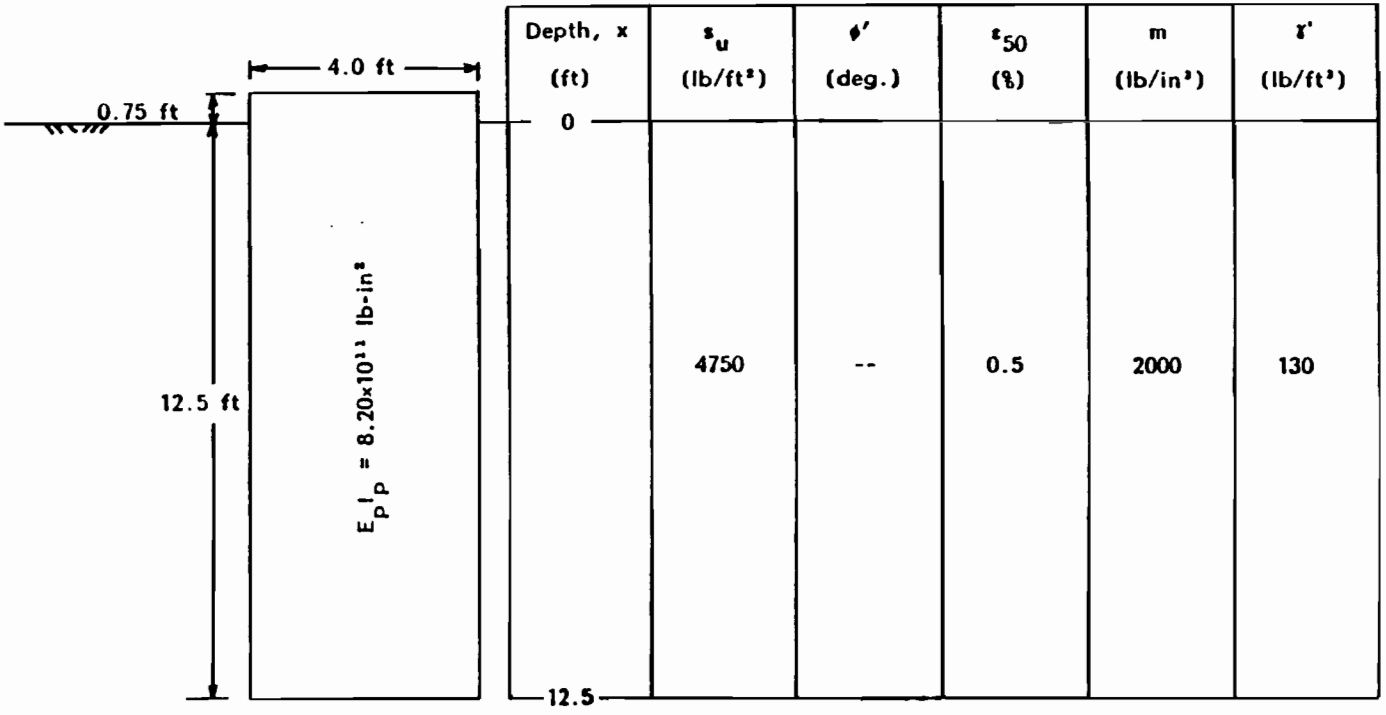

Figure 8.8: Soil and Drilled Shaft Data Used for COM624 Input, Shaft No. 22.

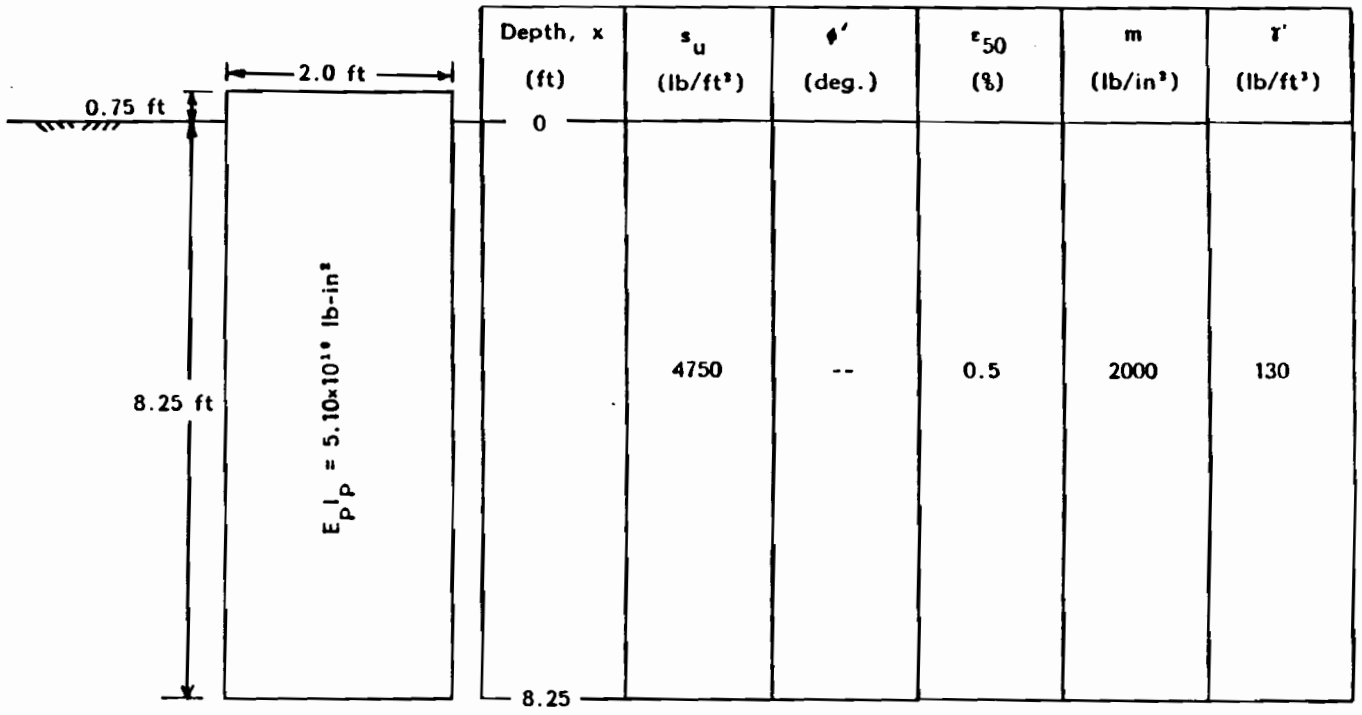

Figure 8.9: Soil and Drilled Shaft Data Used for COM624 Input, Shaft No. 23.

Table 8.4

Length-to-Diameter Ratios and Ultimate Shear Forces for Analyses with Modified Procedures

Shaft No.	Length-to-Diameter Ratio	$F_{B,max}$ ($\times 10^3$ lb)
15	2.1	167.6
16	3.1	61.4
17	4.0	23.3
18	4.0	197.7
19	6.7	10.6
20	6.7	70.8
21	3.9	59.7
22	3.1	59.7
23	4.1	14.9

Table 8.5

Results from Analyses Using Conventional and Modified Procedures
Top of Shaft Deflections

Shaft No.	P_t ($\times 10^3$ lb)	Measured y_t (in)	Conventional Procedures y_t (in)	Modified Procedures y_t (in)
15				
	5.56	0.014	0.044	0.024
	11.1	0.034	0.34	0.14
	16.7	0.061	1.1	0.37
	22.2	0.092	3.0	0.80
16				
	4.17	0.036	0.043	0.034
	8.33	0.14	0.28	0.18
	12.5	0.30	0.90	0.48
	16.7	0.51	2.05	1.16
17				
	4.69	0.016	0.17	0.15
	9.38	0.038	0.34	0.29
	14.1	0.082	0.52	0.46
	18.8	0.15	0.75	0.64
18				
	6.25	0.007	0.034	0.033
	12.5	0.02	0.10	0.086
	18.8	0.041	0.27	0.17
	25.0	0.068	0.66	0.30

Table 8.5 (cont.)

Shaft No.	P_t ($\times 10^3$ lb)	Measured y_t (in)	Conventional Procedures y_t (in)	Modified Procedures y_t (in)
19				
	4.69	0.10	0.28	0.27
	9.38	0.30	0.58	0.56
	14.1	0.56	1.02	0.97
	18.8	1.0	1.72	1.56
20				
	6.25	0.13	0.21	0.21
	12.5	0.35	0.55	0.54
	18.8	0.53	1.1	0.98
	25.0	0.73	2.3	1.6
21				
	100	0.22	0.069	0.066
	200	0.68	0.84	0.54
	300	1.4	4.1	2.6
	400	2.3	14.2	8.4
22				
	75	0.13	0.068	0.048
	150	0.55	0.95	0.48
	225	1.25	4.72	2.40
	300	2.1	17.2	7.90
23				
	25	0.08	0.054	0.046
	50	0.18	0.57	0.30
	75	0.34	2.7	1.10
	100	0.60	10.2	3.5

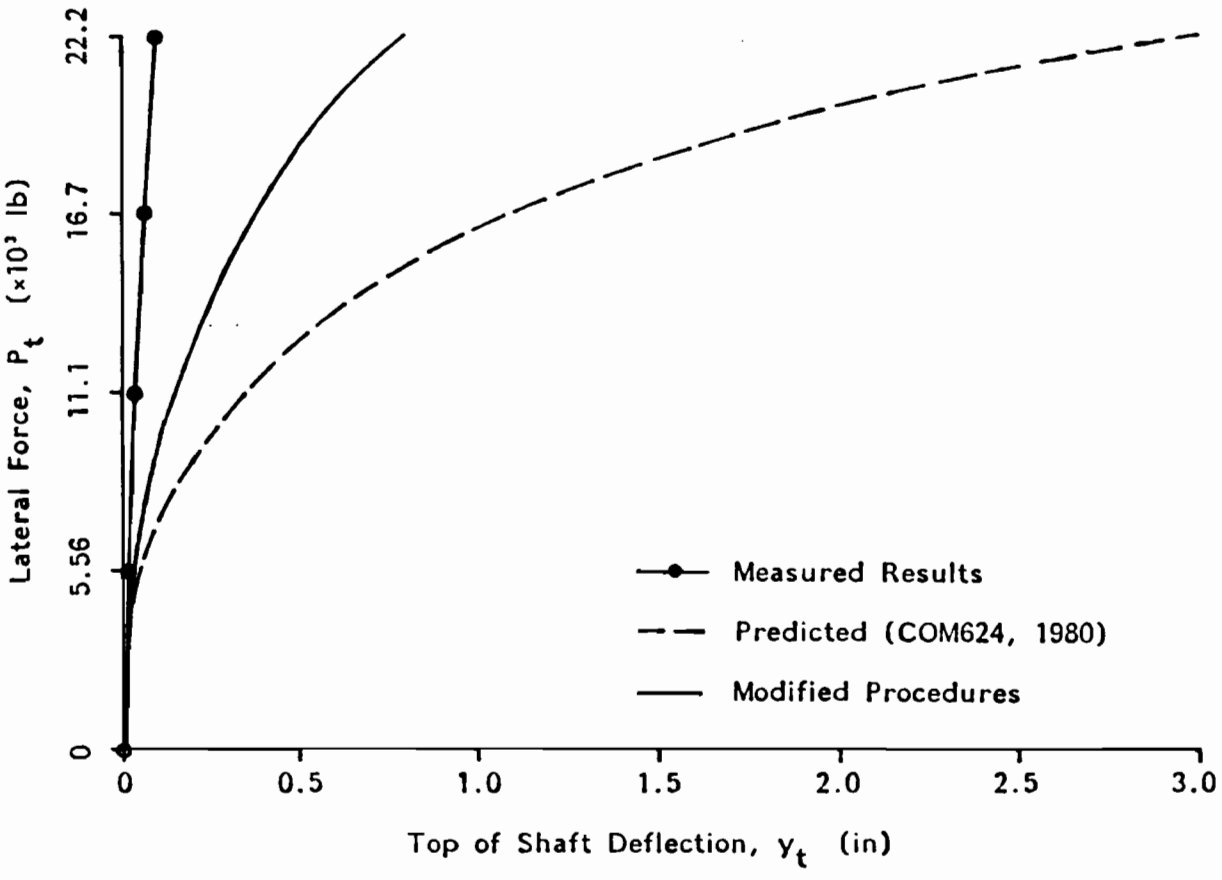

Figure 8.10: Top of Shaft Deflection versus Lateral Force for Shaft No. 15. - Conventional and Modified Procedures

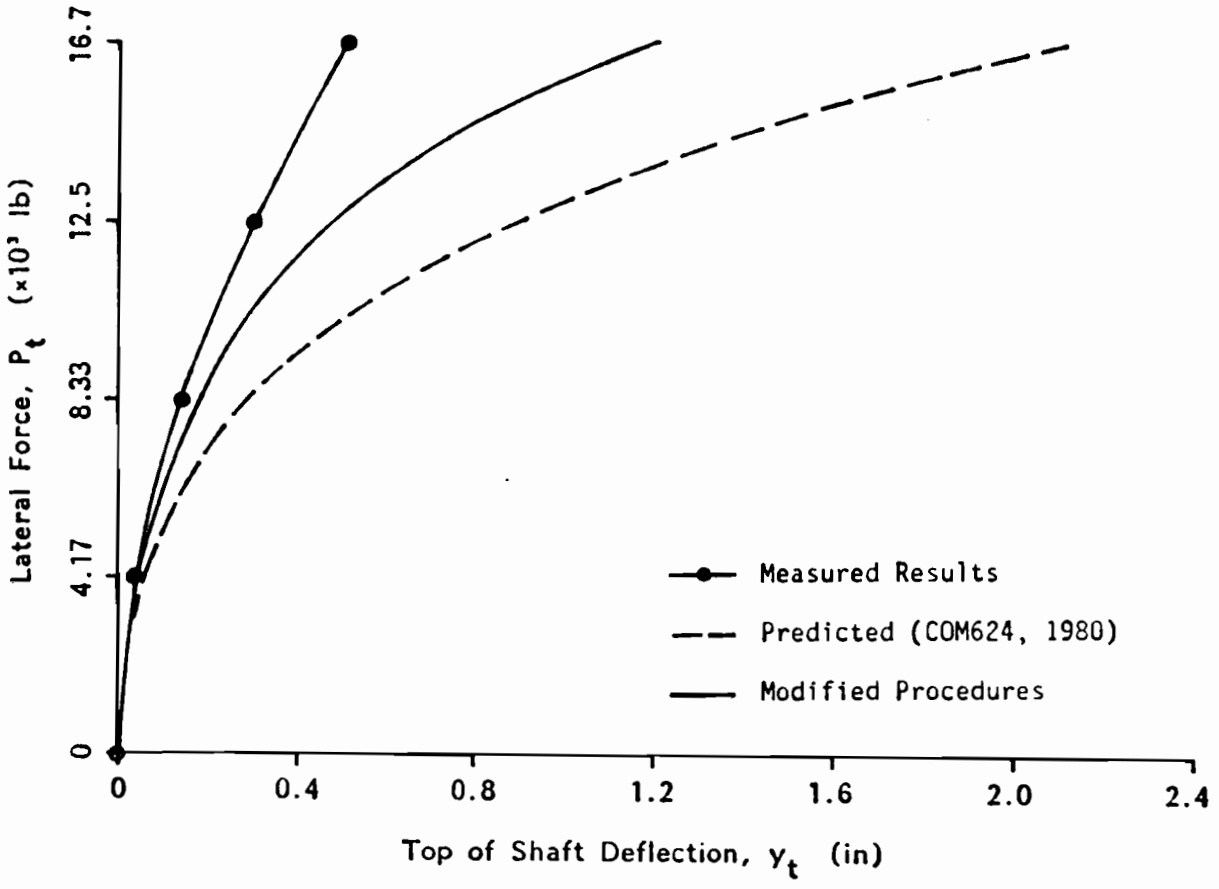

Figure 8.11: Top of Shaft Deflection versus Lateral Force for Shaft No. 16. - Conventional and Modified Procedures

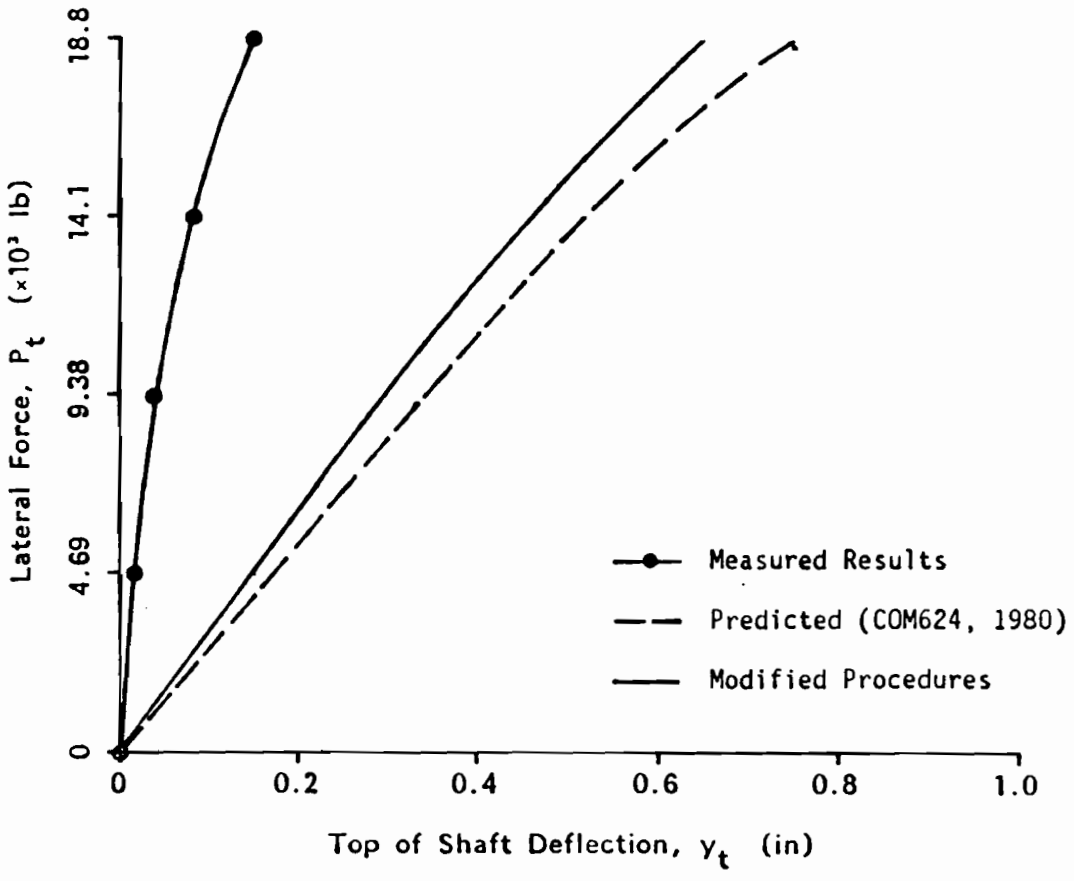

Figure 8.12: Top of Shaft Deflection versus Lateral Force for Shaft No. 17. - Conventional and Modified Procedures

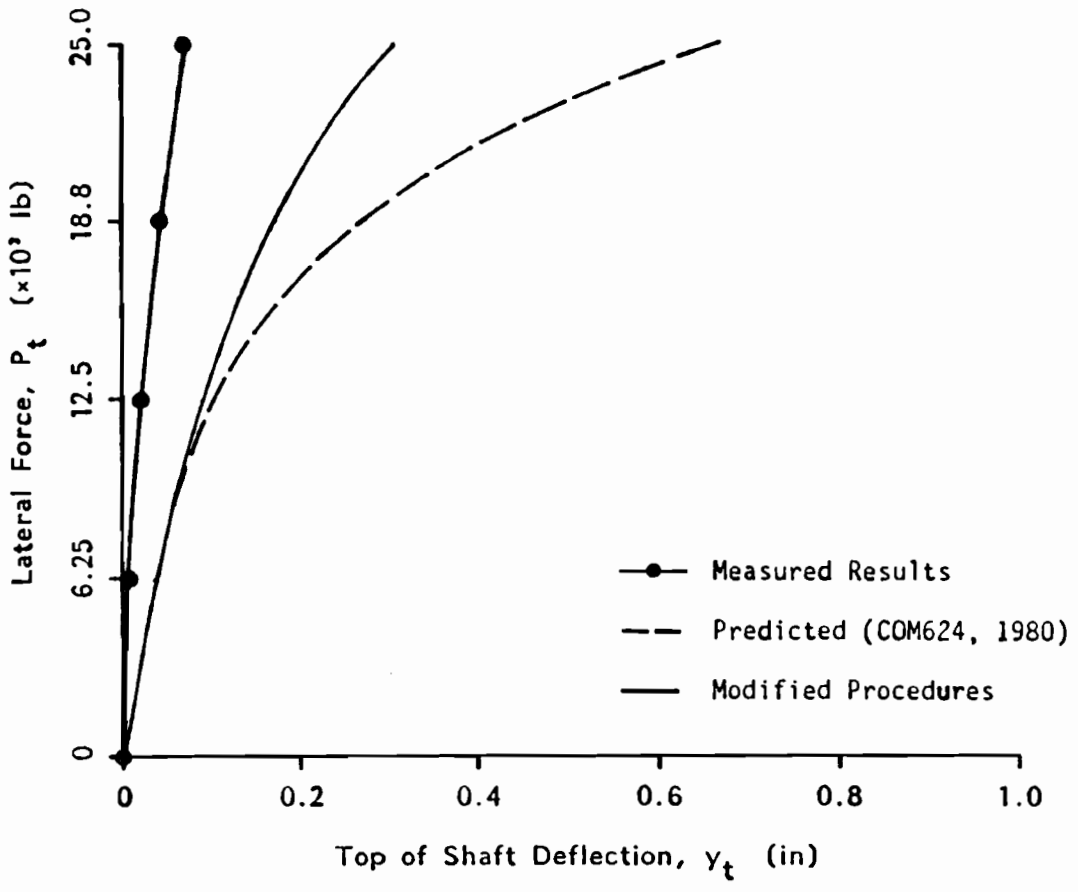

Figure 8.13: Top of Shaft Deflection versus Lateral Force for Shaft No. 18. - Conventional and Modified Procedures

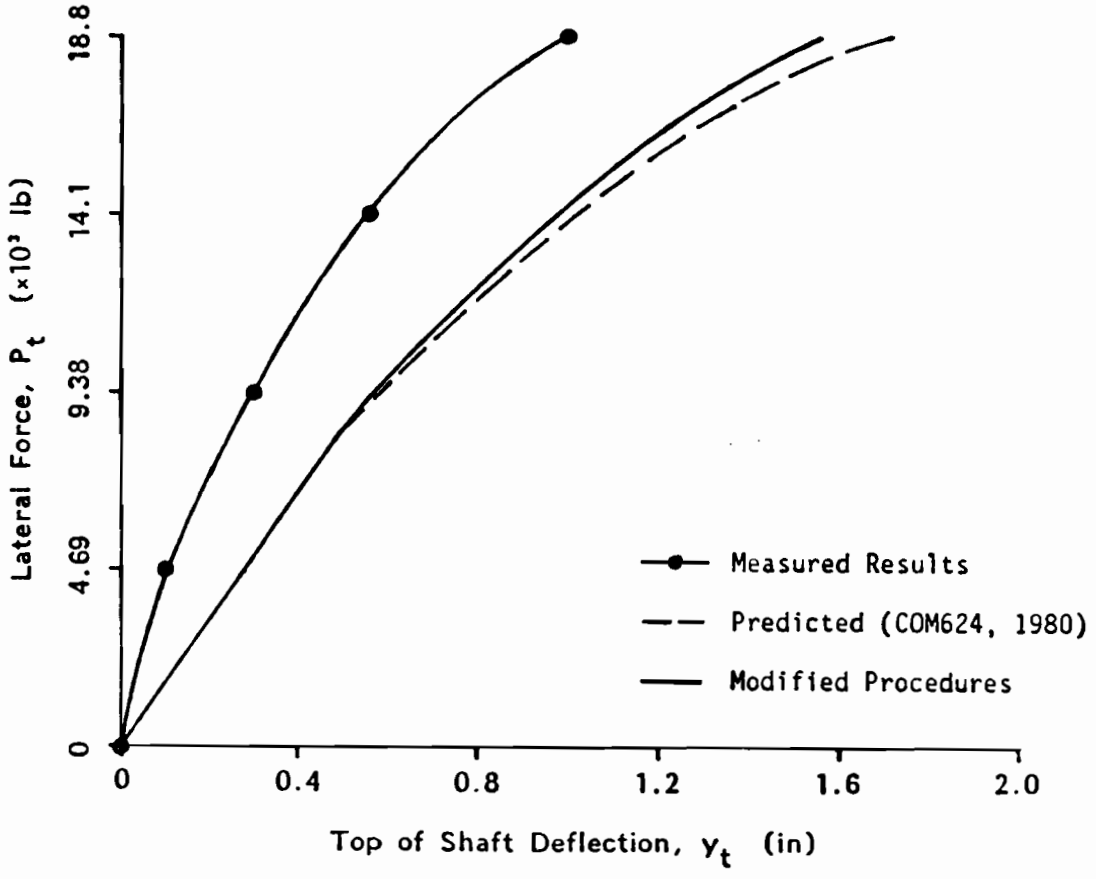

Figure 8.14: Top of Shaft Deflection versus Lateral Force for Shaft No. 19. - Conventional and Modified Procedures

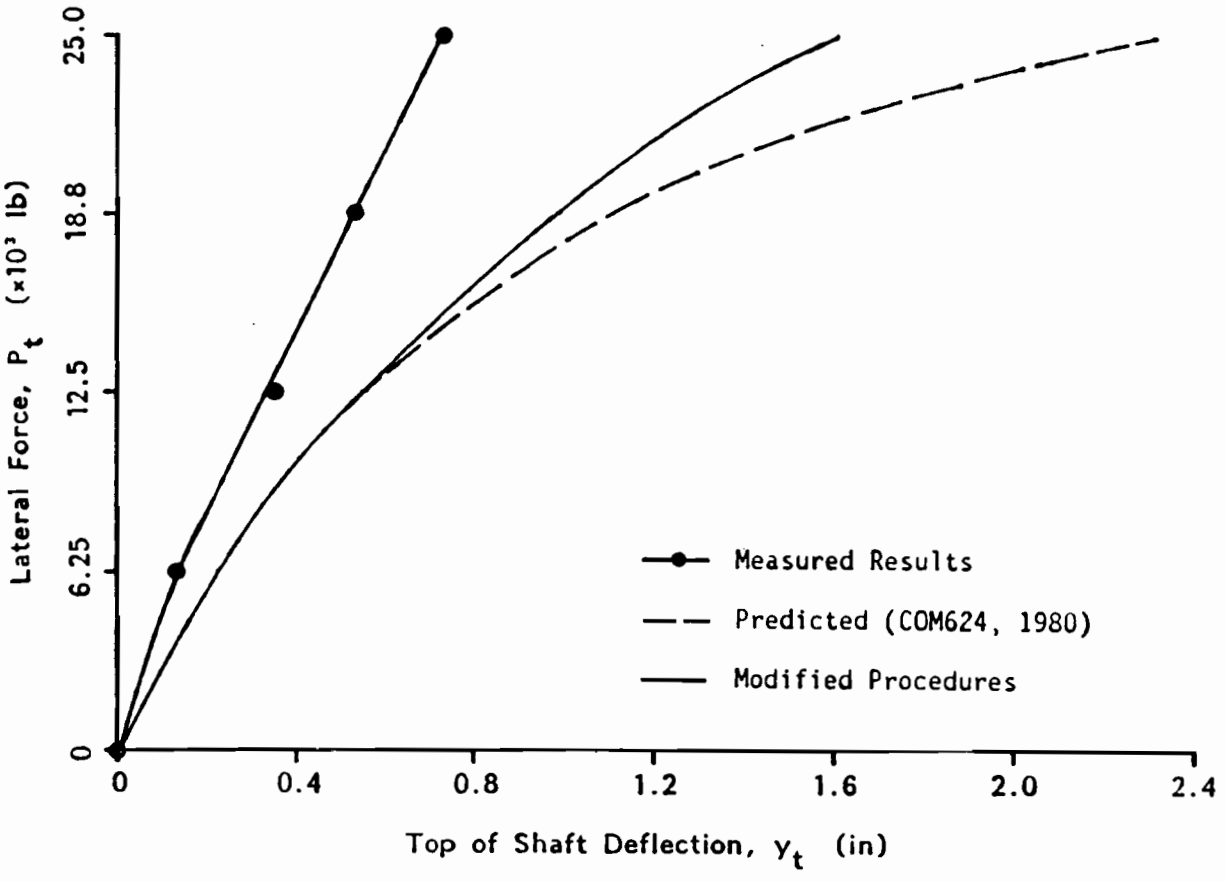

Figure 8.15: Top of Shaft Deflection versus Lateral Force for Shaft No. 20. - Conventional and Modified Procedures

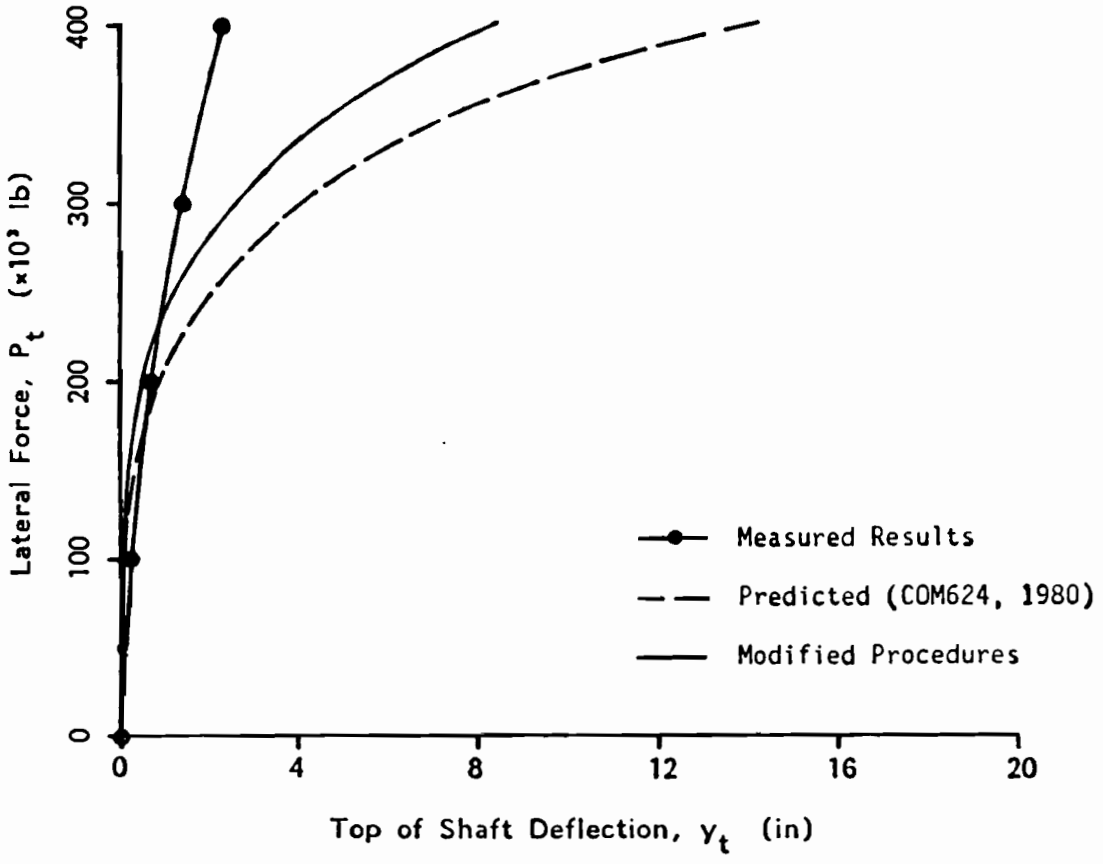

Figure 8.16: Top of Shaft Deflection versus Lateral Force for Shaft No. 21. - Conventional and Modified Procedures

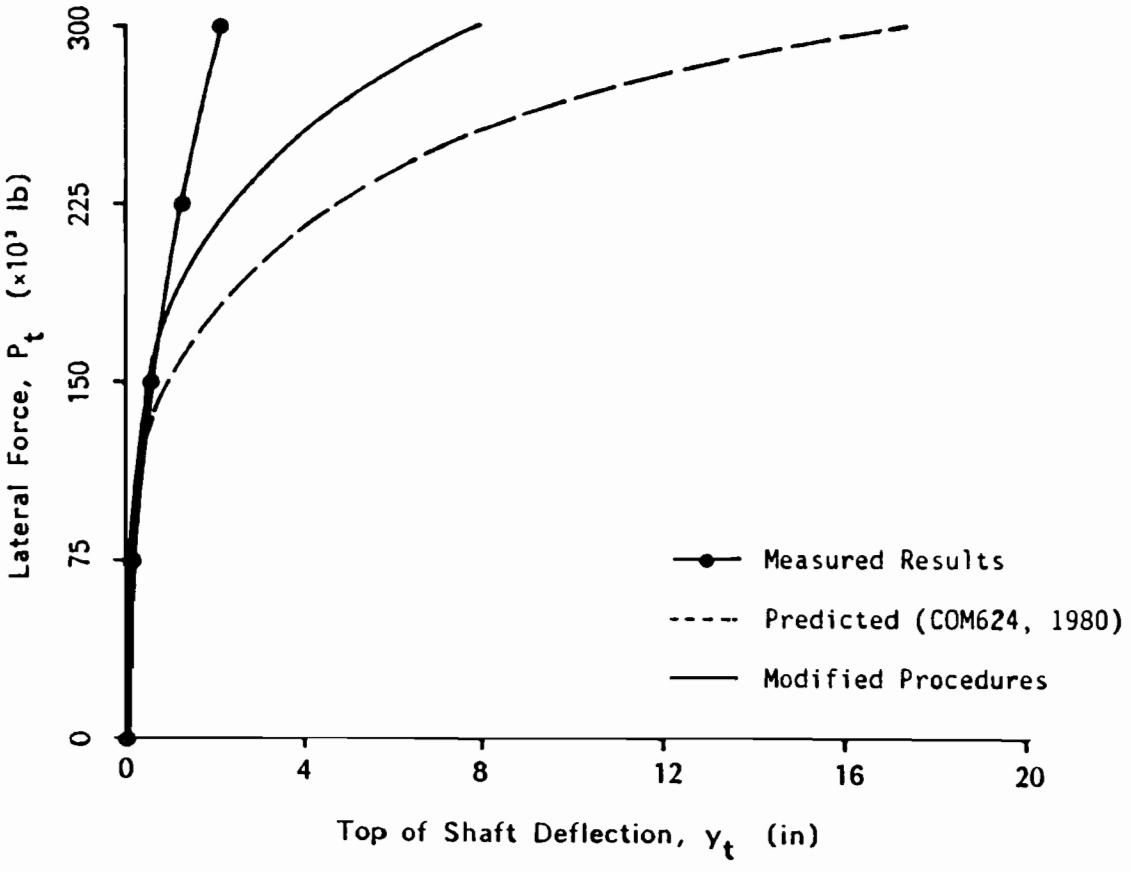

Figure 8.17: Top of Shaft Deflection versus Lateral Force for Shaft No. 22. - Conventional and Modified Procedures

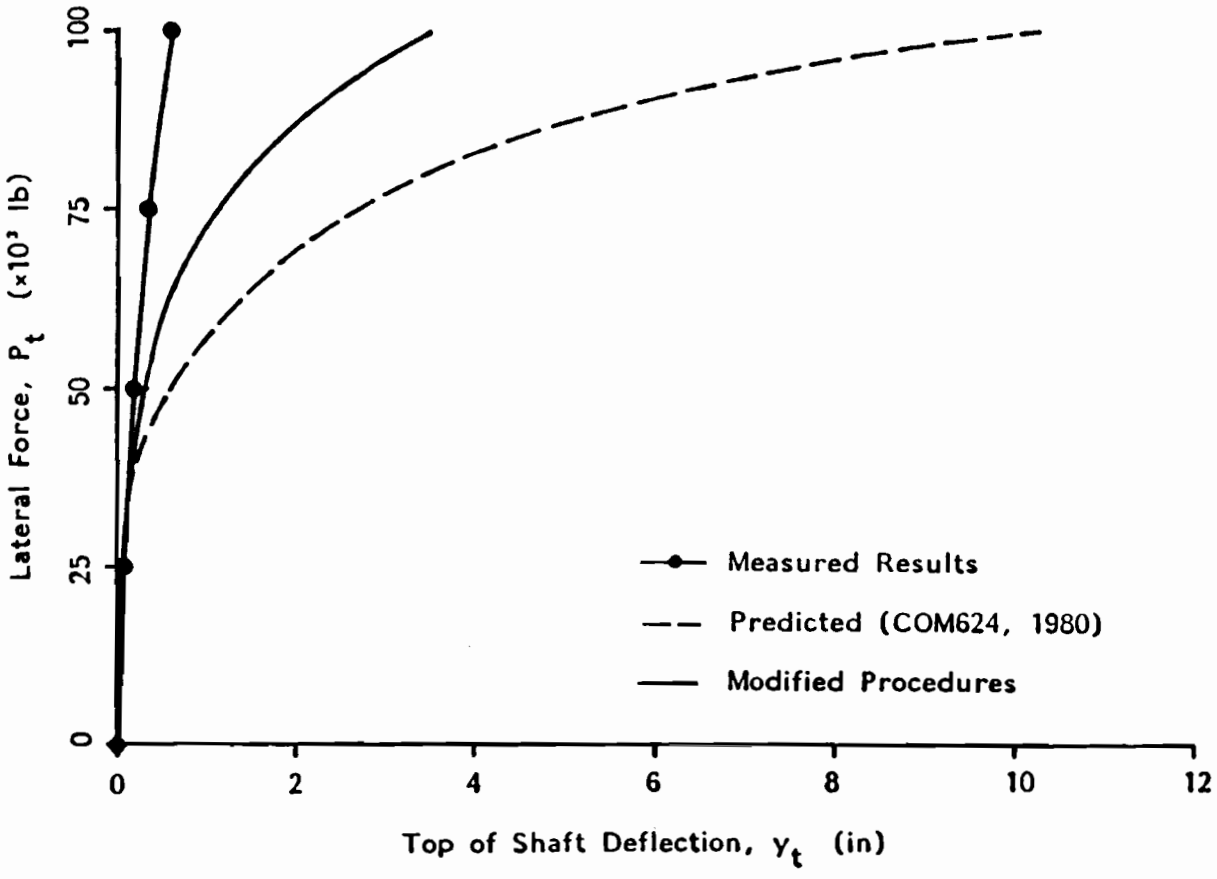

Figure 8.18: Top of Shaft Deflection versus Lateral Force for Shaft No. 23. - Conventional and Modified Procedures

8.2.1 Top of Shaft Deflection

The predicted top of shaft deflections exceeded the measured values for both analyses except for the smaller loadings analyzed for shafts No. 21 through 23. However, the predicted deflections from the analyses using the modified procedures were generally in better agreement with the measured values than those from the analyses using the conventional procedures.

Since the drilled shafts were loaded by various methods and tested completely independent of each other, a statistical comparison between predicted and measured deflections can be best achieved using deflections at a reference load. For the present study, the reference loads were chosen as one-half the largest loads applied to the shafts in the load tests. The reference loads for each shaft along with the corresponding measured and predicted deflections from both procedures are presented in Table 8.6. The average and standard deviation of the ratios of the predicted-to-measured deflection were 6.24 and 7.05, respectively, for the analyses using the conventional procedures. The average and standard deviation were reduced to 3.13 and 2.22, respectively, for the modified procedures.

8.2.2 Deflected Shape of Drilled Shafts

A single point of zero deflection was indicated from all loads except for three loads, applied to shafts No. 18 and 20, under which two points of zero deflection developed. For cases where one point of zero deflection was noted, the point was further down the shaft when the modified procedures were used in comparison to the conventional procedures. This also created smaller base of shaft deflections. The ratios of the distance to the point of zero deflection and the total length of the shaft (L_z/L) are presented in Table 8.7 along with the computed base of shaft deflections. More flexure in the deflected shapes of the drilled shafts was also noted as the length-to-diameter ratio increased. This is illustrated for shafts No. 17 and 19 in Fig. 8.19 where, for the same soil conditions, load and length, the smaller diameter shaft (No. 19) deflected with more curvature than the larger diameter shaft (No. 17).

Table 8.6

Deflections at Reference Load of One-Half the Ultimate Load Applied in Load Tests

Shaft No.	P_t ($\times 10^3$ lb)	Measured y_t (in)	Conventional Procedures y_t (in)	Modified Procedures y_t (in)
15	17.2	0.07	1.65	0.44
16	9.72	0.18	0.43	0.24
17	11.9	0.056	0.38	0.43
18	12.5	0.02	0.10	0.086
19	11.6	0.40	0.79	0.76
20	12.5	0.35	0.55	0.54
21	225	0.80	1.40	0.79
22	200	0.97	1.38	3.00
23	80	0.37	3.41	1.38

Table 8.7

Ratios of Depth to Point of Zero Deflection and Shaft Length, L_z/L and Base of Shaft Deflections

Shaft No.	P_t ($\times 10^3$ lb)	L_z/L, Conv. Proc.	L_z/L Mod. Proc.	Deflection, Conv. Proc. (in)	Deflection, Mod. Proc. (in)
15					
	5.56	0.66	0.72	0.021	0.008
	11.1	0.72	0.80	0.13	0.031
	16.7	0.74	0.84	0.38	0.069
	22.2	0.74	0.86	1.04	0.13
16					
	4.17	0.67	0.69	0.015	0.010
	8.33	0.72	0.75	0.099	0.048
	12.5	0.74	0.79	0.30	0.12
	16.7	0.75	0.78	0.67	0.31
17					
	4.69	0.68	0.72	0.066	0.46
	9.38	0.68	0.72	0.13	0.091
	14.1	0.68	0.71	0.21	0.15
	18.8	0.68	0.70	0.31	0.22
18					
	6.25	**[1]	**	**	**
	12.5	0.72	0.74	0.009	0.0007
	18.8	0.63	0.82	0.056	0.007
	25.0	0.73	0.84	0.19	0.021

**[1] - Two points of zero deflection were noted

Table 8.7 cont.

Shaft No.	P_t ($\times 10^3$ lb)	L_z/L, Conv. Proc.	L_z/L Mod. Proc.	Deflection, Conv. Proc. (in)	Deflection, Mod. Proc. (in)
19					
	4.69	0.65	0.66	0.051	0.043
	9.38	0.66	0.66	0.11	0.089
	14.1	0.68	0.69	0.20	0.16
	18.8	0.70	0.72	0.38	0.27
20					
	6.25	**[1]	**	**	**
	12.5	0.71	**	0.002	**
	18.8	0.72	0.75	0.085	0.006
	25.0	0.73	0.83	0.39	0.046
21					
	100	0.73	0.79	0.011	0.004
	200	0.73	0.83	0.30	0.083
	300	0.73	0.82	1.6	0.51
	400	0.73	0.82	5.6	1.8
22					
	75	0.72	0.79	0.018	0.007
	150	0.72	0.84	0.345	0.079
	225	0.72	0.83	1.77	0.46
	300	0.73	0.82	6.45	1.69
23					
	25	0.73	0.80	0.006	0.002
	50	0.73	0.86	0.17	0.034
	75	0.73	0.91	0.93	0.090
	100	0.74	0.90	3.61	0.37

**[1] - Two points of zero deflection were noted

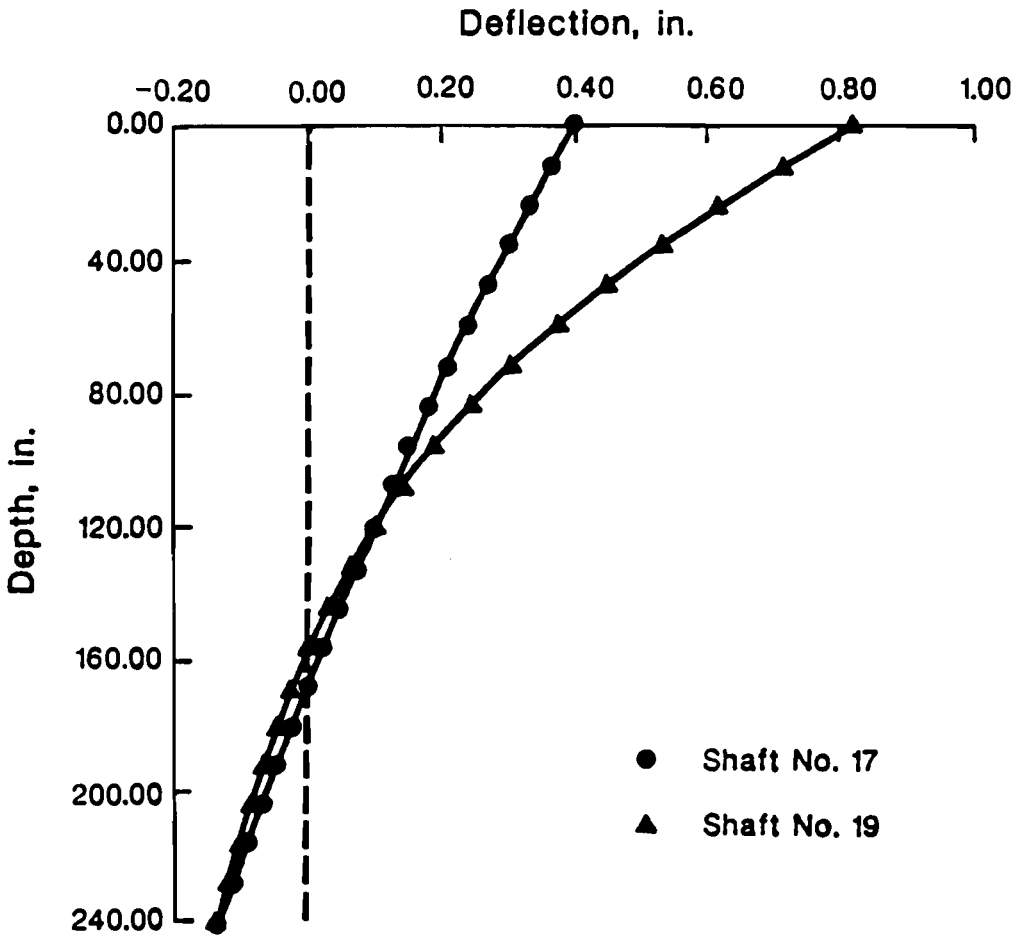

Figure 8.19: Deflected Shape of Shafts No. 17 and 19 at Lateral Force = 9.38 $\times 10^3$ lb

8.3 CONCLUSION

For the drilled shafts described in this chapter, as well as those described in Chapters 4, 5 and 7, analyses with the modified procedures reduce the discrepancies between computed and measured responses of "short" drilled shafts when compared to analyses with the conventional procedures.

CHAPTER 9. SUMMARY AND RECOMMENDATIONS

In the previous chapters, the analysis of laterally loaded drilled shafts was studied for two specific cases. The first case, discussed in Chapter 3, was that of a drilled shaft with only two points of zero deflection. A simplified procedure to determine the length of drilled shaft required to achieve two points of zero deflection was developed for two p-y curve criteria which produce p-y curves with initial linear portions; the criteria for stiff-clay-below-the-water-table and sand. This was accomplished by relating nonlinear soil responses to linear responses. The simplified procedure for these two criteria provided an excellent estimate of the length of shaft required to achieve two points of zero deflection and should be used as an aide in the design of laterally loaded drilled shafts. Additional studies are warranted to extend a similar procedure for other p-y criteria which do not have initial, linear portions.

The second case, covered in Chapter 4 through 8, concerned the analysis of laterally loaded "short" drilled shafts which have only a single point of zero deflection. Twenty load tests on "short" drilled shafts were analyzed using current, conventional procedures and modified procedures developed in this study. The modified procedures, discussed in chapter 6, consisted of three modifications. Two of the modifications involved changes to the p-y curves namely, reducing the characteristic deflection, y_{50}, and increasing the ultimate soil resistance, p_{ult}, below the first point of zero deflection. The third modification introduces a shear force, F_B, to the base of the shaft. Analyses with the modified procedures produced better agreement with measured responses of "short" drilled shafts than analyses with the conventional procedures; however, computed responses still exceeded the measured in most cases. It is recommended that the modified procedures, described in this study, be incorporated into analysis and that additional study on the behavior of "short" drilled shafts be performed by continuing analyses on available load tests and/or testing actual "short" drilled shafts in the field.

REFERENCES

1. Adams, J.I., and Radhakrishna, H.S., "The Lateral Capacity of Deep Augered Footings," Proceedings, Eighth International Conference of Soil Mechanics and Foundation Engineering, Moscow, International Society of Soil Mechanics and Foundation Engineering, Vol. 2.1, 1973, pp. 1-8.

2. Bhushan, K., Haley, S.C. and Fong, P.T., "Lateral Load Tests on Drilled Pires in Stiff Clay," Proceedings, American Society of Civil Engineers, Vol. 104, No. GT8, August, 1979, pp. 969-985.

3. Colye, H.M., Bartoskewitz, R.E. and Berger, W.J., "Bearing Capacity Prediction by Wave Equation Analysis: State of the Art," Texas A&M University Texas Transportation Institute Research Report 125-8F, August, 1973.

4. Electric Power Research Institute, Laterally Loaded Drilled Pier Research, Volumes I and II, prepared by GAI Consultants, Research Project 1280-1, January, 1982.

5. Focht, J.A., Jr., and McClelland, B., "Analysis of Laterally Loaded Piles by Difference Equation Solution," The Texas Engineer, Texas Section, American Society of Civil Engineers, 1955.

6. Gleser, S.M., "Lateral Load Tests on Vertical Fixed-Head and Free-Head Piles," Symposium on Lateral Load Tests on Piles, American Society Testing Materials, Special Training Publication No. 154, 1953, pp. 75-101.

7. Hetenyi, M., Beams on Elastic Foundation, University of Michigan Press, Ann Harbor, Michigan, 1946.

8. Howe, R.J., "A Numerical Method for Predicting the Behavior of Laterally Loaded Piling," TS Memorandum 9, Shell Oil Company, Houston, Texas, 1955.

9. Huang, W. and Cheng, W.H., "Transmission Pole Caisson Foundation Tests," Sargent and Lundy, for Pennsylvania Power and Light Company, August 1977.

10. Leicht, T.J., "Load Deformation Characteristics of Pile Foundations," M.S. Thesis, University of Texas, Austin, Texas, August, 1986.

11. Matlock, H., "Correlations for Design of Laterally Loaded Piles in Soft Clay," Proceedings, Second Annual Offshore Technology Conference, Houston, Texas, Paper No. OTC 1204, Vol. I, 1970, pp. 577-594.

12. Matlock, H, and Reese, L.C., "Generalized Solutions for Laterally Loaded Piles," Transactions, American Society of Civil Engineers, Vol. 127, Part I, 1962, pp. 1220-1251.

13. McClelland, B. and Focht, J.A., Jr., "Soil Modulus for Laterally Loaded Piles," Transactions, American Society of Civil Engineers, Vol. 123, 1958, pp. 1049-1086.

14. Reese, L.C., Behavior of Piles and Pile Groups Under Lateral Load, U.S. Department of Transportation, Federal Highway Adminstration, Office of Research, Washington, D.C., July, 1983.

15. Reese, L.C., personal communication, 1985.

16. Reese, L.C., Cox, W.R. and Koop, F.D., "Analysis of Laterally Loaded Piles in Sand," Proceedings, Fifth Annual Technology Conference, Houston, Texas, Vol. II., Paper No. OTC 2080, 1974, pp. 473-485.

17. Reese, L.C., Cox, W.R. and Koop, F.D., "Field Testing and Analysis of Laterally Loaded Piles in Stiff Clay," Proceedings, Seventh Annual Technology Conference, Houston, Texas, Vol. II., Paper No. OTC 2312, 1975, pp. 672-690.

18. Reese, L.C. and Matlock, H., "Nondimensional Solutions for Laterally Loaded Piles with Soil Modulus Assumed Proportional to Depth," Proceedings, Eighth Texas Conference on Soil Mechanics and Foundation Engineering, Special Publication No. 29, Bureau of Engineering Research, The University of Texas, Austin, Texas, September, 1956.

19. Reese, L.C. and Sullivan, W.R., Documentation of Computer Program COM624, Parts I and II, Geotechnical Engineering Center, Department of Civil Engineering, Unversity of Texas, Austin, Texas, 1980.

20. Reese, L.C. and Welch, R.C., "Lateral Loading of Deep Foundations in Stiff Clay," Proceedings, American Society of Civil Engineers, Vol. 101, No. GT7, February, 1975, pp. 633-649.

21. Skempton, A.W., "The Bearing Capacity of Clays," Proceedings, Building Research Congress, Division I, London, England, 1951, pp. 180-189.

22. Timoshenko, S.P., Strength of Materials, Part II, Advanced Theory and Problems, Second Edition - Tenth Printing, D. Van Nostrand Company, Inc., 1941.

APPENDIX

APPENDIX. RESULTS OF COMPUTER ANALYSES FOR TWO POINTS OF ZERO DEFLECTION

The following are the results from the analyses for two points of zero deflection considering the two p-y curve criteria. The equivalent quantitites, m' and T', and the ratios m'/m_i and y_t/D for the stiff clay and sand are presented in Table A.1 and A.2, respectively.

Table A.1
Results for Analyses in Stiff Clay Below the Water Table

Dimensional Quantities, Effective Soil Modulus Variation With Depth and Non-Dimensional Variables

Medium Stiff Clay m = 500 lb/in^3

Diameter (in)	T' (in)	m' (lb/in^3)	y_t/b	m'/m_i
12	23.61	500.0	0.00608	1.0
12	24.38	426.5	0.00967	0.853
12	29.79	156.4	0.0479	0.313
30	49.12	500.0	0.000933	1.0
30	50.42	439.0	0.00162	0.878
30	52.08	373.1	0.00289	0.746
30	56.25	253.9	0.00643	0.508
30	62.50	149.9	0.0134	0.300
30	67.08	105.3	0.0246	0.211
48	71.59	500.0	0.000198	1.0
48	71.88	490.0	0.000421	0.95
48	73.54	437.0	0.000725	0.874
48	77.71	331.7	0.00150	0.663
48	81.88	255.5	0.00273	0.511
48	86.04	199.3	0.00427	0.399
48	93.54	131.3	0.00835	0.263

Table A.1 cont.

Medium Stiff Clay m = 500 lb/in³

Diameter (in)	T' (in)	m' (lb/in³)	y_t/b	m'/m_i
60	85.54	500.0	0.000253	1.0
60	86.46	474.0	0.00038	0.948
60	89.58	396.9	0.000775	0.794
60	94.79	299.2	0.001395	0.598
60	98.96	241.3	0.00213	0.483
60	107.29	161.1	0.00398	0.322

Very Stiff Clay m = 2000 lb/in³

12	17.89	2000.0	0.00823	1.0
12	18.54	1674.6	0.014	0.837
12	18.96	1498.5	0.0207	0.749
12	19.79	1208.5	0.0313	0.604
30	37.23	2000.0	0.00201	1.0
30	38.54	1681.5	0.00377	0.841
30	40.63	1292.3	0.00803	0.646
30	43.54	913.7	0.0154	0.457
30	48.13	554.0	0.0306	0.277
48	54.25	2000.0	0.000796	1.0
48	54.79	1903.5	0.000923	0.952
48	57.29	1522.9	0.00244	0.761
48	60.42	1167.7	0.00485	0.584
48	64.17	864.1	0.00867	0.432

Table A.1 cont.

Very Stiff Clay m = 2000 lb/in^3

Diameter (in)	T' (in)	m' (lb/in^3)	y_t/b	m'/m_i
60	64.83	2000.0	0.000588	1.0
60	67.71	1609.3	0.00124	0.805
60	69.79	1383.0	0.00227	0.691
60	72.92	1111.0	0.00363	0.555
60	76.46	876.4	0.00548	0.438
60	79.79	708.0	0.00795	0.354

Table A.2
Results for Analyses in Sand

Dimensional Quantities, Effective Soil Modulus Variation With Depth and Non-Dimensional Variables

Loose Sand $m = 20\ lb/in^3$

Diameter (in)	T' (in)	m' (lb/in^3)	y_t/b	m'/m_i
12	44.95	20.00	0.0159	1.0
12	47.50	15.18	0.0883	0.759
12	52.10	9.58	0.4425	0.479
12	59.38	4.97	1.742	0.249
30	93.51	20.00	0.0192	1.0
30	95.83	17.69	0.0291	0.885
30	100.0	14.30	0.0527	0.715
30	100.0	14.30	0.0813	0.715
48	136.28	20.00	0.02125	1.0
48	137.50	19.12	0.02354	0.956
48	141.67	16.47	0.0367	0.824
48	141.67	16.47	0.0510	0.824
60	162.84	20.00	0.0225	1.0
60	164.58	18.96	0.0278	0.948
60	166.67	17.81	0.0353	0.890
60	168.75	16.73	0.0432	0.837

Table A.2 cont.

Medium Dense Sand m = 60 lb/in^3

Diameter (in)	T' (in)	m' (lb/in^3)	y_t/b	m'/m_i
12	36.08	60.00	0.00665	1.0
12	39.58	37.77	0.0513	0.630
12	42.71	25.83	0.2275	0.431
12	47.71	14.85	0.8667	0.248
30	75.06	60.00	0.0101	1.0
30	77.71	50.47	0.0157	0.841
30	80.21	43.08	0.0301	0.718
30	83.33	35.58	0.0463	0.592
30	85.83	30.69	0.0877	0.512
30	88.54	26.28	0.143	0.438
30	93.75	19.75	0.304	0.329
48	109.39	60.00	0.01127	1.0
48	110.42	57.27	0.0125	0.955
48	113.54	49.81	0.01925	0.830
48	118.75	39.81	0.0383	0.663
48	121.88	34.96	0.0596	0.583
60	130.72	0.119	0.00198	1.0
60	131.25	58.79	0.1127	1.0
60	132.92	55.20	0.01483	0.920
60	138.54	44.87	0.029	0.748
60	143.75	37.31	0.0453	0.622

Table A.2 cont.

Very Dense Sand m = 125 lb/in^3

Diameter (in)	T' (in)	m' (lb/in^3)	y_t/b	m'/m_i
12	31.16	125.00	0.00521	1.0
12	33.96	81.27	0.03175	0.650
12	36.46	56.97	0.13	0.456
12	39.79	36.79	0.466	0.294
12	45.83	18.15	1.513	0.145
12	50.63	11.04	4.242	0.088
30	64.82	125.00	0.0063	1.0
30	65.42	119.37	0.00903	0.955
30	70.83	80.20	0.0278	0.642
30	74.79	61.10	0.0823	0.489
30	78.13	49.13	0.167	0.393
48	94.46	125.00	0.0070	1.0
48	95.83	116.29	0.01146	0.930
48	101.88	85.66	0.02875	0.685
48	105.21	72.93	0.0504	0.583
48	109.38	60.05	0.0771	0.480
60	114.58	115.94	0.00893	0.928
60	116.67	105.95	0.0165	0.848
60	120.80	88.90	0.0267	0.711
60	125.00	75.04	0.0382	0.600
60	126.04	71.99	0.0508	0.576